2017

Identification of Novel Ligands and Structural Requirements for Heterodimerization of the Liver X Receptor Alpha

Shimpi Bedi
Wright State University

IDENTIFICATION OF NOVEL LIGANDS AND STRUCTURAL REQUIREMENTS FOR HETERODIMERIZATION OF THE LIVER X RECEPTOR ALPHA

A dissertation submitted in partial fulfillment of the
requirements for the degree of
Doctor of Philosophy

By

SHIMPI BEDI
M.S., Wright State University, 2009
B.S., Panjab University, 1988

2017
Wright State University

WRIGHT STATE UNIVERSITY
GRADUATE SCHOOL

April 25, 2017

I HEREBY RECOMMEND THAT THE DISSERTATION PREPARED UNDER MY SUPERVISION BY Shimpi Bedi ENTITLED Identification of Novel Ligands and Requirements for Heterodimerization of the Liver X Receptor Alpha BE ACCEPTED IN PARTIAL FULFILLMENT OF THE REQUIREMENTS FOR THE DEGREE OF Doctor of Philosophy.

_____

Stanley Dean Rider, Jr., Ph.D.
Dissertation Director

_____

Mill W. Miller, Ph.D.
Director, Biomedical Sciences
Ph.D. Program

_____

Robert E. W. Fyffe, Ph.D.
Vice President for Research and
Dean of the Graduate School

Committee on
Final Examination

_____
Stanley Dean Rider, Jr., Ph.D.

_____
Jerry Alter., Ph.D.

_____
Lawrence J. Prochaska, Ph.D.

_____
Katherine Excoffon, Ph.D.

_____
Nicholas V. Reo, Ph.D.

_____
J. Ashot Kozak, Ph.D.

ABSTRACT

Bedi, Shimpi Ph.D., Biomedical Sciences Ph.D. program, Department of Biochemistry and Molecular Biology, Wright State University, 2017. Identification of novel ligands and structural requirements for heterodimerization of the liver X receptor alpha.

LXRs, LXRα (NR1H3) and LXRβ (NR1H2), are ligand-activated transcription factors that are members of the nuclear receptor superfamily. Oxysterols and nonsteroidal synthetic compounds bind directly to LXRs and influence the expression of LXR dependent genes. The use of murine models and LXR-selective agonists have established the important role of LXRs as sterol sensors that govern the absorption, transport, and catabolism of cholesterol. Upon activation, these receptors have been shown to increase reverse cholesterol transport from the macrophage back to the liver to aid in the removal of excess cholesterol. Not surprisingly, LXR dysregulation is a feature of several human diseases, including metabolic syndrome. Due to their roles in the regulation of lipid and cholesterol metabolism, LXRs are potentially attractive pharmaceutical targets. As ligand binding and dimerization play pivotal roles in modulating LXR activity, the identification of novel ligands and requirements for LXR dimerization can potentially aid the drug development process. Herein, using a variety of biophysical assays, including fluorescence based assays coupled with *in silico* molecular modeling, I have identified medium chain fatty acids and/or their metabolites as the novel endogenous agonists of LXRα. There is mounting evidence that ligand induced dimerization regulates the transcriptional output of nuclear receptors. Thus, it is important to identify factors that

modulate protein-protein interactions. This work demonstrated that (a) LXRα binds PPARα with a high affinity (low nanomolar concentration), (b) ligands for LXRα alter the binding dissociation constant values of LXRα-PPARα interaction, and (c) ligand binding induces conformational changes in the dimer secondary structure. Furthermore, site-directed mutagenesis investigated the strength of individual contributions of residues located in the ligand binding domain to dimerization and transactivation properties of LXRα. Data herein highlight the importance of hydrophobic interactions and salt bridges at the interface, and suggest that key interface residues are required for the ligand-dependent activation of LXRα in a promoter specific manner. Mutagenesis of LXRα L414 to an arginine revealed the importance of this site in dimerization, specifically with RXRα. This work showed that this particular mutation specifically abolished dimerization with RXRα. Taken together, this study provided insights into the functional roles of fatty acids as novel LXRα ligands and the effects mutations may have in modulating molecular interactions and activity profile of LXRα.

TABLE OF CONTENTS

INTRODUCTION 1

Metabolic syndrome 1

Liver X receptor (LXR) 6

LXR structure and function 6

LXRα isoforms 6

LXRα target genes 6

LXR-RXR dimerization 6

Domain structure 8

Ligand binding domain (LBD) 9

Crystal structure of LXRα-RXRβ 10

Agonist binding to the LBD 9

Ligand binding mode 10

Ligands of LXRα 14

Heterodimerization of LXRα 16

Binding partners of LXRα 16

LXRα interface 17

Identification of residues required for dimer formation 18

Sequence alignment of LBDs 20

Solvent accessibility of LXRα LBD residues 21

TABLE OF CONTENTS (continued)

Regulation of LXRα 22

Function of LXRα 22

Reverse cholesterol transport 26

Cholesterol synthesis 26

Cholesterol uptake 27

Intestinal cholesterol absorption 27

Fecal neutral sterol excretion via intestine 27

Apolipoprotein-mediated lipid efflux via ABCA1 28

HDL-cholesterol and ApoA1 28

Animal Models of LXRα 29

LDL and HDL 30

HYPOTHESIS 32

Development of hypothesis 31

Hypothesis 32

CHAPTER I 33

Abstract 34

Introduction 35

Materials and Methods 37

Purification of recombinant hLXRα 37

TABLE OF CONTENTS (continued)

Reagents 37

Direct Fluorescent ligand binding assays 37

Displacement of bound fluorescent BODIPY C16:0-CoA 37

Intrinsic quenching of LXRα aromatic amino acids 38

Secondary structure determination through CD 38

Mammalian expression plasmids 39

Cell culture and transactivation assay 39

Molecular docking 40

Statistical analysis 40

Results 41

Protein expression and purification 41

Direct Fluorescent ligand binding assay 43

Displacement of bound fluorescent BODIPY C16:0-CoA 47

Intrinsic quenching of LXR aromatic amino acids 51

Secondary structure determination through CD 56

In silico molecular docking 61

Luciferase reporter assay 65

Discussion 69

TABLE OF CONTENTS (continued)

CHAPTER II **74**

Abstract 75

Introduction 77

Materials and Methods 80

Chemicals 80

Construction of plasmids 80

Protein expression 81

Recombinant protein purification 81

Hex docking of LBDs 82

Fluorescent protein-protein binding assay 82

Forster resonance energy transfer 83

Secondary structure determination through CD 84

Results 86

Purification of recombinant proteins 86

Hex docking of LBDs of LXRα and PPARα 88

Fluorescent protein-protein binding assay 91

Forster resonance energy transfer 94

Secondary structure determination through CD 98

Discussion 101

TABLE OF CONTENTS (continued)

CHAPTER III **102**

Abstract 103

Introduction 104

Materials and Methods 107

Chemicals 107

Mutagenesis for generation of LXRα mutants 107

Purification of recombinant proteins 107

Intrinsic quenching of LXRα aromatic amino acids 108

Circular dichroism spectroscopy 108

Protein-protein binding 109

Bimolecular fluorescence complementation assay 109

Molecular docking 110

Mammalian expression plasmids 110

Cell culture and transfection assays 111

Statistical analysis 111

Results 112

Generation of LXRα mutants 112

Mutant LXRα purification 116

Ligand binding profile of hLXRα mutants 118

TABLE OF CONTENTS (continued)

Docking simulation for ligand binding free energies 122

Protein Protein binding assay 124

CD spectroscopy to determine structural changes 129

Bimolecular fluorescence complementation assay 134

Luciferase reporter assay 137

Discussion 144

SUMMARY AND CONCLUSIONS **149**

BIBLIOGRAPHY **158**

LIST OF ABBREVIATIONS **186**

LIST OF FIGURES

INTRODUCTION

1. Dietary lipids are ligands of nuclear receptors 2

2. Liver X receptor (LXR) domain organization 5

3. LXR-RXR target genes 7

4. LXRβ-RXRα crystal structure 12

5. Agonist binding in the NR LBD 13

6. Sequence alignment of LXRα LBD 20

7. Solvent accessibility of LXRα LBD 21

8. LXR is an oxysterol sensor 24

CHAPTER I

9. Purification of recombinant LXRα protein 42

10. Binding of fluorescent ligands to LXRα 45

11. Displacement of BODIPY C16:0-CoA by LXRα 49

12. Quenching of LXRα aromatic amino acids by FA 53

13. Ligand induced structural changes in LXRα secondary structure 58

14. Docking of ligands in LXRα LBD 63

15. Luciferase reporter assay 67

LIST OF FIGURES (continued)

CHAPTER II

16. SDS-PAGE and Coomassie blue staining of purified proteins 87

17. Hex docking of LBDs of LXRα and PPARα 89

18. Fluorescent protein-protein binding assay 92

19. FRET between LXRα and PPARα 96

20. CD spectrum of LXRα mutants with PPARα with ligands.....99

CHAPTER III

21. Contacts across LXRα dimer interface.....113

22. SDS-PAGE of purified LXRα mutant proteins.....117

23. Intrinsic quenching assay of LXRα mutant proteins.....120

24. Protein-protein binding of LXRα mutants with PPARα.....126

25. Far UV CD spectrum of PPARα with LXRα mutants 131

26. Visualization of protein complexes in living cells (BiFC).....135

27. Luciferase reporter assay activity of hSREBP-1c promoter 139

28. Luciferase reporter assay activity of hApoA-1 promoter.....142

APPENDIX

S1. FRET showing LXRα binding to MCFA and MCFA-acyl CoA 177

S2. Displacement assay with LCFA.....178

S3. Intrinsic quenching of LXRα with LCFA or acyl CoA 179

S4. CD spectroscopy of LXRα with LCFA or acyl CoA.....180

S5. Ligand binding of LXRα mutants to 25-HC.....181

S6. LigPlot analysis of T-0901317 binding to LXRα mutants 182

S7. Fluorescent protein-protein binding to RXRα 183

S8. CD structural changes LXRα/PPARα due to ligand binding 184

S9. Western blotting to show protein expression levels.....185

LIST OF TABLES

CHAPTER I

1. Binding affinities of LXRα for non-fluorescent ligands 55

2. Secondary structure composition of LXRα in the presence of ligands 60

3. Binding free energies of ligand binding to LXRα.....64

CHAPTER III

4. Exposure of amino acid residues predicted at LXRα interface 115

5. Binding free energies of T-17 binding to LXRα.....123

6. Binding affinities of PPAR binding for LXRα mutants 128

7. CD changes of LXRα mutants with PPARα.....133

APPENDIX

S 1. Affinity of LXRα for LCFA or acyl CoA.....175

S 2. Secondary structure of LXRα with LCFA or acyl CoA 176

ACKNOWLEDGEMENTS

I would like to express my appreciation and thanks to my previous advisor, the late Dr. Heather. A. Hostetler, who passed away before the completion of my graduate training. Her insight and direction has contributed immensely to shaping my dissertation project. I would like to thank and extend my gratitude to my present mentor, Dr. Stanley Dean Rider, Jr., who has been no less instrumental in completing this project. I greatly benefited from his support and guidance. The completion of my dissertation and success in graduate school would not have been possible without his help.

I would also like to thank my committee members, Dr. Alter, Dr. Prochaska, Dr. Excoffon, Dr. Reo, and Dr. Kozak for serving as my committee members. Your advice on both research as well as career choices has been priceless.

I would especially like to thank all the previous Hostetler lab members for their friendship and support. My time at Wright state was made enjoyable due to the many friends that I have made over the years.

DEDICATION

I am grateful to my friends and family for their unconditional love, encouragement, and motivation.

For my parents for always believing in me and for encouraging me to follow my dreams

For my loving husband and daughter whose invaluable support during the final stages of Ph.D. is greatly appreciated

INTRODUCTION

METABOLIC SYNDROME

Nuclear receptors (NRs), described as *metabolic nuclear receptors* by Francis *et al*., 2003 are activated by dietary nutrients or metabolite intermediates which act as metabolic and toxicological sensors (Fig.1). These receptors allow the organism to adapt and survive in an ever-changing environment by inducing the appropriate metabolic genes and pathways. It has been demonstrated that nuclear receptors play central roles in; (a) energy and glucose metabolism through peroxisome proliferator-activated receptor gamma (PPAR γ); (b) fatty acid, triglyceride, and lipoprotein metabolism via PPAR α, δ, and γ; (c) reverse cholesterol transport and cholesterol absorption through the liver X receptors (LXRs); (d) bile acid metabolism through the farnesoid X receptor (FXR) and LXRs; and (e) the defense against xeno and endobiotics by the pregnane X receptor/steroid and xenobiotic receptor (PXR) (*1, 2*). An intricate signaling network allows these receptors to maintain normal homeostasis of glucose, cholesterol, triglycerides, and bile acids. Any disturbances in the equilibrium of this network is associated with elevated circulating levels of free fatty acids, bile acids, oxysterols, leading to dysregulation of the transcriptional activities of the nuclear receptors (*3*). Much attention has been given to the role of NRs in the pathophysiology of metabolic diseases including metabolic syndrome.

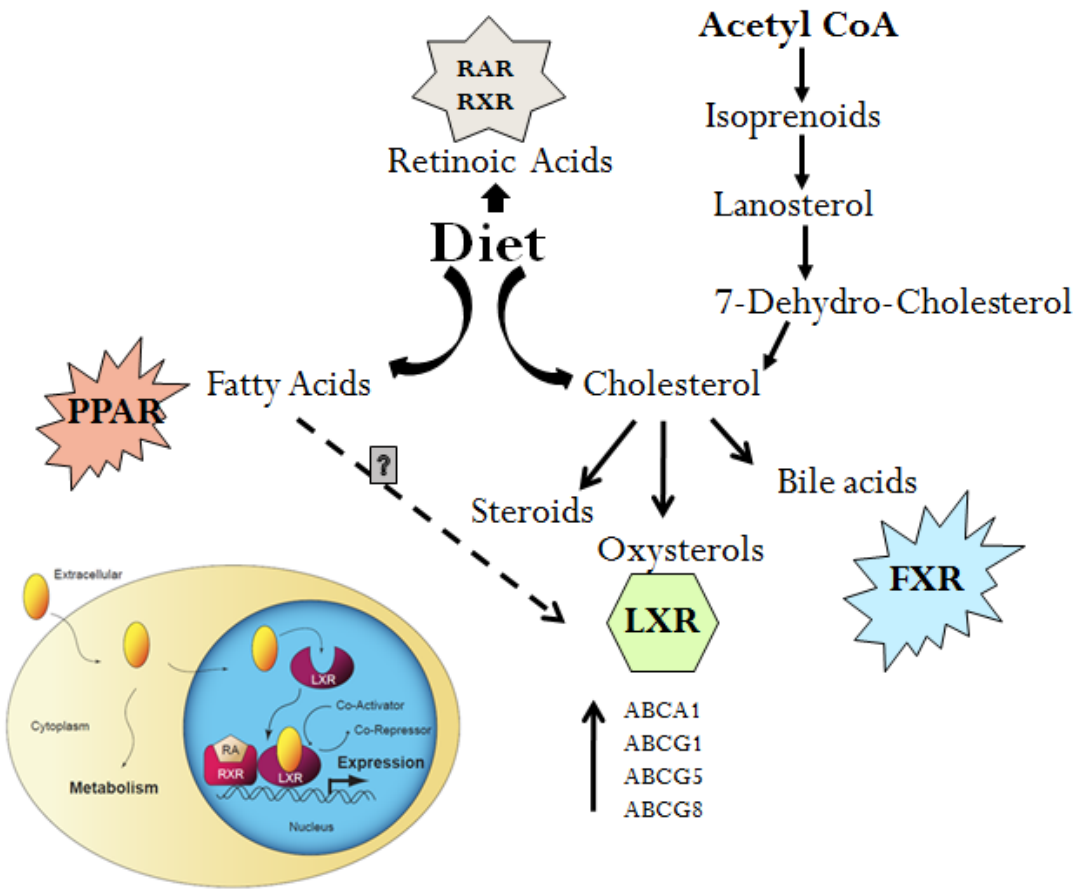
RAR
RXR
Retinoic Acids
Acetyl CoA
Isoprenoids
Lanosterol
7-Dehydro-Cholesterol
Diet
PPAR
Fatty Acids
Cholesterol
?
Steroids
Oxysterols
Bile acids
FXR
LXR
ABCA1
ABCG1
ABCG5
ABCG8
Extracellular
Cytoplasm
Metabolism
LXR
Co-Activator
Co-Repressor
RA
RXR
LXR
Expression
Nucleus

Fig.1. Dietary lipids are endogenous ligands for nuclear receptors. Ligands for the nuclear receptors, LXR, PPAR, and FXR are derived from the diet and from the biosynthetic pathways that generate cholesterol and fatty acids from acetyl coenzyme A. These lipophilic ligands diffuse through the nuclear membrane, bind to and stimulate the transcriptional activities of the receptors. Image modified from (*2*).

Metabolic syndrome is a clinical condition that is characterized by multiple cardiovascular risk factors including obesity, hypertension, dyslipidemia, and abnormal glucose metabolism. It is strongly associated with higher cardiovascular and total mortality (*4, 5, 6*). Given that the activities of NRs are modulated via direct DNA binding and by small endogenous lipophilic molecules as well as exogenous synthetic molecules, they represent attractive therapeutic targets for the treatment of metabolic syndrome (*7, 8, 9*).

The NR superfamily consists of 48 members in humans and 49 in mice. While they are conserved from human to C. *elegans*, they are not present in plants and yeast, suggesting their essential function in animal cells. NRs are composed of several domains that mediate DNA-binding, dimerization, ligand binding, and transcriptional activities. Synergistic and high-affinity dimeric DNA binding of nuclear receptors requires two independent dimerization functions, one located within the DNA-binding domain (DBD) and the second located in the ligand-binding domain (LBD) (*10*) (Fig. 2). NRs are classified based on phylogeny, structure, and their ligand binding properties (*11*). The segregation into these classes are indicative of their unique DNA binding properties, ligands, and dimerization status on target genes.

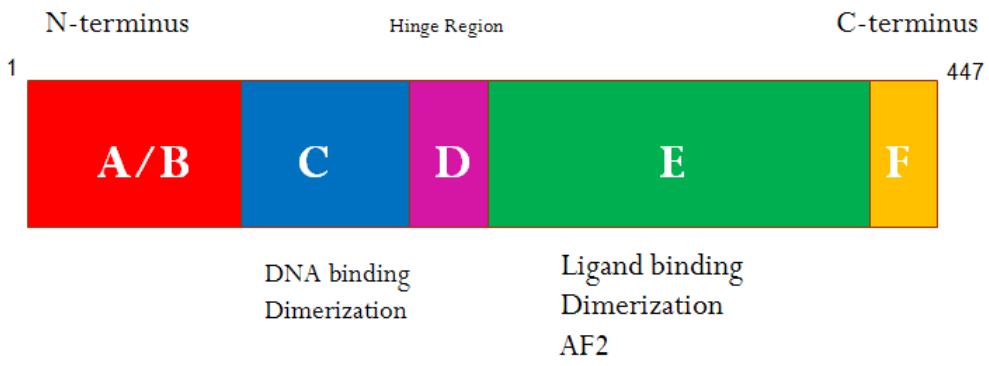

Fig.2. Schematic of the domain organization of LXRα that typifies nuclear receptors. A central DNA-binding domain or C domain is flanked by an N-terminal A/B domain and a C-terminal ligand binding domain (LBD). The LBD harbors a ligand-dependent transcriptional activity, a strong dimerization interface, and a ligand binding pocket.

LIVER X RECEPTOR (LXR)

Liver X receptors belong to a large family of nuclear hormone receptors that play important roles in cholesterol and lipid metabolism (*12, 13*). P. Willy and D. J. Mangelsdorf, 1995 cloned LXRα by low stringency screening of a rat liver cDNA library and named it based on its liver-rich expression pattern. *In vitro* transcription/translation showed full-length hLXRα to contain 447 amino acids (M, 49,000) (*14*). LXRs were initially classified as orphan receptors but were deorphanized with the identification of oxysterols as their physiological ligands. Several other ligands, both natural and synthetic, have since been classified as LXR ligands. There are two LXR isoforms in mammals, termed LXRα (NR1H3) and LXRβ (NR1H2). Both isoforms are highly related and share 78% identity of their amino acid sequences in both DNA and ligand-binding domains. The expression pattern of the two LXR isoforms varies; whereas LXRα is expressed in metabolically active tissues such as liver, spleen, intestine, kidney, lung, and adipose tissues, LXRβ is ubiquitously expressed in all tissues examined (*15*).

LXRs form obligate heterodimers with the retinoid X receptor (RXR) and regulate the expression of genes involved in bile acid and cholesterol metabolism through binding to LXR response elements (LXREs) in the promoter regions of the target genes (*10*) (Fig. 3). These targets include ATP-binding cassette transporters A1, G5, and G8 (ABCA1, ABCG5, ABCG8), apolipoprotein E (Apo E), and cholesterol ester transport protein (CETP).

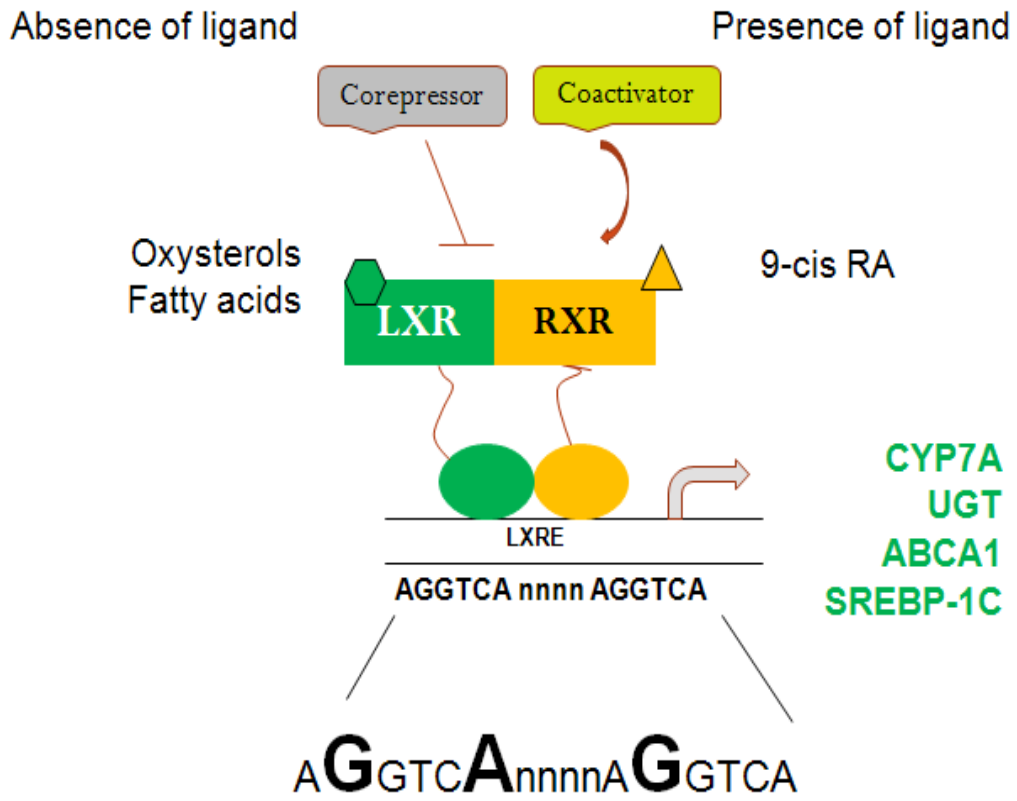

Fig.3. LXR and RXR form an obligate heterodimer that recognizes and binds to a direct repeat of DR4 response element in the regulatory regions of their target genes. In the absence of ligand, co-repressors are bound to the heterodimer and inhibit the transcription of target genes. Upon ligand binding to either LXR or RXR, co-activator proteins are recruited that initiate transcriptional activity.

Additional targets of LXR are fatty acid synthase (FAS) and SREBP-1c that are key lipogenic enzymes (*16, 17*). LXRE consists of two hexanucleotide sequences (AGGTCA) separated by four bases (DR-4 element) (*18*) (Fig. 3). The LXR/RXR heterodimer is activated by ligand binding to either partner and is, therefore, termed as a permissive heterodimer. The mode of activation is similar to that observed with other members of the hormone receptors. In the absence of ligand, the NRs repress transcription via direct interactions with transcriptional co-repressor proteins such as N-CoR (NR co-repressor) and SMRT (silencing mediator of retinoid- and thyroid-responsive transcription), and subsequent recruitment of the histone deacetylase complex to target genes. Upon ligand binding, there is a conformational change within the ligand binding domain (LBD) of the NR that results in the exchange of co-repressor complex with the recruitment of coactivators. The coactivator bound state converts the receptor from an inactive to an active state and exhibits enhanced levels of gene transcription (*19*).

STRUCTURE OF LXR

LXR contain two well-defined structural domains: a DNA-binding domain (DBD) and a ligand binding domain (LBD). The N-terminal region of LXR is highly variable and has a ligand independent transactivation function. The DBD and LBD are linked via a hinge region that displays very low amino acid identity and similarity between receptors. The function of the hinge region is poorly understood, however, it can influence transcription due to phosphorylation (*11*). The most conserved region within the nuclear receptors is the DBD that is composed of two zinc finger motifs. The first zinc finger contains the proximal- or P-box region, a short motif, responsible for

recognizing the promoter and allowing the receptor to bind differentially to target genes (*20*). The tertiary structure of the DBD contains alpha helices that bind to specific DNA sequences called hormone response elements. The DBD is not only involved in response element binding, but also serves as an allosteric transmitter of signals to other regions of the receptor molecule (*21*). Located within the second zinc finger is the distal- or D-box that provides a dimerization interface for nuclear receptor dimerization. Nuclear receptors bind to DNA as heterodimers, homodimers, or monomers, depending on the class of NRs (*22*).

Most nuclear receptors contain residues N-terminal to the DBD that mediate ligand-independent transactivation function (AF-1 function). The AF-1 sequence is not very well conserved across the nuclear receptor superfamily. This region can activate transcription in a constitutive manner. There is evidence that the AF1 activation function displays cells and promoter specificity (*23*). Allosteric interactions between subunits allow the receptor to function as efficient regulatory switches. The overall structure of the receptor may be altered in a subtle or dramatic manner as a result of allosteric interactions (*24*).

The LBD exhibits at least 78% amino acid sequence identity between the two LXR isoforms and constitutes the principal dimerization interface of this protein family. The multifunctional LBD mediates dimerization, ligand binding, and ligand-dependent transcriptional activity (*25*). X-ray crystallography established the apo and holo LXRα LBD as organized as a three-layered α-helical sandwich structure (Fig. 4). The helices have been designated H1 to H12 that are arranged in an antiparallel helix sandwich. Since the three dimensional crystal structure is derived from the LBD of LXRα, regions of high flexibility are not visible. Located at the core of the LBD is a hydrophobic ligand-binding

pocket (LBP) that accommodates the hydrophobic ligands (*26*). Several LXR LBD structures complexed with ligands have been determined (*26-29)*. Regardless of the type of bound ligand, the LBD maintains the same overall arrangement of the alpha helices. Ligand binding causes a major conformational change in the LBD. The structural transition upon ligand binding has been described as a 'mouse trap' mechanism. In the absence of ligand, H12 is located away from the LBD body. Ligand binding results in the positioning of H12 to a new position on the surface of LBD that entraps the ligand (active conformation) (*30*) (Fig. 5). This forms a hydrophobic binding groove for the binding of coactivator such as steroid receptor coactivator (SRC) family of proteins. The coregulators bind the receptors using LXXLL motifs located within their polypeptides and bind helix 12 via a charge clamp. The recruiting of transcriptional coregulators triggers activation or suppression of target genes (*31*). Antagonist may inhibit coactivator binding by sterically blocking the positioning of helix 12 over the LBD core structure or by promoting corepressor recruitment (*26*). Thus, nuclear receptors are molecular switches that may be turned off or on depending on the positioning of H12 of the LBD relative to the rest of the LBD.

Visual inspection of the LXRα LBD reveals that the LBP is shaped as a straight cylinder and extends between helix 12 and the beta sheet located at the entrance of the pocket. The volume of the LXRα LBP is in the range 700-800 A^3. The ligands are positioned centrally and the ligand-LBP interactions involve residues from helices 3, 5 and 7. Hydrophobic interactions and hydrogen bonds between the ligand and key residues in the LBP determine the strength and specificity of LBD-ligand complex. The hydrophilic region of the LBP, located near helices 1 and 5 and the β-sheet region found

between helices 5, possesses several polar and charged amino acids. Key residues His 421 and Trp 443 (helices 11 and 12) located in the LXRα LBP stabilize the active conformation of LXRα through direct interactions with the ligand (*26*).

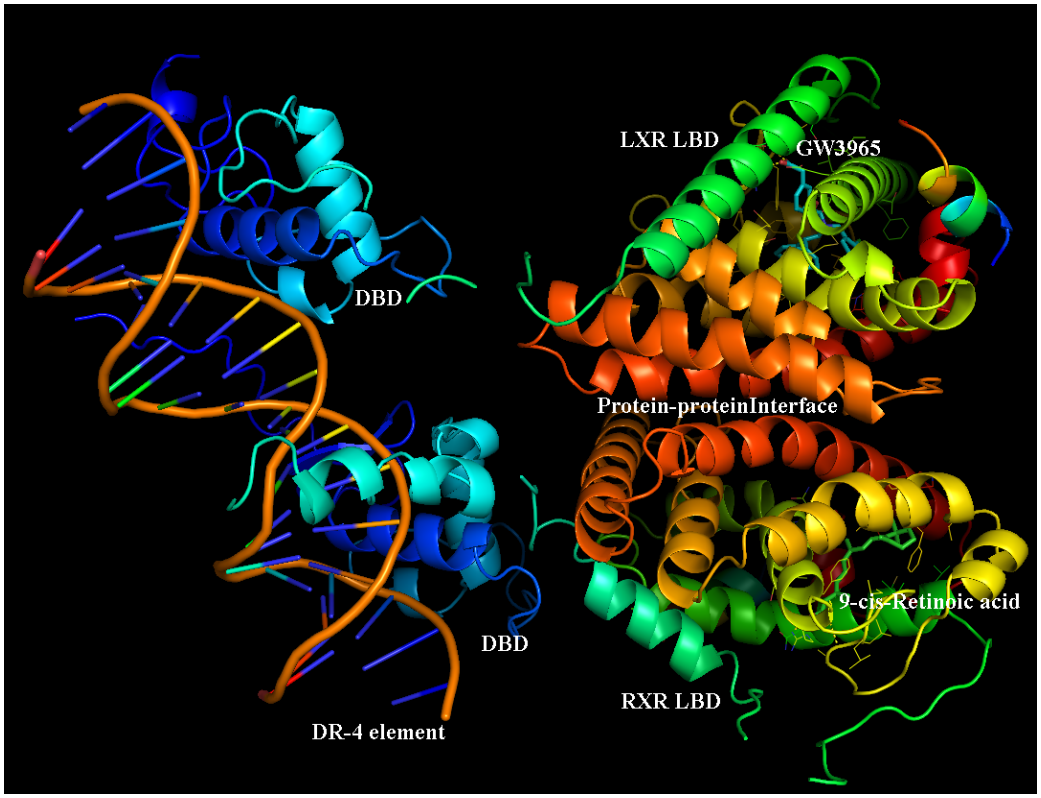

Fig.4. Crystal structure of LXRβ-RXRα complex on the DR-4 element in the presence of respective agonists: GW3965 (LXRβ) and 9-cis Retinoid acid (RXRα). Image adapted from the RCSB PDB entry 4NQA. Sections of the protein are not visible owing to residual mobility in the crystal structure.

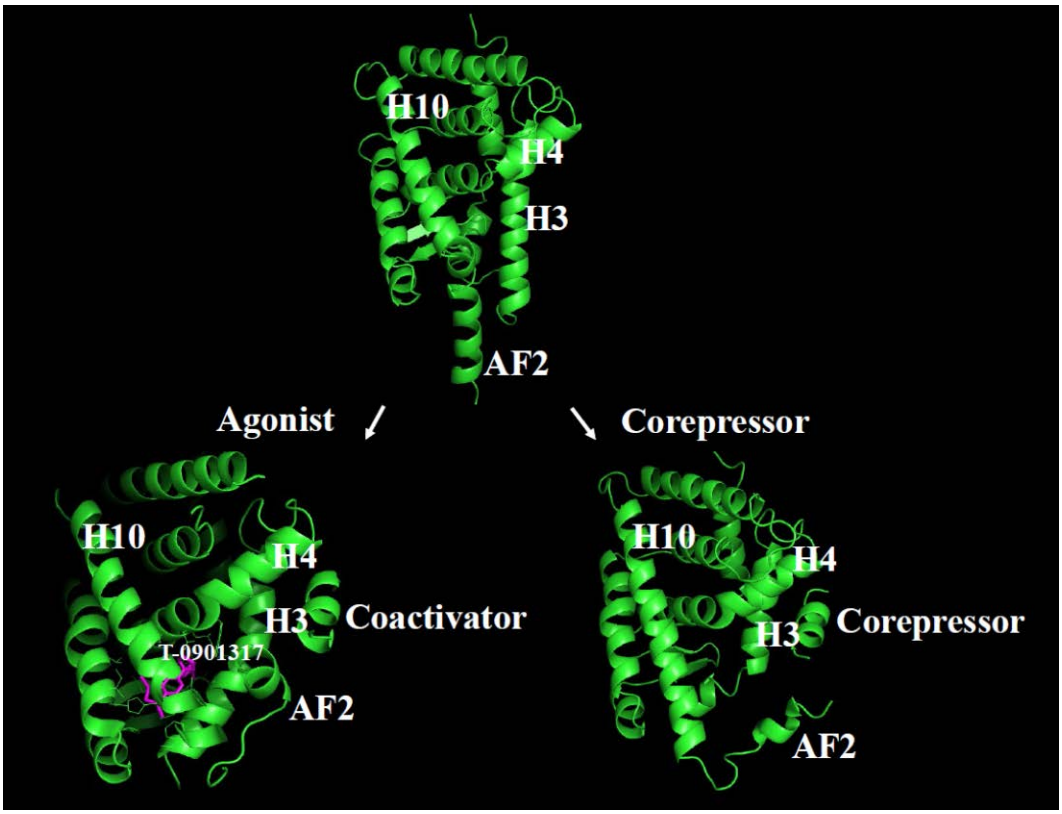

Fig.5. Agonist binding in the LBD induces a conformational change in C-terminal helix 12 (AF2). In the active state, AF-2 forms a lid over the hydrophobic ligand binding pocket to facilitate coactivator recruitment. In the absence of ligand, corepressor binds the LBD to prevent gene transcription. Image adapted from reference (30).

To date more than a dozen high resolution structures of LXR with various ligands and in complexes with RXR have been deposited in the Protein Data Bank (PDB) (*26*, *32*). Using these crystal structures, it has been possible to identify putative residues that may be involved with binding, the nature of the protein-protein interface, and the conformational changes undergone by the proteins upon binding other macromolecules. Considerable attention has recently been devoted to the regulation of the novel heterodimeric pair composed of LXRα and PPARα. Because the LXRα-PPARα LBDs have not been crystallized in a complex, the exact nature of protein-protein interactions is unclear. However, the LBDs of each of these proteins have individually been crystallized and might prove useful for predicting important interactions leading to LXRα-PPARα heterodimerization. Molecular docking has proved to be a valuable tool for the determination of the complex structure between two proteins by utilizing the structures from the individually crystallized subunits as input. Among the popular protein docking tools available to carry out such studies are AutoDOCK, HADDOCK, HEX, and ZDOCK.

Ligands of LXR

Endogenous Agonists

Oxidized cholesterol derivatives (oxysterols) are endogenous ligands for LXR. Among the oxysterols, 22(R)-hydroxycholesterol and 20(S)-hydroxycholesterol, 24(S)-hydroxycholesterol, and 24(S), 25-epoxycholesterol bind LXR with the strongest affinities at concentrations consistent with those found in tissues (K_d values ranging from 0.1-0.4 μM). Intermediates of cholesterol biosynthesis also activate LXRs through direct

high affinity binding. 24(S), 25-epoxycholesterol is produced in a shunt of the mevalonate pathway and activates LXR (*15*). Other intermediates such as desmosterol and zymosterol also activate LXR (*33*). Fatty acids are known to modulate activation of LXRα. Whereas trans-9, trans-11- conjugated linoleic acid transcriptionally regulates LXR target genes (ABCA1 and ABCG1) in human macrophages, polyunsaturated fatty acids antagonize ligand-dependent activation of LXRα by oxysterols (*34-36*).

Endogenous Antagonists

Highly unsaturated fatty acid, such as arachidonic acid, interfere with the activation of SREBP-1c by functioning as a competitive antagonist of the activating LXRα ligand. Arachidonate blocks activation of a synthetic LXR-dependent promoter in transfected human embryonic kidney 293-cells (*36*). In addition, antagonists such as prostaglandin $F_{2\alpha}$, small heterodimer partner interacting leucine zipper protein (SMILE), and ursodeoxycholic acid have also been reported (*37*).

Exogenous Natural Ligands

Compounds derived from plants or fungi modulate LXR activity. These include phytosterols and terpenes that bind LXRs (EC_{50} in the range of 33-136 nM as determined in a coactivator peptide recruitment assay). Other reported natural agonists include acanthoic acid, viperidone, polycarpol, and gorgostone derivative. Among the natural compounds that act as LXR antagonists are guttiferone (IC_{50} value of 3.4 μM), riccardin C, naringenin, genistein, taurine (2-aminoethanesulfonic acid), and dahuang (*38*).

Synthetic Ligands

Strong synthetic agonists such as T0901317 and GW3965 have been developed and used as valuable tools in biomedical research (*39*, *40*). Both agonists have EC_{50} values in

the low nanomolar range for both isoforms of LXR. T0901317 is a non-steroidal synthetic ligand composed of a tertiary sulfonamide and a bistrifluoromethyl carbinol (EC_{50} value is 20 nM). Various studies have identified hydrogen binding between the head group of T-0901317 and key residues in the LXR LBP to be critical for coactivator recruitment and subsequent activation of LXR. GW3965 is another non-steroidal, tertiary benzylamide that selectively activates LXRα (EC_{50} value is 648±178 nM). Both ligands are associated with hypertriglyceridemic effects in mouse model, therefore, preventing the use of these agonists in clinical trials in human subjects (*41*, *42*). Multiple research groups have modified existing ligands to develop novel ligands that are potent agonists, exhibit anti-inflammatory activity without the concomitant hypertriglyceridemic effects. Present research has continued to focus on developing potent ligands that might exhibit enhanced specificity and selectivity for LXRβ over LXRα.

HETERODIMERIZATION OF LXR

LXRα, in addition to forming dimers with RXR, binds peroxisome proliferator-activated receptor α (PPARα) (*43*, *44*). Little research has followed to investigate the quantitative values, namely the dissociation constant values (K_d), for the heterodimer composed of full-length LXRα and PPARα proteins in the presence of LXRα ligands. Our laboratory has previously reported the effect of endogenous PPARα ligands on LXRα-PPARα interaction. We concluded that whereas palmitic acid, oleoyl CoA, and linoleic acid enhance LXRα-PPARα interactions, oleic acid, palmitoyl CoA, and eicosapentaenoic acid inhibit this interaction. LXRα-PPARα heterodimer has the ability to bind both the LXR response element (LXRE) and PPAR response element (PPRE).

However, the affinities with which LXRα-PPARα complex binds its response elements is lower than their corresponding dimers formed with RXRα [*44*]. A new PPARα-LXRα response element has recently been identified that regulates a semi-distinct set of genes or pathways ((Klingler, A. M., 2016. Novel Insight into the Role of LXRα in Metabolic Regulation via DNA Binding as a Heterodimer with PPARα and as a Homodimer (Master's thesis) Ohio Link Document number: wright1472486254)). Ligand binding to either or both protein(s) could affect the secondary structure of the complex, co-factor recruitment, and the ability to bind DNA for gene regulation. Examination of the effects of ligand binding on the formation of heterodimeric complexes will provide insight into the regulatory features of these systems.

The reported crystal structure of LXRα-RXRβ (1UHL) provides important information about the residues that form the dimer core. The LXRα-RXRα, and presumably LXRα-PPARα, interface is formed mainly by the interactions of residues that are components of helices H9 and H10 of LXRα. Significant changes in accessible surface area were observed in residues H383, E387, and H390 located in helix 9 upon LXRα dimerization resulting in the formation of novel salt bridges (*26*). The relative contribution of the individual amino acid residues to receptor dimerization is unknown. The most common approach to determine which residues contribute to binding utilizes site directed mutagenesis. The best candidates for LXRα mutagenesis should be the amino acid residues which strongly interact with the partner receptor. Mutation of putative contact points at the LXRα interface is expected to exhibit one or all of the following defects: (1) failure to form heterodimers, (2) failure to form heterodimers with PPARα, but not RXRα, or vice versa, (3) reduced heterodimerization along with

enhanced LXRα homodimerization, and (4) altered affinity of the mutant LXRα for its ligands, DNA, or coactivators due to allosteric effects.

Visual examination of the interface of the three-dimensional crystal structure of LXRα LBD shows that residues H383, E387, H390, L414, and R415 could provide direct sites of interaction at the protein-protein interface (*26*). Modifications of any one or a combination of these residues may cause subtle repositioning of residues or provide additional stabilization to the interface resulting in selective LXRα dimerization properties. Alternatively, mutations at these sites may not be accommodated in the heterodimer three-dimensional structure due to unfavorable electrostatic or steric interactions both close and distant to the interface. This will result in the inability of the LXRα to form dimers with either RXRα or PPARα. Because the LBD is associated with ligand binding, mutations in the LBD may perturb ligand binding. For example, a mutation in the LXRα LBD (R415A) exhibits a phenotype similar to that of a mutant lacking the AF2 helix and is unable to transactivate an ADH-LXRE x2-luc reporter in response to T-0901317 addition (*45*). Whether mutations at the interface may impact the ligand binding properties of LXRα has yet to be tested.

Alignment of human sequence of the LXRα LBD to corresponding sequences of other species and receptors such as farnesoid X receptor (FXR), VDR, PPAR, and retinoid acid receptor (RAR) shows complete conservation of residues at positions homologous to E379, L414, and R415 in LXRα (Fig. 6). The conservation strongly suggests an important structural and/or functional role of these residues. In addition, LXRα residues H383, E387, and H390 have charged residues at corresponding positions in other nuclear receptors. To identify the residues that are essential for dimerization,

surface area of LXRα that is accessible to the solvent was calculated using Swiss PDB Viewer (SPDBV) software. Fig. 7 illustrates that the LXRα LBD has been colored according to the solvent accessibility of the residues (least accessible or buried residues are colored violet and most exposed residues are colored red). LXRα residues (H383, E387, H390, and R415) within helices 9 and 10 are more exposed (green) compared to residues in their vicinity (blue). The LXRα-RXRβ complex reveals that H383, E387, and H390 of LXRα could stabilize intermolecular contacts by forming salt bridges with E465, A469, and E472 of RXRβ (corresponding to E394, A398, and E401 of RXRα) (*26*). However, the proof of the identity of PPARα residues that participate in protein-protein interactions with LXRα awaits the crystal structure of the LXRα-PPARα complex.

Several studies have demonstrated that modification of amino acid residues at the interface is sufficient to alter the dimerization properties of the nuclear receptors (*22*, *46*, *47*). For example, mutation of mouse RXRα alters its dimer specificity, such that mRXRα Y402A is deficient in dimerization with the Retinoid A receptor (RAR), PPAR, and the vitamin D receptor (VDR), but acquires an enhanced tendency to form homodimers (*22*). Since LXRα can heterodimerize to either RXRα or PPARα, this suggests that modification of LXRα interface may provide a mechanism to determine the heterodimer choice.

Fig.6. Alignment of helices 9 and 10 of the LBDs of hLXRα, hFXR, hVDR, hPPARα, and hRXR (top). Amino acid residues predicted to be critical for dimerization based on the crystal structure of LXRα LBD are colored in red. Alignment of helix 10 of LXRα LBD (bottom) showing complete conservation of amino acid residues among species.

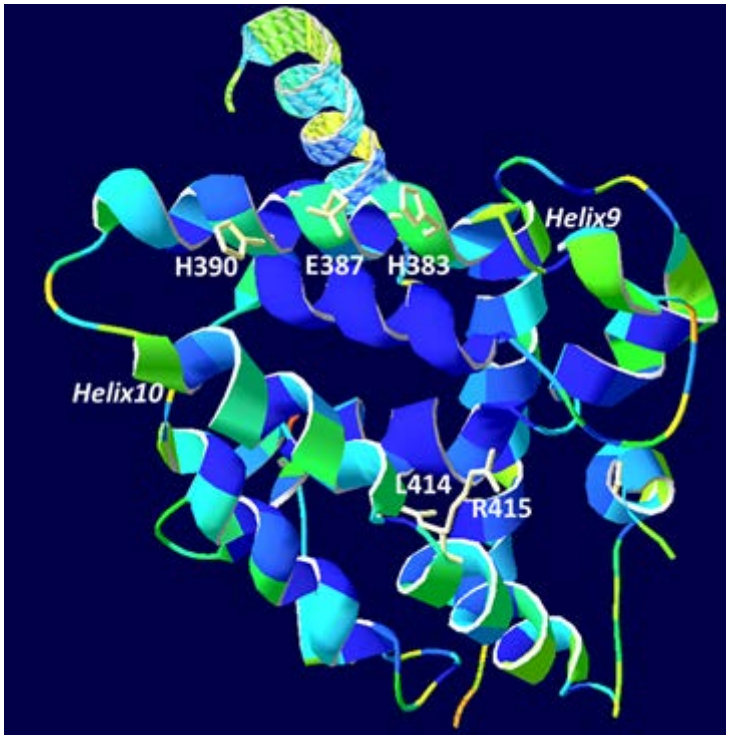

Fig.7. Solvent accessibility of LXRα residues showing surface exposed residues. Multiple potential protein-protein binding sites were identified by computational analysis using the reported crystal structure of LXRα-RXRβ heterodimer. LXRα LBD was extracted from PDB entry 1UHL using SPDBV. Helices are colored based on solvent accessibility: green regions are more exposed compared to regions in blue.

REGULATION OF LXR EXPRESSION AND ACTIVITY

LXR signaling is modulated by both ligand binding and changes in receptor expression. Expression of LXRα in human macrophages, adipocytes, hepatocytes, skin fibroblasts and myotubes is controlled by an autoregulatory mechanism suggesting that LXRα can regulate its own expression. This activity is mediated through the presence of a functional LXRE located in the promoter of the human, but does not occur in mouse, LXRα (*48*). Interestingly, a functional peroxisome proliferator-response element (PPRE) has been identified in the human and rodent LXR gene promoter; it suggests that PPAR could regulate the LXR pathway (*49*). Indeed, agonists of PPAR α and γ stimulate LXRα expression in human and rodent macrophages, adipocytes, and hepatocytes (*50*). Insulin and bacterial lipopolysaccharide have also been demonstrated to modulate the expression of LXRα. Additionally, LXRs can be posttranslationally modified through phosphorylation (Protein kinase A and C), acetylation, and sumoylation. These modifications have been shown to affect LXR's stability, gene specificity, and transactivation properties (*51-54*).

FUNCTION OF LXR

There is abundant evidence that indicates that LXR-RXR heterodimers control various aspects of cholesterol transport, metabolism, and biosynthesis (*15*). LXRs act as cholesterol sensors to prevent cells from accumulating toxic levels of cholesterol through triggering various adaptive mechanisms. For example, oxidized form of low-density lipoproteins (ox-LDL) are recognized and internalized by the scavenger receptor CD36 in the macrophages. Intracellular catabolism of ox-LDL leads to the generation of

endogenous LXR ligands (oxysterol) which upregulate ATP-binding cassette transporter (ABCA1) (Fig. 8) (*13*). The removal of excess cholesterol from macrophage foam cells by high density lipoprotein and its principal apolipoprotein, apoA-1 prevents cells from oxysterol-induced toxicity. In general, activation of LXR results in: (a) stimulation of reverse cholesterol transport- a pathway that removes excess cholesterol from peripheral tissues to liver and conversion of cholesterol to bile for biliary excretion, (b) inhibition of intestinal cholesterol absorption, and (c) inhibition of cholesterol synthesis and uptake by the cells.

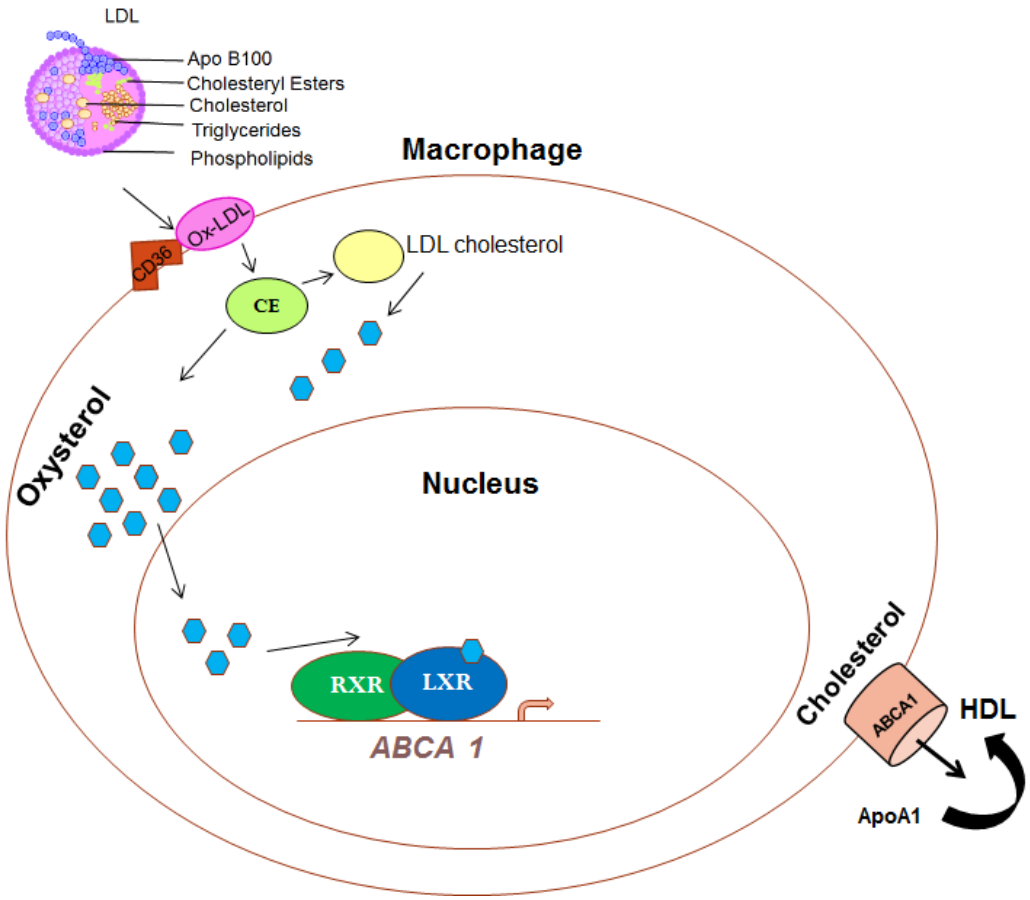
LDL
Apo B100
Cholesteryl Esters
Cholesterol
Triglycerides
Phospholipids
Macrophage
Ox-LDL
CD36
LDL cholesterol
CE
Oxysterol
Nucleus
RXR
LXR
ABCA 1
Cholesterol
ABCA1
HDL
ApoA1

Fig.8. Model showing LXRα mediated cholesterol efflux to HDL via ABCA1 from macrophages. Binding of oxidized-LDL (Ox-LDL) to cell surface receptors such as CD36 leads to internalization and degradation generating ligands for the activation of LXR/RXR heterodimer on target genes such as ABCA1. Upregulation of ABCA1 results in enhanced efflux of cholesterol to apoA1 component of HDL. Image adapted from the reference (13).

LXR and Reverse cholesterol transport: Reverse cholesterol transport (RCT) is a pathway by which excess cholesterol is transported from peripheral tissues to the liver followed by biliary secretion and subsequent disposal via the feces. Free cholesterol can leave the macrophage either through a transporter-independent mechanism or dependent on cholesterol transporters, mainly the ABCA1 and ABCG1. Another key player in cholesterol efflux and macrophage-specific RCT is apoE. Interestingly, LXR agonists induce the transcription of ABCA1 and apoE that raise HDL-C levels and reduce atherosclerosis in animal models (*55-57*). The ability of LXR to promote macrophage reverse cholesterol transport makes it a potential therapeutic target in the prevention of atherosclerotic vascular disease.

LXR and Cholesterol synthesis: LXRs, in addition to regulating cholesterol metabolism, are involved in induction of fatty acid and triglyceride biosynthesis in response to feeding. This mechanism ensures that excess acetyl-CoA, an intermediate product of glucose metabolism, is converted into fats and triglycerides. Activation of LXR stimulates fatty acid synthesis through upregulation of key enzymes implicated in hepatic lipogenesis. The major isoform responsible for hepatic lipogenesis is LXRα. The lipogenic effect is mediated by increased expression of sterol regulatory element-binding protein-1c (SREBP-1c) (*51*). Yoshikawa *et al,* 2001 have identified two LXREs within the SREBP-1c gene promoter, and demonstrated that agonists of LXR and RXR increase its transcriptional activity (*58*). In addition to directly regulating SREBP-1c expression, LXR regulates several other lipogenic enzymes including acetyl-CoA carboxylase (ACC), fatty acid synthase (FAS), and stearoyl-CoA desaturase-1 (SCD-1) (*59*).

LXR and cholesterol uptake: LXR helps maintain cholesterol homeostasis not only through promotion of cholesterol efflux, but also through suppression of low-density lipoprotein (LDL) uptake. The major part of cholesterol in human blood is transported within LDL-C. The LDLR mediates the removal of LDL and remnant lipoproteins from circulation by binding to apolipoprotein B-100 and ApoE. LXR agonists GW3965 and T0901317 markedly inhibit the binding and uptake of LDL by cells. The mechanism for feedback inhibition of cholesterol uptake is independent of and complementary to the sterol regulatory element-binding protein pathway (*60*).

LXR and intestinal cholesterol absorption: LXR activation results in a reduced absorption of intestinal cholesterol by regulating the expression of genes such as ABCG5/ABCG8 and Niemann-Pick C1-like 1 involved in this process. The enhanced expression of ABCG5/ABCG8 transports absorbed cholesterol back to the lumen of the intestine. Therefore, it is unsurprising that administration of LXR agonists decreases intestinal net cholesterol absorption in mice (*60*). This observation suggests that intestine-specific agonists of LXR might prove beneficial in promoting cholesterol efflux in chronic disorders such as atherosclerosis, inflammation, and cancer.

LXR and fecal neutral sterol excretion via intestine: Consistent with its role in controlling key steps in removal of excess cholesterol from the body, LXR activation leads to increased fecal sterol loss in mice models. Administration of LXR agonist T-0901317 to mice enhances removal of blood-derived free cholesterol through transintestinal cholesterol excretion. This effect is independent of ABCA1-mediated elevation of HDL and the presence of ABCA1 in liver and intestine (*60*). Thus, excretion

of excess cholesterol via the intestine represents an alternative route for cholesterol disposal.

Apolipoprotein-mediated cellular lipid efflux and ABCA1: The expression of ABCA1 is tightly regulated by the cellular content of cholesterol, through oxysterol-dependent activation of LXR. An LXR response element has been identified in the human ABCA1 promoter that binds both isoforms of LXR and mediates transcriptional induction of the promoter by LXR ligands. This suggests that the expression of ABCA1 and the process of cellular cholesterol efflux are controlled, at least in part, by the LXR signaling pathway. *In vivo* data has further underscored the potential usefulness of synthetic LXR agonists in the prevention or treatment of atherosclerosis via induction of ABCA1 in macrophages and fibroblasts (*61*).

HDL-cholesterol and ApoA1: Since cholesterol is a water-insoluble molecule, it must be packaged and transported within the plasma in the form of lipid/protein (lipoprotein) complexes. High-density lipoprotein (HDL) particles transport cholesterol from tissues back to the liver for excretion. HDL exists in two forms, one containing apolipoprotein A-1 (ApoA-I) and apolipoprotein A-II (Apo-II), and one containing ApoA-I alone. The cardioprotective effect of HDL is largely due to ApoA-1 (*13, 62*). Experimental manipulations to increase production of ApoA-1 has been associated with reduced atherogenicity. ApoA-1 promoter contains a functional PPRE (*63*) that makes fibrates and PPAR agonists interesting options for enhancing HDL levels. However, the beneficial effects of LXR and/or PPAR activation are accompanied by enhanced hepatic lipogenesis and high triglyceride levels. This observation has hampered the use of LXR and PPAR agonists in the treatment of cardiovascular, metabolic, and/or inflammatory

diseases. There is a need for novel strategies to increase endogenous ApoA-1 that would be a major step in treating lipid-related cardiovascular disease (*64*). Whether manipulation of LXRα-PPARα heterodimeric pair presents an alternative route for enhancement of ApoA1 has not been investigated yet.

ANIMAL MODELS

Insights into LXR function in metabolism have been provided by the generation of LXR mutant mice. These studies have allowed better definition of the role of LXRs in lipid synthesis, clearance, and catabolism. LXRα, but not LXRβ, knockout mice accumulate large amounts of cholesterol esters in the liver after being fed a high-fat cholesterol diet due to failure of inducing expression of CYP7A1 gene (*19*). In contrast to this observation in rodents, LXRα agonist treatment suppresses the expression of CYP7A1 in primary human hepatocytes (*60).* These results highlight the mechanisms different species employ to regulate cholesterol homeostasis. To date, the use of mouse models of atherosclerosis have shown an ability of LXR to decrease atherosclerosis via ABCA1 expression. Overexpression of the human ABCA1 transgene in normal mice led to an increase in HDL and decrease in atherosclerosis suggesting that enhancement of HDL may be a useful route to pursue in the development of anti-atherosclerotic therapies. However, the development of LXR agonists for the treatment of metabolic syndrome has been difficult due to undesirable properties in animal models (*65*). Nevertheless, majority of the studies provide evidence that LXRs are key players in maintaining metabolic homeostasis in health and disease by regulating inflammation and lipid/carbohydrate metabolism.

LDL and HDL: “Bad” and “Good” Cholesterol

Complex particles called lipoproteins carry cholesterol in the plasma. These molecules have a central core containing cholesterol esters and triglycerides that is surrounded by free cholesterol, phospholipids, and apolipoproteins. Two important types of lipoproteins are low-density lipoprotein (LDL) and high-density lipoprotein (HDL). The role of LDLs, particularly the role of oxidized LDL, in damaging arterial walls leading to the development of atherosclerotic lesions is well documented. On the other hand, epidemiological studies have demonstrated an inverse relationship between HDL cholesterol levels and cardiovascular disease risk. Thus, lowering of cholesterol-rich LDL lipoproteins or upregulation of HDL through apoA-I may be crucial in patients with coronary artery disease and individuals prone to atherosclerosis (*64*).

DEVELOPMENT OF HYPOTHESIS

First, there is evidence of fatty acids modulating LXR activity suggesting that interaction of fatty acids with LXRα may play a role in LXRα function. These data synthesized the hypothesis that there may be direct interaction between LXRα and fatty acids (*34-36*). Second, activation of LXRα-RXRα and PPARα-RXRα complexes via agonist treatment could induce lipid accumulation via stimulation of SREBP-1c and its response genes encoding key lipogenic enzymes (*39, 51*). Despite continuous efforts of the pharmaceutical industry to design compounds that can circumvent triglyceridemia and steatosis associated with the activation of these complexes, no specific drug has provided therapeutic benefits. Activation of LXRα-PPARα provides an alternate route of LXRα activation by which these side effects may be minimized. In the absence of quantitative information about the binding of full length LXRα to PPARα, the dissociation constant values for binding had to be determined both in the absence and in presence of ligands. Previous experiments have indicated that the dimerization interface and the ligand-binding pocket of the NRs are energetically linked (*45*) suggesting that ligand binding modulates the side-chain dynamics of key residues at the interface.

The objectives of this study are to elucidate (1) whether fatty acids constitute high affinity ligands of LXRα, (2) quantitatively characterize the LXRα-PPARα interaction, and (3) identify positions within the LBD of LXRα that are required for its transactivation properties. The ability to generate engineered receptors that are capable of selectively forming distinct dimeric complexes may prove useful in enhancing our understanding of the distinct roles of each heterodimeric pair.

I tested the overall **hypothesis that ligand binding determines heterodimer choice through rearrangement of critical residues in helices 9 and 10.** The specific aims of this thesis are: (Specific aim 1) An investigation of the effect of chain length and degree of unsaturation on fatty acid binding to LXRα; (Specific aim 2) The effect of LXRα ligands on the heterodimerization of wild-type LXRα with its novel partner receptor PPARα was studied; and (Specific aim 3) The effects of mutating LXRα interface residues H383, E387, H390, L414, and R415 on heterodimerization, ligand binding, and transactivation properties of LXRα were determined. A previously reported LXRα mutant R415A (lacks LXRα-RXRα transactivation activity in the context of ADH promoter when treated with an LXRα agonist T-0901317) (*45*) and novel LXRα mutants (H383E, E387Q, H390Q, and L414R) were used to investigate whether mutations of LXRα selectively impact dimerization, ligand binding, and/or transactivation properties.

CHAPTER I

FATTY ACID BINDING PROFILE OF THE LIVER X RECEPTOR ALPHA

1. Abstract

Liver X receptor (LXR) alpha is a nuclear receptor that responds to oxysterols and cholesterol overload by stimulating cholesterol efflux, transport, conversion to bile acids, and excretion. Synthetic (T-0901317, GW3695) and endogenous (oxysterols) ligands bind to LXRα which then regulates LXRα action. LXRα activity is also modulated by fatty acids (FA) but the ligand binding specificity of FA and acyl-CoA derivatives for LXRα remains unknown. I investigated whether LXRα binds FA or FA acyl-CoA with affinities that mimic *in vivo* concentrations, examined the effect of FA chain length and the degree of unsaturation on binding, and investigated if FA regulate LXRα activation. Saturated medium chain FA (MCFA) exhibited binding affinities in low nanomolar concentration range, while long-chain fatty acyl CoA did not bind or bound weakly to LXRα. Circular dichroism and computational docking confirmed that MCFA bound to the LXRα ligand binding pocket similar to the known agonist (T0901317) but without inducing a major conformational change. Transactivation assays showed MCFA activated LXRα, whereas LCFA caused no effect. These results suggest that LXRα functions as a receptor for saturated FA or acyl-CoA of C_{10} and C_{12} in length.

2. Introduction

Nuclear hormone receptors are ligand activated transcription factors that mediate the transcriptional effects of steroid, thyroid, and retinoid hormones (*14, 66-68*). Among the dietary nutrients that act as ligands and serve as signaling molecules to regulate cellular metabolism are oxysterols and fatty acids (*15, 69, 70*). These compounds directly bind to the nuclear receptor ligand-binding domain (LBD) and induce conformational changes to trigger the exchange of corepressors with the coactivators leading to the repression or activation of the target genes (*11, 71*). Liver X receptors (LXR) are ligand activated nuclear receptors belonging to the steroid hormone receptor superfamily that specifically bind to and are activated by oxysterols. Both isoforms of LXR form heterodimers with the retinoid X receptor (RXR) which then bind to specific DNA elements to regulate gene transcription. The LXR-RXR complex exhibits basal levels of transcription in the absence of a ligand. Upon ligand activation, LXRs act as transcription factors to regulate the expression of genes involved in cholesterol transport, lipid metabolism, and carbohydrate metabolism. There are two LXR isoforms: the alpha isoform is found in metabolically active tissue such as liver, kidney whereas the beta isoform is ubiquitously expressed (*72*). Although both isoforms are involved in regulating cholesterol homeostasis, the alpha isoform is the predominant isoform that functions as a master hepatic lipogenic transcription factor (*73*).

In LXRα knockout mice, the CYP7a1 gene (which is involved in cholesterol metabolism) is down regulated, resulting in accumulation of cholesterol in the liver. Genes involved in hepatic fatty acid biosynthesis, such as sterol regulatory element binding protein (SREBP-1), stearoyl CoA desaturase (SCD) and fatty acid synthase

(FAS) are also down regulated in LXRα deficient mice, and LXRβ was unable to compensate for this loss of LXRα. In LXRβ- deficient mice, expression of the above genes remains unaffected (*74, 75*). Furthermore, patients with non-alcoholic fatty liver disease (NAFLD) and hepatitis C virus induced steatosis have elevated levels of LXRα and its target gene involved in lipogenesis (*76-78*). Not surprisingly, LXRs are attractive drug targets for the treatment of diabetes and metabolic disorders (*79-81*).

Although oxysterols are classical endogenous ligands of LXRs, fatty acids have been reported to inhibit oxysterol binding to LXR. The inhibition depends on the degree of unsaturation of the fatty acids; polyunsaturated fatty acids are more potent inhibitors of oxysterol binding compared to monounsaturated FA suggesting that fatty acids or fatty acyl-CoAs may directly bind LXRα (*35, 82-84*). Furthermore, LXRα can form a heterodimeric pair with PPARα (*43*), and each of the two proteins individually binds fatty acids (*36, 85*). This creates complexity in understanding and characterization of individual signaling pathways. To differentiate the direct and indirect effects of PPAR ligands (FA) on LXRα, it is important to quantify the binding affinities of fatty acid binding to LXRα. The main goal of this study is to test the hypothesis that LXRα serves as a fatty acid receptor through investigating fatty acid binding to LXRα.

3. **Materials and Methods**

Purification of Recombinant hLXRα: Plasmids for full-length hLXRα recombinant protein expression were transformed into Rosetta 2 competent cells. Protein was purified through affinity chromatography with the GST tag and on-column digestion as described (*44*). Protein concentrations were estimated by the Bradford assay (Bio-Rad, Hercules, CA). Protein purity was determined by sodium dodecyl sulfate-polyacrylamide gel electrophoresis (SDS-PAGE) followed by Coomassie Blue staining and Western blotting (*44*).

Reagents: Fluorescent fatty acids (BODIPY-C16 and BODIPY-C12) were purchased from Molecular Probes, Inc. (Eugene, OR). BODIPY C12-CoA and BODIPY C16-CoA were synthesized and purified by HPLC as previously described, and found to be >99% pure and unhydrolyzed (*86*).

Fluorescent Ligand Binding Assays: Fluorescent ligand (BODIPY C16, BODIPY C12, BODIPY C12-CoA or BODIPY C16-CoA) binding measurements were performed using 0.1 μM LXRα with increasing concentrations of fluorescent ligand in phosphate buffered saline (PBS), pH7.4. Fluorescence emission spectra (excitation, 465 nm; emission, 490-550 nm) were obtained at 24°C with a PC1 photon counting spectrofluorometer (ISS Inc., Champaign, IL), and corrected for background (protein only and fluorescent ligand only). Maximal intensities were used to calculate the apparent dissociation constant (K_d) (*86, 87*). All ligand concentrations were below the critical micelle concentrations and were delivered using ethanol as a solvent.

Displacement of Bound Fluorescent BODIPY C16-Co by Non-fluorescent Ligands: To examine further whether fatty acids could bind LXRα directly and displace a

fluorescent ligand, putative ligands were assessed for displacement using recombinant LXRα and BODIPY labeled C16-CoA in PBS, pH7.4. 0.1 μM LXRα was mixed with 0.1 μM of BODIPY C16-CoA and the maximal fluorescence intensity was measured. The effect of increasing concentrations of fatty acids or fatty acyl CoA was measured by quenching fluorescence of BODIPY C16-CoA at 24^0C. All spectra were corrected for background as described above for BODIPY. Changes in fluorescence intensity were used to calculate the inhibition constant (K_i) values (*86, 87*).

Quenching of LXRα Aromatic Amino Acid Residues by Non-fluorescent Ligands: The direct binding of LXRα to non-fluorescent ligands was determined by quenching of intrinsic LXRα aromatic amino acid fluorescence. LXRα (0.1 μM) was titrated with increasing concentrations of ligand in PBS, pH7.4. Emission spectra from 300-400 nm were obtained with a PC1 photon counting spectrofluorometer (ISS Inc., Champaign, IL) at 24°C using an excitation of 280 nm. Data were corrected for background and inner filter effects, and maximal intensities were used to calculate the apparent dissociation constant (K_d) (*86, 87*).

Secondary structure determination: Effect of ligand binding on LXRα circular dichroism: Circular dichroic spectra of hLXRα (0.6 μM in 600 μM HEPES pH 8.0, 24 μM dithiothreitol, 6 μM EDTA, 6mM KCl and 0.6 % glycerol) were monitored in the presence and absence of fatty acids and fatty acyl-CoA (0.6 μM) with a Jasco J-815 spectropolarimeter. Ligand stock solutions were prepared in ethanol or KH_2PO_4 pH 8.0 as vehicle. Spectra were scanned from 260 to 187 nm using a bandwidth of 2.0 nm and sensitivity of 10 millidegrees. The scan rate of 50 nm/min using a time constant of 1 s was used. Ten scans were averaged and percent

compositions of α-helices, β-strands, turns and unordered structures were estimated using the CONTIN/LL program of the CDpro software package (*44*, *86-89*).

Mammalian Expression Plasmids: hPPARα and hLXRα from 6xHis-GST-hPPARα and 6xHis-GST-hLXRα were transferred into the multiple cloning site of pSG5 (Stratagene; *Bam*H1-end-filled *Bgl*II) to produce pSG5-hPPARα and pSG5-hLXRα respectively as described (*44*). The human sterol regulatory element binding protein 1c (hSREBP-1c) minimal promoter (-520 to -310) containing the LXRE (*90*) was cloned into the pGEM-T easy vector (Promega) and subsequently transferred into *Kpn*I-*Xho*I sites of pGL4.17 (Promega) to produce hSREBP-1c-pGL4.17. All plasmid constructs were confirmed by DNA sequencing.

Cell culture and Transactivation assay: COS-7 cells (ATCC, Manassas, VA) were grown in DMEM supplemented with 10 % fetal bovine serum (Invitrogen, Grand Island, NY) at 37°C with 5% CO_2 in a humidified chamber. Cells were seeded onto 24-well culture plates and transfected with 0.4 μg of each full-length mammalian expression vector (pSG5-hPPARα or pSG5-hLXRα) or empty vector (pSG5), 0.4 μg of the LXRE LUC reporter construct (hSREBP1c-pGL4.17), and 0.04 μg of the internal transfection control plasmid pRL-CMV (Promega Corp., Madison, WI) with Lipofectamine™ 2000 (Invitrogen, Grand Island, NY). Following transfection incubation, the serum-free DMEM was added for 2 h, ligands (10 μM) were added, and the cells were grown for an additional 20 h. Fatty acids were added as a complex with bovine serum albumin (BSA) as described (*44, 86, 89*). Firefly luciferase activity, normalized to *Renilla* luciferase (for transfection efficiency), was determined with the dual luciferase reporter assays system (Promega, Madison, WI) and measured with a

SAFIRE^2 microtiter plate reader (Tecan Systems, Inc. San Jose, CA). All samples were normalized against the sample with no ligand.

Molecular docking: In silico docking of ligands was performed using the LBD from LXRα extracted from the crystal structure of LXRα-RXRβ complex (PDB entry 1UHL). AutoDock Vina 1.1.2 and FlexiDock module of SYBYL-X 2.0 (Tripos, St. Louis, MO) were used to dock ligands of interest to the LXRα LBD and to estimate the binding free energies of receptor-ligand binding as described (89).

Statistical Analysis: Data were analyzed by SigmaPlot™ (Systat Software, San Jose, CA) using the ligand binding macro (one site saturation). Binding curves were generated by plotting changes in fluorescence as a function of total ligand concentration. Free ligand concentrations for each ligand tested were determined by subtracting the protein bound fraction from the total ligand concentration using the following equation:

$L_{free} = L_{total} - L_{bound}$, where $L_{bound} = (\Delta_{FL}/\Delta_{FL\ max})*[\text{Protein}_{\ active}]$.

The dissociation constant values (K_d) were generated using the free ligand concentrations. K_i to K_d conversions were performed by using the following equation:

$EC_{50\ ligand}$/ [BODIPY C16-CoA] = K_i Ligand/K_d [BODIPY C16-CoA] (*85-87*).

One-way ANOVA was used to evaluate overall significance. All results were expressed as means ± the standard error. The confidence limit of $p < 0.05$ was considered statistically significant (*44, 86, 89*).

4. Results

Protein Expression and Purification: Full-length recombinant hLXRα protein was purified as described previously (*44*). The protein with a molecular mass of 51768 Da migrated at approximately 50 kDa size on SDS-PAGE and it was estimated to be at least 85% pure (Fig. 9). Western blots using antibodies for LXRα showed that the 50 kDa band was full-length, untagged LXRα.

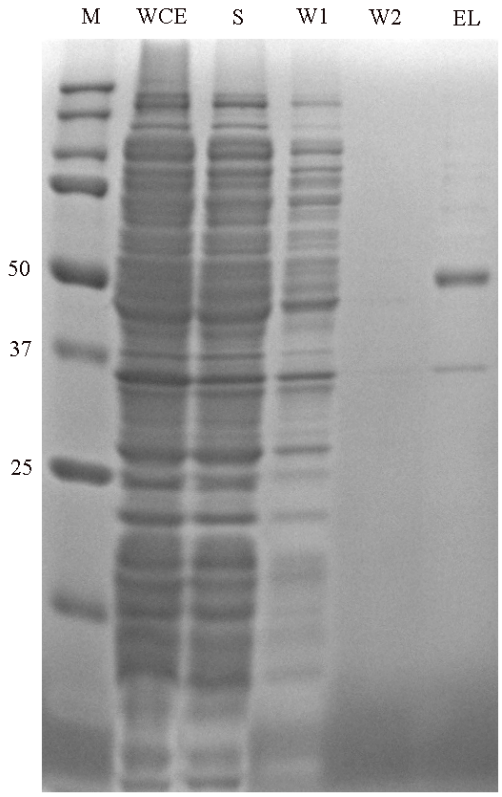

Fig.9. SDS-PAGE and Coomassie blue stained gel showing purification steps of full length hLXRα protein using affinity chromatography. The prominent band corresponding to 50 kDa represents untagged full-length proteins. Lane 1 (Marker), Lane 2 (WCE= whole cell extract), Lane 3 (S=Clarified supernatant), Lanes 4, 5 (W1 and W2= Washes with lysis and ATP buffers respectively), and Lane 6 (EL= Elute fraction after a 4 hour treatment with PreScission Protease).

Binding of fluorescent fatty acid and fatty acyl-CoA to LXRα: Since the FA and FA acyl CoA are not fluorescent, BODIPY derivative was conjugated to the ligands for use in the protein-ligand binding studies. Low concentrations of BODIPY C16:0-CoA (25nM) were used for binding experiments due to its limited solubility. BODIPY fatty acid fluoresce only when bound to the protein. Titration of LXRα with BODIPY C12-CoA or BODIPY C16-CoA resulted in increased fluorescence at 515 nm (Fig. 10A, 10C) which saturated at 15 nM (Fig. 10B) and 32 nM (Fig. 10D) respectively. Sharp binding profiles implied the approach of stoichiometric binding conditions. In these instances, straight line extrapolations from the low ligand concentration portion of the binding and the high ligand concentration portion of the curve intersect at a point that has the concentration axis value approximately equal to the concentration ligand binding sites (91). Thus, it was determined that the percentage of active protein present in the sample is much lower than 100 nM. Multiple titrations of LXRα with various high affinity ligands suggested that the percentage of active protein present in the preparation was approximately 12%.

The apparent binding constants (K_d) using free ligand concentrations were estimated to be 4 ± 0.5 nM for BODIPY C12 CoA and 21 ± 5 nM for BODIPY C16 CoA suggesting that BODIPY C12:0-CoA and BODIPY C16:0-CoA can bind LXRα as high affinity ligands. Similar studies using fatty acids showed little or no changes in the fluorescence intensity, suggesting that these molecules bound relatively weaker compared to their CoA derivatives (data not shown). The binding of C12:0-CoA, and not C12:0 FA, was further confirmed through using aromatic residues (Tyr/Trp) in LXRα as intrinsic donor and BODIPY labeled ligands as the corresponding acceptor

FRET assay. FRET was observed between LXRα protein and BODIPY C12:0-CoA, but not C12:0 FA (Fig. S1). Taken together, our results show that BODIPY C12:0-CoA and BODIPY C16:0-CoA can bind as high affinity ligands to LXRα.

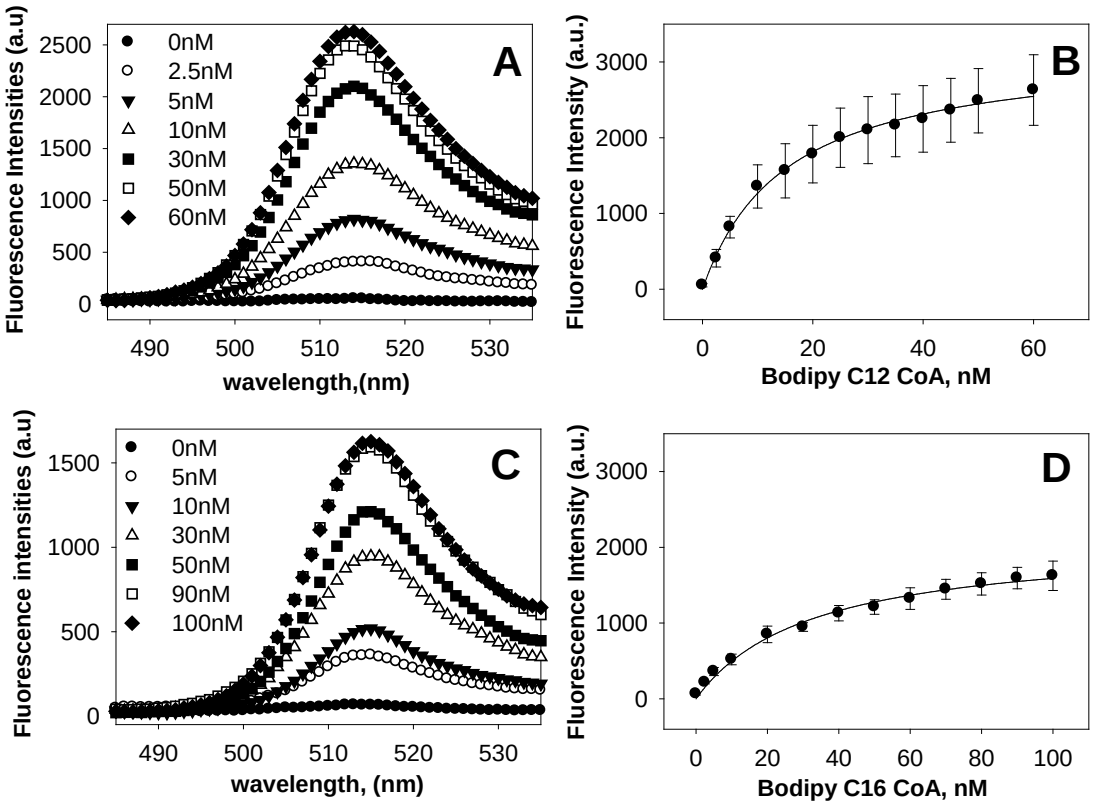
A
Fluorescence Intensities (a.u)
wavelength,(nm)
0nM
2.5nM
5nM
10nM
30nM
50nM
60nM
B
Fluorescence Intensity (a.u.)
Bodipy C12 CoA, nM
C
Fluorescence intensities (a.u)
wavelength, (nm)
0nM
5nM
10nM
30nM
50nM
90nM
100nM
D
Fluorescence Intensity (a.u.)
Bodipy C16 CoA, nM

Fig. 10: LXRα binds fluorescently labeled saturated fatty acyl-CoA. **(A)** Fluorescence emission spectra of 0.1 μM LXRα titrated with 0 (filled circles), 2.5 (open circles), 5 (filled triangles), 10 (open triangles), 30 (filled squares), 50 (open squares), and 60 nM (filled diamonds) of BODIPY C12-CoA upon excitation at 465 nm demonstrating that the enhanced fluorescence intensity of BODIPY C12:0-CoA is a result of direct binding with LXRα. **(B)** Plot of LXRα maximal fluorescence emission as a function of total BODIPY C12:0-CoA. (**C**) Corrected fluorescence emission spectra of 0.1 μM LXRα titrated with 0 (filled circles), 5 (open circles), 10 (filled triangles), 30 (open triangles), 50 (filled squares), 90 (open squares), and 100 nM (filled diamonds) of BODIPY C16-CoA upon excitation at 465 nm demonstrating that the enhanced fluorescence intensity as a result of binding to LXRα. (**D**) Plot of LXR maximal fluorescence emission as a function of total BODIPY C16-CoA.

Binding of endogenous FA and FA-CoA to LXRα – Displacement of bound BODIPY C16-CoA: To determine the ligand specificity of LXRα for fatty acids, FA and FA-CoA of different chain lengths and degree of unsaturation were examined for their ability to displace BODIPY C16:0-CoA from the LXRα ligand binding pocket. The BODIPY C16:0-CoA-LXRα complex was titrated with increasing concentrations of non-fluorescent FA or FA-acyl CoA until the effect plateaued. The decrease in fluorescent intensity was used to calculate the efficiency (K_i) of the non-fluorescent ligand. By comparing the percent displacement of a variety of fatty acids or fatty acyl-CoA for a given concentration range, the relative affinities for binding of these lipids were estimated. Whereas decanoic acid, octanoyl-CoA, and lauroyl-CoA caused a 20-50 % decrease in the BODIPY fluorescence (Fig. 11 B, D, F), other ligands exhibited a smaller effect (Fig. 11A, C, E, G, H). Displacement of BODIPY C16:0-CoA by its non-fluorescent analog C16:0-CoA validates earlier concerns that ligand modifications to render them fluorescent alter the ligand binding properties. This was confirmed through direct binding of BODIPY C16:0 CoA and C16:0 CoA to LXRα that exhibited a slight (two-fold) decrease in the binding affinity of the fluorescent ligand (Fig. 10 D, 12 H). Of all fatty acids and fatty acyl-CoA tested, decanoic acid and octanoyl CoA showed the highest degree of displacement (Fig. 11B, D). Long chain fatty acids were not able to displace BODIPY C16:0-CoA at concentrations as high as 1600 nM, suggesting that these ligands might either bind poorly or not at all to LXRα (Fig. S2 B, C). By comparison, LXR agonists T-0901317 and 22 (R) Hydroxycholesterol (positive controls) displaced the LXRα bound Bodipy C16 CoA by 30% and 50% respectively (Fig. 11I, Fig. S2A). These results taken together suggest that LXRα preferentially binds

medium chain fatty acyl CoA and these ligands compete to some extent for binding to the same site on LXRα as BODIPY fatty acyl CoA. K_i values for the ligands suggest that the binding affinities of the studied ligands are 22 (R) Hydroxycholesterol and T-0901317> octanoyl-CoA> lauroyl-CoA>palmitoyl-CoA>lauric acid and decanoyl-CoA (Supp.Table 1).

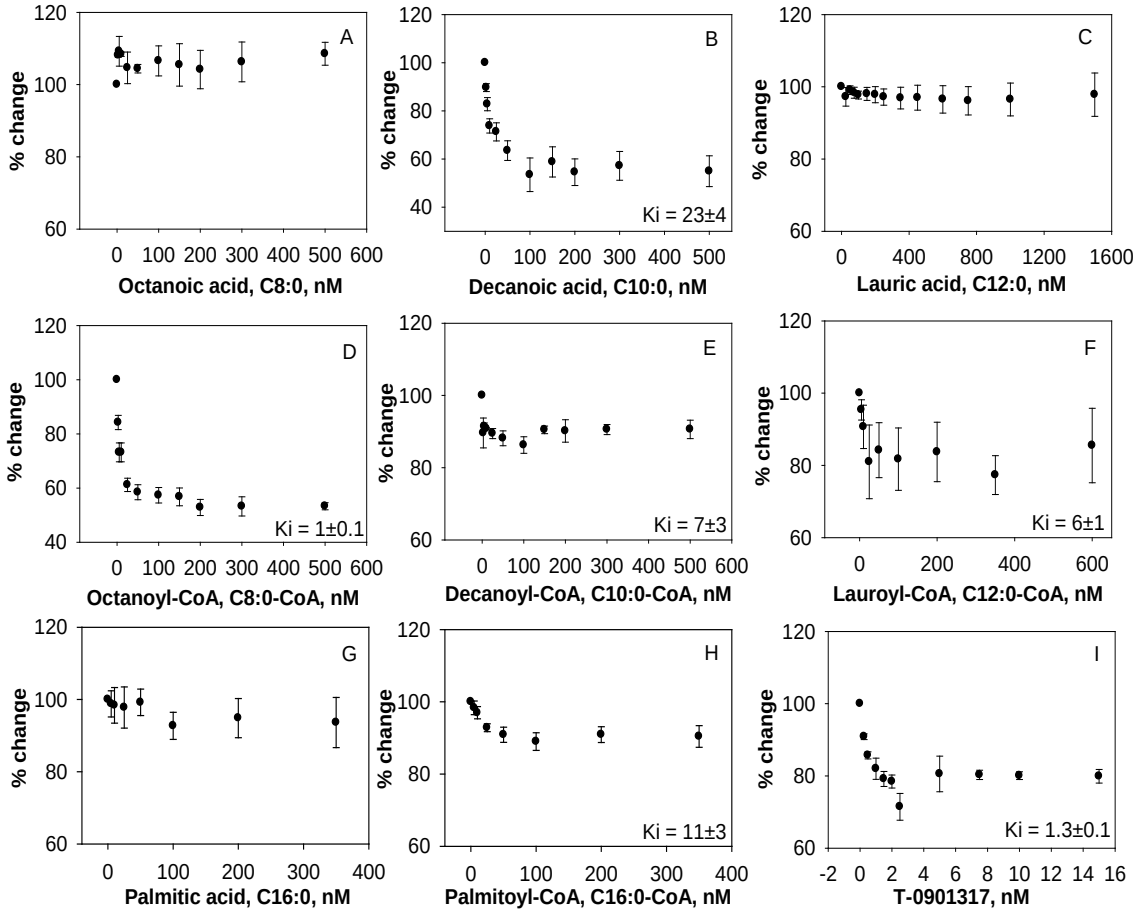
A
% change
Octanoic acid, C8:0, nM
B
Ki = 23±4
Decanoic acid, C10:0, nM
C
Lauric acid, C12:0, nM
D
Ki = 1±0.1
Octanoyl-CoA, C8:0-CoA, nM
E
Ki = 7±3
Decanoyl-CoA, C10:0-CoA, nM
F
Ki = 6±1
Lauroyl-CoA, C12:0-CoA, nM
G
Palmitic acid, C16:0, nM
H
Ki = 11±3
Palmitoyl-CoA, C16:0-CoA, nM
I
Ki = 1.3±0.1
T-0901317, nM

Fig. 11: Displacement assay of BODIPY C16:0-CoA bound LXR. BODIPY C16:0-CoA bound to LXRα was displaced with naturally occurring fatty acids or fatty acyl-CoA. The fall in fluorescence due to displacement of BODIPY C16-CoA from LXRα is expressed as percent changes when titrated with the following ligands: (**A)** octanoic acid, (**B)** decanoic acid, (**C**) lauric acid, (**D**) octanoyl-CoA, (**E**) decanoyl-CoA, (**F)** lauroyl-CoA, (**G**) palmitic acid, (**H**) palmitoyl-CoA, and (**I**) T-0901317. Data are presented as percent change in fluorescence intensity of BODIPY C16-CoA at 515nm plotted as a function of ligand concentrations. All values are the average for at least three independent determinations. Error bars represent standard errors (S.E.)

Binding of endogenous FA and FA-CoA to LXRα – Quenching of intrinsic aromatic amino acid fluorescence: To verify that fatty acids bind to LXRα, we tested these ligands using an intrinsic protein fluorescence using excitation at 280 nm and emission at 342 nm. Purified recombinant LXRα (100 nM) was incubated with medium chain saturated fatty acids, monounsaturated long chain fatty acids, polyunsaturated fatty acids, and the corresponding fatty acyl CoA derivatives. Titration with octanoic acid (Fig. 12A) did not result in decreased LXRα fluorescence. However, addition of decanoic acid and lauric acid resulted in decreased fluorescence, with the maximum change occurring at very low nanomolar concentrations (Fig. 12B, C). Interestingly, estimation of active protein (12%) obtained through the non-fluorescent ligand binding curves was consistent with the estimation obtained through BODIPY labeled fatty acyl CoA binding to LXRα.

The apparent K_d values of the remaining ligands binding to LXRα were measured and are listed in Table 1. Titration of LXRα with monounsaturated and polyunsaturated FA yielded no significant quenching of the intrinsic fluorescence suggesting either little or no binding (Fig. S3). Binding with T-0901317 and 25-hydroxycholesterol (positive controls) yielded binding curves that exhibited saturation with the maximal changes in the intensities at 10 nM and 100 nM respectively (Fig. 12I, Fig. S3L). The apparent K_d values of unlabeled C12:0-CoA obtained from the intrinsic quenching was consistent with the value obtained with BODIPY labeled ligand. However, the K_d values of C16:0-CoA differ between the two assays (Table 1). Since quenching of intrinsic protein fluorescence is a more direct method for the determination of binding affinity, it is a more accurate measure of ligand binding. Despite differences between the fluorescent

methods to measure the apparent K_d values of the ligands, our findings suggest that fatty acids bind LXRα in the nanomolar concentration range. The observed decrease in the intrinsic fluorescence may be a result of direct interaction of LXRα aromatic amino acids with the ligands tested or ligand induced conformational changes bringing the aromatic amino acids in close proximity to the ligand.

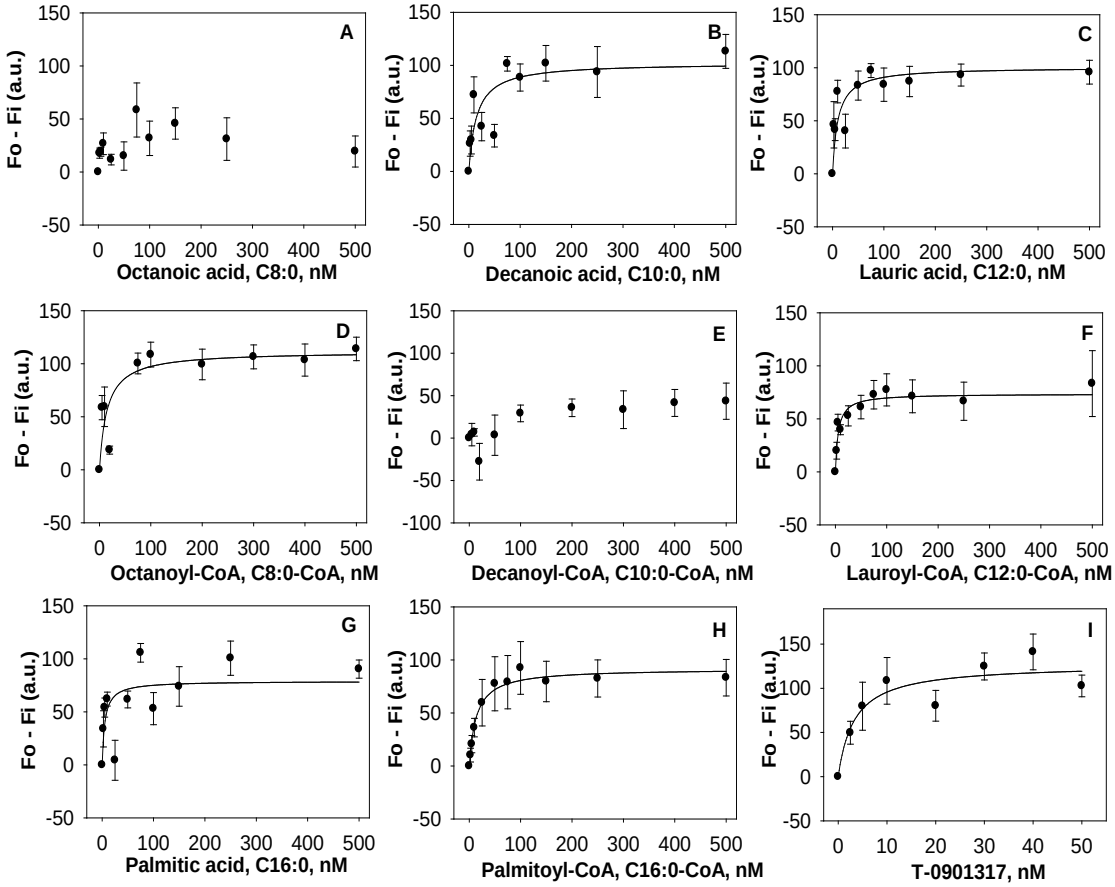
A
Fo - Fi (a.u.)
Octanoic acid, C8:0, nM
B
Decanoic acid, C10:0, nM
C
Lauric acid, C12:0, nM
D
Octanoyl-CoA, C8:0-CoA, nM
E
Decanoyl-CoA, C10:0-CoA, nM
F
Lauroyl-CoA, C12:0-CoA, nM
G
Palmitic acid, C16:0, nM
H
Palmitoyl-CoA, C16:0-CoA, nM
I
T-0901317, nM

Fig. 12: Interaction of naturally-occurring fatty acids and fatty acyl-CoA with LXRα. Direct binding assay based on quenching of 0.1 μM LXRα aromatic amino acid fluorescence emission when titrated with the following ligands: (**A**) Octanoic acid (**B**) Decanoic acid, (**C**) Lauric acid, (**D**) octanoyl-CoA, (**E**) decanoyl-CoA (**F**) lauroyl-CoA, (**G**) palmitic acid, (**H**) palmitoyl-CoA, and (**I**) T-0901317. Data are presented as the change in fluorescence intensity (F_0- F_i) plotted as a function of total ligand concentration. All values represent mean ± S.E., $n \geq 3$.

Table 1. Affinity of hLXRα for non-fluorescent ligands determined by quenching of hLXRα aromatic amino acid fluorescence (K_d) and ligand efficiencies determined by displacement of hLXRα-bound BODIPY C16-CoA (K_i).

Ligand	Chain length: double bonds (position)	K_d protein fluorescence	K_d displacement assay
Octanoic acid	C8:0	N.D.	N.D
Octanoyl-CoA	C8:0	6±1	5±1
Decanoic acid	C10:0	17±8	21±6
Decanoyl-CoA	C10:0	N.D.	N.D.
Lauric acid	C12:0	3±1	N.D.
Lauroyl-CoA	C12:0	14±3	12±2
Palmitic acid	C16:0	N.D.	N.D.
Palmitoyl-CoA	C16:0	6±3	5±2
T-0901317		3±1	N.D.

Values represent the mean ± S.E. ($n \geq 3$). ND, not determined.

Effect of endogenous fatty acids and fatty acyl-CoAs on hLXRα secondary structure: Ligand-induced nuclear receptors exhibit the ability of ligand to induce conformational changes in the secondary structure of the proteins. Changes in LXRα intrinsic fluorescence as a result of ligand binding suggested that these changes may correlate with secondary structure changes of the protein. Circular dichroism (CD) was used to quantitatively measure changes in the LXRα CD spectrum due to fatty acid and fatty acyl CoA binding. Fig. 13 shows the far UV circular dichroic spectrum of LXRα in the absence or presence of ligands tested. The LXRα spectrum exhibited a large positive peak at 192 nm and two negative peaks at 207 and 222 nm. Quantitative analysis using the CDPro software suggested the presence of 26% α-helical, 22 % β-structure, 20 % turns, and 32 % unordered structures in unliganded-LXRα (Table 2). In relation to the ligand-free state, addition of fatty acids and fatty acyl-CoA caused changes in molar ellipticity at 192 nm, 207 nm, and 222 nm (Fig. 13A-H). The calculated structure (Table 2) showed that C16:0-CoA produced an increase in content and size of the α–helix region. No statistically significant changes were observed with other fatty acids and fatty acyl CoA although small changes in the CD spectra were evident with C8:0-CoA, C10:0, C12:0-CoA, and C16:0 (Fig. 13D, B, E, F, G). Changes observed with these ligands were clearly different from those produced by the solvent. Significant changes in β-sheet content were observed with C8:0-CoA and C10:0 in agreement with the fact that both ligands resulted in changes in intrinsic fluorescence of LXRα. CD spectral shifts observed with C12:0 and C16:0 were limited to turns and unordered structures (Table 2). T-0901317, a higher affinity LXR ligand, caused a smaller shift in the CD spectrum compared to 25-HC (Fig. 13I). Significant binding of palmitoleic acid and

eicosapentaenoic acid to LXRα was not observed although perturbations were observed with these ligands. No significant differences were observed with the polyunsaturated fatty acids tested (Fig. S4, Supp. Table 2).Taken together, these results suggest that fatty acids and fatty acyl CoA binding to LXRα causes reorganization of the protein structure with subtle differences observed between various ligands tested.

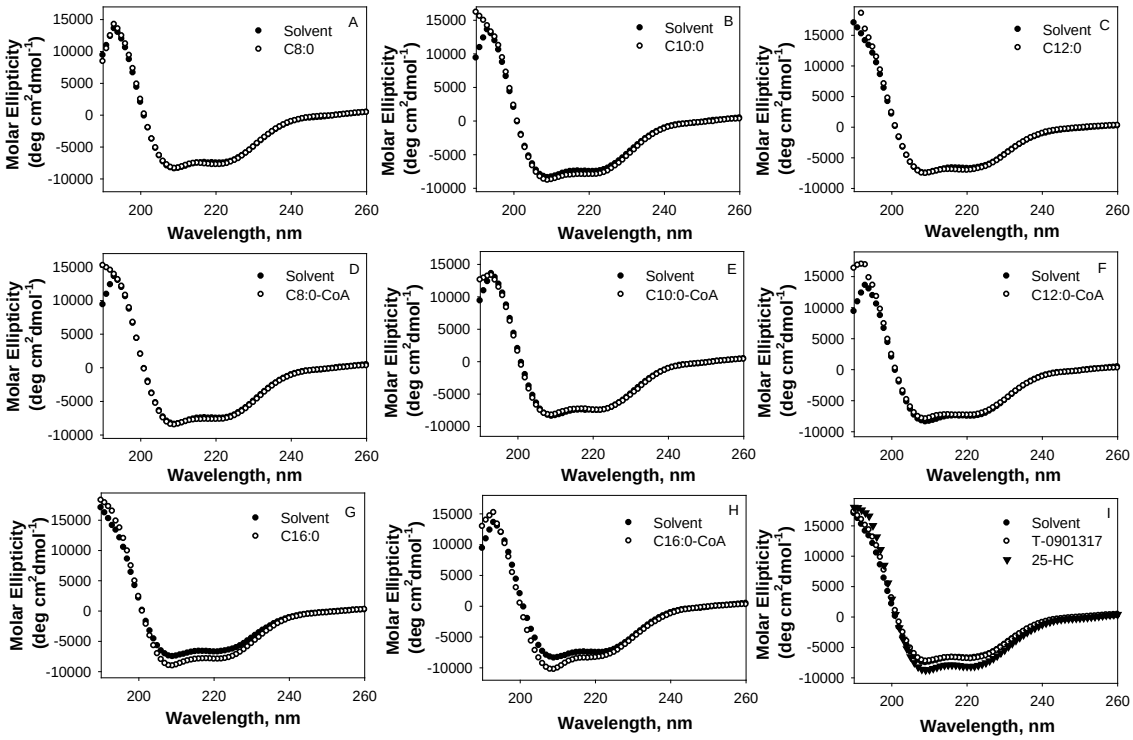
A
Solvent
C8:0
B
Solvent
C10:0
C
Solvent
C12:0
D
Solvent
C8:0-CoA
E
Solvent
C10:0-CoA
F
Solvent
C12:0-CoA
G
Solvent
C16:0
H
Solvent
C16:0-CoA
I
Solvent
T-0901317
25-HC
Molar Ellipticity (deg cm2dmol-1)
Wavelength, nm

Fig. 13: Far UV circular dichroic spectra of LXRα in the absence (filled circles) and presence of added ligand at a concentration of 0.6 μM: (**A**) octanoic acid, C8:0 (open circles) or (**D**) Octanoyl-CoA, C8:0-CoA (open circles); (**B**) decanoic acid, C10:0 (open circles) or (**E**) decanoyl-CoA, C10:0-CoA (open circles); (**C**) lauric acid, C12:0 (open circles) or (**F**) lauroyl-CoA, C12:0-CoA (open circles); (**G**) palmitic acid, C16:0 (open circles) or (**H**) palmitoyl-CoA, C16:0-CoA (open circles); (**I**) T-0901317 (open circles) or 25-HC (filled triangle). Each spectrum represents an average of 10 scans for a given representative spectrum from at least three replicates.

Table 2. Secondary structures of hLXRα protein in the presence of fatty acids and fatty acyl-CoAs

Ligand	α-helix regular H(r)%	α-helix distort H(d)%	β-sheet regular S(r)%	β-sheet distort S(d)%	Turns T%	Unordered U%
Ethanol	13.9 ± 0.4	11.9 ± 0.2	13.3 ± 0.3	8.8 ± 0	19.6 ± 0.8	32.4 ± 1.5
C8:0	14.4 ± 0.5	12.0 ± 0.2	12.5 ± 0.6	8.5 ± 0.1	19.6 ± 0.2	32.8 ± 0.5
C8:0-CoA	14.2 ± 1.1	11.5 ± 0.8	15.8 ± 0.5***	8.9 ± 0.5	19.8 ± 1.3	32.2 ± 3.1
C10:0	13.6 ± 0.6	11.5 ± 0.1	15.3 ± 0.5**	9.2 ±	21.2 ± 0.1	29.0 ± 0.2
C10:0-CoA	15.3 ± 2.7	11.7 ± 0.4	15.7 ± 1.5*	0.1* 8.1 ± 0.8	17.7 ± 3.4	36.7.0 ± 6.4
C12:0	12.1 ± 1.6	9.9 ± 0.3	17.9 ± 0.6	10.5 ±	20.5 ± 0.1*	28.9 ± 0.4*
C12:0-CoA	13.9 ± 0.6	11.3 ± 0.6	14.5 ± 1.2	0.2 9.6 ± 0.3	19.9 ± 1	30.6± 1.4
C16:0	13.7 ± 1.7	11.4 ± 1.2	15.9 ± 3.9	9.5 ± 0.9	22.1 ± 0.8*	27 ± 2.5
C16:0-CoA	17.2 ± 2.5	12.8 ± 0.8	12.6 ± 3.7	8.1 ± 0.7	18.1 ± 2.8	35.2 ±4.8
25-HC	14.7 ± 0.3**	11.9 ± 0.3**	12.9 ± 0.9	8.9 ±0.3	21.4 ± 0.1**	30.1 ± 0.4*
T0901317	12.1 ± 1.3	10.5 ± 0.6	16.8 ± 1.5	9.7 ± 0.3	21.3± 0.2**	29.4 ± 0.2**

Significant difference between hLXRα with solvent compared to the absence or presence of fatty acids or fatty acyl-CoA (in Ethanol) determined by t-test * = $P<0.05$, ** = $P<0.01$, *** = $P<0.001$.

Docking of ligands: Computational methods allow identification of novel ligands for nuclear receptors. Molecular docking using AutoDock Vina and SYBYL Tripos was used to investigate the steric and electrostatic complementarity between the LXRα LBD and putative ligands. The availability of LXRα LBD crystal structure allows employment of structure-based virtual screening of various fatty acids and fatty acyl CoA (*26*). The existing structure of LXRα-RXRβ complex in the presence of T-0901317 (PDB 1UHL) was used as a template to screen putative ligands of LXRα. As a first step, LXRα synthetic agonist T-0901317 was docked as a control to validate the docking parameters. The theoretical docking study of ligands gave results in terms of energy and orientation of ligands. Since SYBYL utilizes a more computationally expensive force field method compared to the inexpensive grid-based method to estimate the binding energies, differences in values between the two methods was not surprising. As seen in Fig. 14D, T-0901317 fits centrally inside the ligand binding pocket with the hydroxyl head group coordinated by hydrogen bonding to H421. This orientation of T-0901317 in the LXRα ligand binding pocket is similar to that proposed by Svensson *et al*. (*26*). Docking exercise performed with the fatty acids and fatty acyl CoA shows that these ligands similarly orient themselves centrally in the ligand pocket of LXRα. The polar head group of ligand is situated close to helix 12, and interacts with amino acids H421 and W443 of LXRα in the ligand binding pocket. Whereas lauric acid and lauroyl-CoA ligands completely fit within the ligand binding pocket, the hydrophobic tail of stearoyl-CoA is not accommodated in the pocket of LXRα (Fig. 14A-C). The position of docked ligands resembles that of T-0901317 in the LBD of LXRα as reported in the LXRα-RXRβ heterodimer complex (PDB entry 1UHL) (*26*). The predicted binding free

energies derived by molecular docking listed in Table 3 gave a similar rank order of binding when compared to the apparent K_d values obtained for the fatty acids, fatty acyl-CoA, and T0901317.

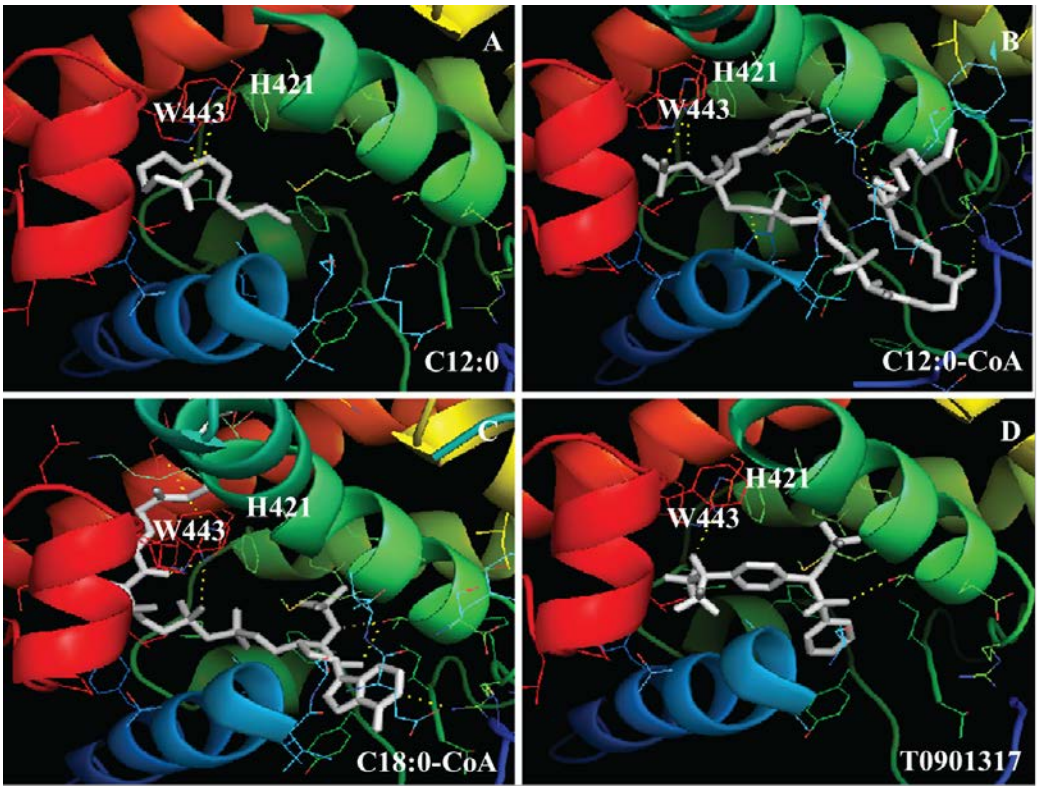

Fig. 14: Ribbon diagrams showing the orientation of ligands (white) (**A**) lauric acid; (**B**) lauroyl-CoA; (**C**) stearoyl-CoA, and (**D**) T-0901317 in the ligand binding pocket of LXRα. Amino acid residues H421 and W443 are shown in stick mode.

Table 3. The binding free energies of the ligand binding to LXRα. The binding free energies are in Kcal. Mol $^{-1}$ for the protein-ligand complexes as estimated by AUTODOCK and SYBYL.

Ligand	**Auto Dock Vina**	**SYBYL**
T-0901317	-10.8	-2047
Lauric Acid	-5.3	-1913
Octanoyl CoA	-9.2	-2413
Decanoyl CoA	-8.8	-2053
Lauroyl CoA	-7.9	-2371
Palmitoyl CoA	-9.1	-2933
Stearoyl CoA	-1.6	-2177

Effect of fatty acids and fatty acyl-CoA on transactivation of LXRE: Transactivation assay was used to confirm the functional significance of lipid binding to LXRα.To determine the cellular activity of fatty acids, a cell based luciferase reporter assay was used to measure the regulation of downstream transcriptional activity of SREBP-1c in the presence of fatty acids (varied in chain length and degree of unsaturation). COS-7 cells were cotransfected with pSG5 empty vector, LXRα alone, PPARα alone, or LXRα with PPARα and analyzed for transactivation of an hSREBP-1c LXRE-luciferase reporter construct in the absence or presence of ligands (Fig. 15). Cells were treated with ligands, and transactivation was measured as percent firefly luciferase activity normalized to *Renilla* luciferase (internal control). The fold of activation was calculated against a no ligand (ethanol) control. In cells overexpressing only hLXRα, LXR agonist 25-hydroxycholesterol (positive control) significantly increased transactivation by 1.5 fold. The addition of the octanoic acid, decanoic acid, and palmitic acid resulted in no significant changes in transactivation activity (Fig. 15), consistent with the weak binding affinity of LXRα for these ligands. Lauric acid or its metabolite was the only fatty acid that activated the reporter expression by 2-fold. This result is in agreement with the binding studies that show binding of lauric acid and lauroyl-CoA to LXRα. At 10uM ligand concentration, arachidonic acid lowered luciferase activity compared to the basal levels consistent with published data that unsaturated fatty acids antagonize ligand dependent activation of the LXR (*35, 82, 83*). The enhanced reporter activity was LXRα, not PPARα, mediated since PPARα alone or in the presence of FA showed very little change in luciferase activity. These data suggest that lauric acid or its metabolite fulfills the requirement of an LXRα endogenous ligand

through which fatty acids regulate LXRα activity.

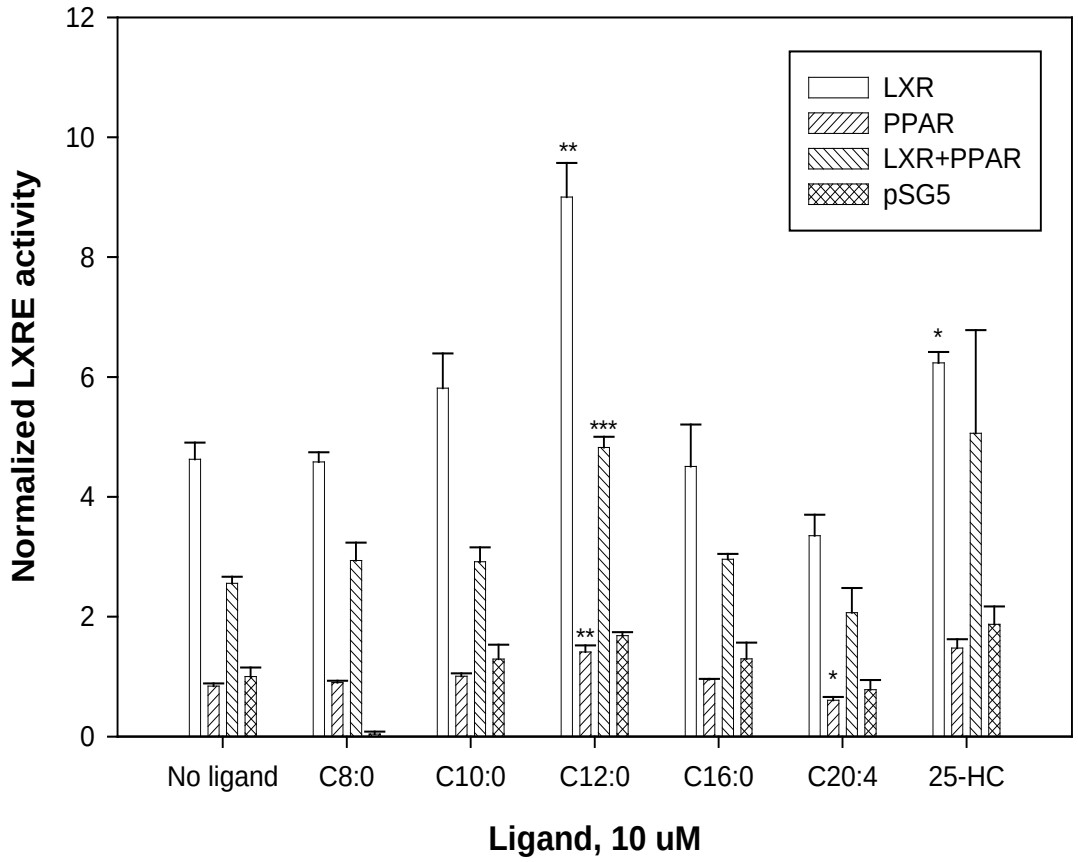
Normalized LXRE activity
12
10
8
6
4
2
0
LXR
PPAR
LXR+PPAR
pSG5
**
**
***
*
*
No ligand
C8:0
C10:0
C12:0
C16:0
C20:4
25-HC
Ligand, 10 uM

Fig. 15: Medium chain fatty acid lauric acid or its metabolite lauroyl-CoA alter LXRα transactivation. COS-7 cells transfected with pSG5 empty vector, LXRα, PPARα, both PPARα and LXRα were analyzed for transactivation of the SREBP-1c-LXRE-luciferase reporter construct in the presence of vehicle *or* 10 μM ligands. The *y-axis* represents values for firefly luciferase activity that have been normalized to *Renilla* luciferase (internal control), where no ligand empty vector (pSG5) sample was arbitrarily set to 1. The bar graph represents the mean values ($n \geq 3$) ± standard error. * $P < 0.05$, ** $P < 0.01$, and *** $P<0.0001$. Asterisks denote significant differences due to ligand as compared to no-ligand controls.

5. Discussion:

The present work demonstrates that medium chain saturated fatty acids and fatty acyl CoA represent high affinity ligands of LXRα that bind at physiological concentrations. Two separate fluorescence based assays confirmed that saturated fatty acyl CoAs binding to LXRα is specific, rather than nonspecific. Changes in aromatic amino acid fluorescence, one of the most direct methods to study ligand induced conformational changes, demonstrated the interactions of LXRα with fatty acids and fatty acyl CoA. The decrease in intrinsic fluorescence of LXRα supports a change in environment in aromatic amino acids upon binding with medium chain fatty acids and fatty acyl CoA. A direct molecular interaction of these ligands with LXRα with well characterized apparent dissociation constants. The deduced K_d value, determined by the intrinsic quenching assay, of T-0901317 (3±1 nM) is in agreement with those reported in the literature (7 nM) (*92*). Using the same assay, the relative affinities of fatty acids showed that binding to LXRα occurs in the low nanomolar concentration range. Furthermore, the apparent K_d values are close to the reported concentrations of free fatty acids present in a cell (*93*). Thus, binding of fatty acids and fatty acyl CoA to LXRα occurs at physiologically relevant concentrations.

Previously reported K_d values for LXRα ligand binding were based on the assumption that total ligand concentration present in the sample was approximately equal to the free ligand concentrations. Since, the protein concentrations under our assay conditions were not below or at the determined K_d values, free ligand concentrations had to be determined to estimate the K_d values. These corrections led to the determination of K_d values that were lower than the previously reported values.

Disagreement was observed between K_d values determined for palmitoyl-CoA binding to LXRα through intrinsic quenching and fluorescent ligand binding assay. This inconsistency may be explained by previously reported work which showed that fluorescent ligands may have a lower affinity than their non-fluorescent counterparts due to the presence of fluorophore (*94*).

The relative binding affinities of various fatty acids and fatty acyl CoA with respect to C16:0-CoA binding through *in vitro* competition LXRα-binding assays were also determined. The observed competition between the fatty acids and existing endogenous or synthetic ligands suggests that these ligands bind at a common site. Established LXRα ligands T-0901317 and 22 (R) Hydroxycholesterol effectively displaced bound BODIPY C16:0-CoA in the receptor competition assay. Medium chain fatty acid (C10:0) and fatty acyl-CoA (C8:0-CoA) successfully competed with BODIPY C16:0-CoA for binding to LXRα at 100 nM and 200 nM concentrations respectively. Incomplete displacement of BODIPY C16:0-CoA by fatty acids suggests that BODIPY dye either interferes with the binding of competing ligands or there are two or more binding sites in the pocket for the occupancy ligands. Long chain fatty acids, such as docosahexaenoic acid and phytanic acid, did not displace the bound ligand. This finding implies that long chain fatty acids or fatty acyl CoA may bind poorly or bind to a different binding site on LXRα, as they do not compete with C16:0-CoA for receptor binding. The literature suggests that particular fatty acids prevent binding of oxysterols to LXRα (*35, 95*). This effect may be mediated through fatty acids competing with oxysterols for the same binding site or allosterically preventing efficient binding of oxysterols in the LXRα ligand binding pocket. The data suggest that oxysterols and long

chain fatty acids do not share the same binding site. It remains to be investigated whether fatty acids induce gene expression similar to LXRα ligands or enhance the interaction of the LXRα with cofactor peptides.

The ability of fatty acids and fatty acyl CoA to induce changes in the secondary structure of LXRα was investigated. Subtle structural changes in the α–helix content, β-structure, and turns were most likely induced after the binding of fatty acyl-CoA and fatty acid binding to LXRα. β-sheet content, as estimated by CD at 190 nm wavelength, was significantly altered by binding of LXRα to medium chain fatty acids and fatty acyl CoA. Although lauric acid and lauroyl CoA binding quenches the intrinsic fluorescence of LXRα, lauric acid alone induces a conformational change in the secondary structure. The binding of C8:0-CoA, C10:0, and C10:0 CoA not only quenches intrinsic fluorescence, but also induces significant conformational changes in LXRα. This finding suggests that ligand induced exposure of the LXRα aromatic amino acids to the solvent may not accompany large conformational changes in the overall structure. Whether conformational changes in the secondary structure of the protein are necessary for its transactivation activity is still unclear although evidence so far suggests that this may be true in the context of LXRα. Furthermore, our results showed that weak binding of LXRα to long chain fatty acids and long chain fatty acyl CoA did not affect the structure of LXRα. Even though LCFA or long chain fatty acyl CoA did not show high affinity binding ,changes in the CD spectra implied that very small conformational changes occurred upon C16:1 and C20:5 binding. One possible explanation for this finding could be non-specific binding of these ligands to various surface domains of LXRα. This finding was not entirely unexpected since LCFA are PPAR ligands (*96*).

The ligand induced changes in the LXRα CD spectra, however, did not always correlate with the binding affinities of ligands tested. One possible explanation for this discrepancy may be that circular dichoric spectra provide a global average of all structural changes, and it is thus possible that changes induced in one domain ameliorated other changes. Alternatively, certain ligands may bind non-specifically to different regions of LXRα and cause differential changes in the overall structure of the proteins.

The structural basis for the selective preference of LXRα for medium chain fatty acids and fatty acyl CoA derivatives and the proposed role of these molecules as LXRα ligands was supported through molecular docking of ligands to the LBD of LXRα. The docking modes demonstrated that the ligand binding pocket of LXRα can easily accommodate the medium chain fatty acyl CoA, but not the longer fatty acids. These theoretical findings are consistent with our binding data suggesting that medium chain fatty acids and medium chain fatty acyl CoA can fit nicely in the LXRα ligand binding pocket. On the other hand, long chain fatty acids and the acyl chains may be too large to fit in the ligand binding pocket of LXRα (volume of 700 A^0) (*26*) inhibiting optimal ligand packing.

Finally, transactivation assays demonstrated that LXRα overexpression alone shows hSREBP-1c promoter activity in luciferase assays, presumably through binding to endogenous RXR. Addition of a fatty acid, particularly, the medium chain fatty acid lauric acid, caused a statistically significant increase in the luciferase reporter assay using the hSREBP-1c promoter in Cos-7 cells. Since the levels of free fatty acids within cells are generally thought to be low and largely bound to intracellular binding proteins,

it is possible that lauroyl-CoA, and not lauric acid, may be the true LXRα ligand. Our binding data agrees very well with this hypothesis. Overexpression of PPARα alone was insufficient to activate the promoter suggesting that the transactivation activity is LXRα mediated. Co-expression of LXRα and PPARα shows repression of transactivation activity observed with LXRα overexpression alone. Taken together, these data support the idea that saturated medium chain fatty acids and fatty acyl CoA are potential LXRα agonists.

In conclusion, fatty acids bind differently to LXR alpha and have distinct effects depending on the chain length and the extent of unsaturation. Future research may explore the possibility that the effects of medium chain triglycerides in the treatment of metabolic disorders may be mediated via activation of LXRα.

CHAPTER II

EFFECT OF LIVER X RECEPTOR ALPHA LIGANDS ON LXRα-PPARα HETERODIMERIZATION – FLUORESCENCE BASED ANALYSIS OF FULL-LENGTH PROTEINS

1. Abstract

Analyzing the effects of ligands on protein-protein interactions is critical for comprehensive understanding of the activation mode of ligand activated transcription factors. Liver X receptor α (LXRα) and peroxisome proliferator-activated receptor α (PPARα) are members of the nuclear receptor superfamily that maintain cholesterol and lipid homeostasis respectively. Each receptor binds to retinoid X receptor (RXR) and specific DNA sequences located within the promoters of their target genes. No crystal structure of LXRα-PPARα complex is available, thus limiting our understanding of how the LBDs of these proteins might interact. Our *in silico* analysis through protein-protein docking (Hex) suggests that LXRα might utilize distinct amino acid residues to interact with each partner receptor. The aim of this study was to show that ligand binding influences LXRα dimerization dissociation constant values. Fluorescence-based *in vitro* assays were used to evaluate the effect of ligands on the relative strength of dimers composed of full-length LXRα and PPARα. Fluorescence quenching of Cy3-labeled PPARα as a result of binding unlabeled LXRα was first used and apparent dissociation constants (K_d) of dimers were determined. A Forster resonance energy transfer (FRET) - based approach was used to determine the K_d values of dimers in the absence or presence of ligands. The values obtained were in agreement with the previous results which confirmed that fluorescent based approaches can accurately measure LXRα-PPARα binding constants. Our results demonstrated that LXRα bound PPARα with a high affinity at low nanomolar concentrations. Exogenous LXRα ligands regulated the strength of this interaction and induced significant changes in the secondary structure of

the dimers. The effects of medium chain fatty acids (C10:0 and C12:0), recently identified as novel ligands of LXRα, on LXRα-PPARα interactions were investigated and it was found from the determined binding K_d values that C10:0 FA enhanced whereas C12:0 weakened LXRα-PPARα interactions. Together, this study suggests that LXRα ligand binding pocket and dimer surface are allosterically coupled and ligands differentially modulate LXRα-PPARα interaction. The latter finding may aid in the discovery of allosteric modulators with unique targeted therapeutic uses.

2. Introduction

The nuclear receptor (NR) family of transcription factors include receptors for steroids, thyroid hormone, and other small hydrophobic molecules. NRs play important roles in maintaining homeostasis, in growth, and development and are frequently dysregulated in diseases (*1, 8*). Peroxisome proliferator-activated receptor (PPARα) and liver X receptor (LXRα) are ligand-activated transcription factors that regulate genes involved in fatty acid and cholesterol homeostasis. Both proteins are activated by ligands (fatty acids and oxysterols respectively) and bind as heterodimers with the 9-cis-retinoic acid receptor (RXR) to activate gene transcription. Administration of LXR ligands in rodents exhibits anti-diabetic and anti-atherosclerotic effects confirming the crucial role LXR plays in cholesterol metabolism. PPAR alpha activation is associated with improved lipoprotein profile and exhibit anti-inflammatory effects in a wide range of pathological conditions. Thus, both receptors are potential drug targets in the treatment of metabolic disorders (*97*).

LXR and PPAR, like other NRs, contain a central DNA binding domain that is linked to a relatively less conserved, multifunctional C-terminal ligand binding domain (LBD) (*43*). The LBD contains binding sites for cofactors, such as corepressors and coactivators, and provides a surface for homodimer or heterodimer formation with the retinoid X receptor (RXR) (*26*) or PPAR. Heterodimer formation is highly regulated by binding to ligands (*43*, *44*). The three dimensional crystal structure of NR heterodimers reveals a common architecture that shows that the ligand binding pocket is distinct from the region that promotes protein-protein interactions (*26*). Ligand binding to either receptor (LXRα or RXRα), or both is sufficient to initiate a downstream cascade of

events resulting in gene activation or repression (*15*). Recent work has been done to understand the regulation of the newly discovered heterodimer composed of LXRα and PPARα (*43*, *44*). In the absence of a three dimensional structure of LXRα with PPARα, a computational model of how the two proteins might interact merits explanation. Since the LBDs of LXRα and PPARα have been crystallized individually, they may be used as models for computational study of their interaction. Hex docking has been proposed to generate a list of plausible models that explores the space of possible conformations of individual components (*98*). In addition, factors that influence the dimerization of these proteins have been identified with respect to PPARα ligands (*44*), but the effects of LXRα ligands on dimerization are not very well characterized.

A majority of *in vitro* studies have utilized truncated proteins (purified LBDs) to investigate the binding affinities of LXRα with RXRα and PPARα (*43*). These studies demonstrated that LXRα ligands (22-R HC and T0901317) and RXRα ligand (9cRA) increased the LXRα-LBD/RXRα-LBD interaction by two to four orders of magnitude. On the other hand, 22-R HC and PPARα ligands (WY 14643 and Bezafibrate) promoted PPARα-LBD/LXRα-LBD interactions by one order of magnitude. However, LBD fragments might behave differently compared to full-length proteins in a complex; and their binding kinetics may be dramatically different. In support of this idea, our laboratory has reported full-length human LXRα-PPARα interaction in the presence of fatty acids (*44*). We showed that long chain polyunsaturated fatty acids inhibit whereas relatively shorter saturated fatty acids enhance this interaction. In the present study, biophysical techniques such as fluorescent and circular dichroism spectroscopies were used to characterize the strength of full-length LXRα-PPARα interaction in the absence

or presence of LXRα ligands. This study demonstrated that LXRα ligands modulate binding dissociation constants describing LXRα-PPARα dimerization and induce conformational changes in the dimers.

3. Materials and Methods

*Chemicals***:** Ligands were purchased from Sigma-Aldrich (St. Louis, MO). Cy3, Alexa fluor 488, and Alexa Fluor 555 protein labeling kits were purchased from Amersham Biosciences (Piscataway, NJ).

*Plasmids***:** Expression vectors for full-length LXRα and PPARα have been previously described (*44, 86*). The hPPARα coding sequence was amplified from cDNA derived from HepG2 cells with the following primers:

5′-c ggatcc ATGGTGGACACGGAAAGCCC-3′ and

5′-c gtcgac CTATCAGTACATGTCCCTGTAG-3′.

In these and subsequent primers, lowercase represents nucleotides outside of the PPARα open-reading frame with restriction sites underlined. The PCR product was cloned into the pGEM-T easy vector (Promega Corporation, Madison, WI) and subsequently transferred into the *Bam* HI / *Sal* I sites of the pGEX-6P derivative to produce 6xHis-GST-hPPARα. Human LXRα (hLXRα) and human retinoid X receptor α (hRXRα) were amplified from cDNA derived from HepG2 cells using the following primers:

5′-ggatccATGTCCTTGTGGCTGGGGGCCCCTGTG-3′ and

5′-aagcttCTCGAGTCATTCGTGCACATCCCAGATCTC-3′ (hLXRα),

5′-cgaattcATGGACACCAAACATTTCCTGCCGCT-3′ and

5′-ctcgagCTAAGTCATTGGGTGCGGCGCCTCC-3′ (hRXRα).

In these and subsequent primers, the lowercase letters represent nucleotides outside of the target sequence with restriction sites underlined. Each PCR product was cloned

into the pGEM-T easy vector (Promega, Madison, WI) and subsequently transferred into the *Bam*HI–*Hin*dIII or *Eco*RI–*Xho*I sites of the pGEX-6P derivative to produce 6xHis-GST-hLXRα and 6xHis-GST-hRXRα, respectively. LXRα and PPARα were expressed as fusion proteins containing an N-terminal poly-histidine GST tag. cDNA encoding full length hLXRα and hPPARα proteins were cloned into a pGEX-6P-3 bacterial expression vector (GE Healthcare), which contains a His and a GST tag upstream of the protease cleavage site (*44, 86*). All plasmid constructs were confirmed by DNA sequencing.

*Protein expression***:** Plasmids for recombinant LXRα and PPARα protein purification were transformed into Rosetta 2 competent cells and used to produce full-length hLXRα and hPPARα proteins Cultures were grown overnite (16h) at 30^{o}C in LB broth containing ampicillin to OD_{600} = 1.2. Protein expression was induced with isopropylthiogalactoside (Sigma, final concentration of 0.1 mM) at 16^{o}C and cultures were allowed to grow for another 4h. Bacteria were pelleted by centrifugation at 8500 rpm for 10 min (Beckman Coultor rotor JA 10) and the pellets were frozen at -80^{o}C.

*Recombinant protein purification***:** Frozen pellets were solubilized in lysis buffer (20 mM Tris, pH 8.0, 300 mM NaCl, 10% glycerol, 1 mM EDTA, pH 8.0 and 1 mM DTT). The resuspension was sonicated six times (30s each) and centrifuged at 12000 rpm for 30 min (Beckman Coultor rotor JA 25.50). Supernatant containing His-GST-tagged protein was applied to a GST column equilibrated in lysis buffer. The GST tag was cleaved by an on-column digestion using PreScission protease. The released proteins were eluted, concentrated, and analyzed using SDS-PAGE and western blotting with specific antibodies (*44, 86*).

*Hex docking of LBDs of LXRα with PPARα***:** The docking analysis was carried out using Hex 8.0.0. Hex explores ways in which two molecules fit together and dock to each other based on shape or charge complementarity (*98*). LXRα LBD (extracted from PDB entry 1UHL) and PPARα LBD (extracted from PDB entry 1K7L) were treated as receptor and ligand respectively for docking. Energy minimized receptor files were prepared using SPDBV and uploaded as inputs into HEX. To dock, the locations of the molecular centroids and the relative orientations of proteins with respect to the intermolecular axis were considered. Water molecules and any other hetero molecules were removed prior to docking. Based on the energy minimization, the best pose of the docked complex was selected.

Protein-protein binding assay- Recombinant PPARα was fluorescently labeled with Cy3 dye using Fluorolink-antibody Cy3 labeling kit (Amersham Biosciences, Pittsburgh, PA). Absorbance measurements were used to characterize the protein-dye conjugates. Emission spectra (560-650 nm) of 25 nM Cy3-labeled PPARα dissolved in PBS were recorded upon excitation at 550 nm with increasing concentrations of unlabeled LXRα in a Cary Eclipse fluorescence spectrophotometer at 24^0C. The spectra were corrected for background (buffer, solvent, and protein alone), and the maximal intensities were recorded. To determine the effects of ligands on LXRα-PPARα interaction, the experiments were repeated in the presence of each ligand at a concentration determined by their binding affinities. The dissociation constants (K_d) were obtained after correcting for bound protein and inactive protein as described above and reported previously (*44*). Binding constants were extracted from binding curves by

nonlinear regression analysis using the ligand binding function in Sigma Plot (SPSS Inc., Chicago, IL) (*44*).

Forster resonance energy transfer (FRET) - To confirm the previous results, recombinant proteins were labeled with fluorescent dyes comprising a FRET pair (Alexa Fluor488/555 dyes). FRET develops when an excited donor fluorophore is in close enough proximity to an acceptor fluorophore so that energy transfer can occur. This technique allows for quantitative measurement of protein interactions and can be demonstrated by the enhanced emission from acceptor or by the decreased emission from the donor. The amount of transferred energy increases exponentially with decreasing distance between fluorophores, while it drops to virtually zero when the distance becomes greater than 10 nm (*99*). Primary amines of the purified recombinant proteins (LXRα and PPARα) are potential labeling targets through the use of protein labeling kits (GE Healthcare Amersham). The dye: protein molar ratio was maintained at 1:1 suggesting the presence of probably one dye label per protein. Since each protein carried approximately a single fluorescent dye, the signal was expected to be proportional to the number of protein-protein binding interactions (*99*). Alexa Fluor 488-labeled LXRα was kept at a constant concentration of 25 nM in PBS, pH 7.4. The sample was excited at 488 nm and emission spectra (500-670 nm) were recorded with increasing concentrations of Alexa Fluor 555-labeled PPARα in a Cary Eclipse fluorescence spectrophotometer. The slit widths for the excitation and emission monochromators were 5 nm each, and the titrations were performed at 24^0C. The spectra were corrected for background (buffer, solvent, and each protein individually) and decrease in the donor's emission was monitored. To determine the effect of ligands on

LXRα-PPARα interactions, the experiments were repeated in the presence of 2.5 to 200 nM of each ligand. This range of ligand concentration was chosen since published data from our laboratory suggested that LXRα and PPARα bind endogenous or synthetic ligands within the concentration range of 2-30 nM. Protein-protein binding curves were generated using the decrease in the donor emission plotted as a function of acceptor concentration. Apparent dissociation constants were estimated from the titration curve as described (*44*, *99*).

Circular dichroism (CD) - A hallmark of nuclear receptors is the ligand induced conformational changes in the secondary structure of the protein. In addition, interactions with partner receptors tend to cause conformational changes upon binding (*85-89, 96*). Circular dichroism (CD) is a spectroscopic technique for studying protein-protein and protein-ligand interactions in solution. Proteins contain a number of chromophores that give rise to CD signals. The CD spectrum can be analyzed to estimate the content of regular secondary structural features such as alpha helices (α-helix) and beta sheets (β-sheet) (*88*). Each of these secondary structures gives rise to a characteristic shape and magnitude of CD spectrum. In the far-UV spectral region (240-180 nm), the chromophore is the peptide bond, and the signal arises when it is located in a regular, folded environment. While changes at 222 or 218 nm can give an estimate of increase in α-helical or β-structure content, more precise estimates of changes in secondary structure accompanying protein-protein or protein-ligand interactions can be made utilizing the previously described software (*88*). CD spectra of protein complexes were obtained by use of a Jasco J-815 CD spectrometer as described previously (*85-89*). Circular dichroic spectra of a mixture of PPARα and wild-type LXRα (0.2 μM each in

30 mM NaCl, 2 mM Tris, pH 8.0, 0.5 μM EDTA, 0.04% glycerol at 22^0C in a 1mM cuvette) were measured in the presence and absence of ligands with a J-815 spectropolarimeter (Jasco Inc., Easton, MD). Spectra was recorded from 260 to 187 nm with a bandwidth of 2.0 nm, sensitivity of 10 millidegrees, scan rate of 50 nm/min and a time constant of 1 s. Ten scans were averaged for analysis of percent compositions of α-helices, β-strands, turns and unordered structures using the CONTIN program of the CDpro software package (*85-89*, *96*).

To determine if physical interactions between LXRα and PPARα were altered upon ligand binding to either protein, CD spectra were obtained from individual proteins (0.4 uM), as well as protein combinations, in the absence or presence of ligands. Replicate spectra were recorded five times over the far-UV region from 186 to 260 nm with a 2 nm bandwidth, 10 millidegree sensitivity, 50 nm/min scan rate, and 1 s time constant. CD spectra of each receptor with ligand was compared to the spectrum for that receptor in the absence of ligand to determine ligand-induced conformational changes in the receptor. The CD spectra of each heterodimeric pair with ligand was compared to (a) the same receptor-receptor pair in the absence of ligand (b) the calculated average of the spectra of the individual receptors in the absence of ligand, and (c) the calculated average of the spectra of the individual receptors each in the presence of ligand. The CD spectrum of the mixed proteins was compared to a theoretical spectrum of proteins as described (*44*).

4. Results

Purification of recombinant proteins: Bacterial expression of highly soluble and stable His-GST tagged full-length LXRα and PPARα proteins was detected by immunoblotting (data not shown). Subsequent purification through affinity chromatography, electrophoresis, and immunoblot of purified PPARα and LXRα proteins showed major protein bands at molecular weight of approximately 52 kDa and 50 kDa respectively (Fig. 16). Immunoblot using anti-PPAR and anti-LXR antibodies recognized the bands confirming that the preparation contained PPARα and LXRα proteins. Assessment of the folding of the recombinant purified proteins into native structure was monitored by circular dichroism spectroscopy

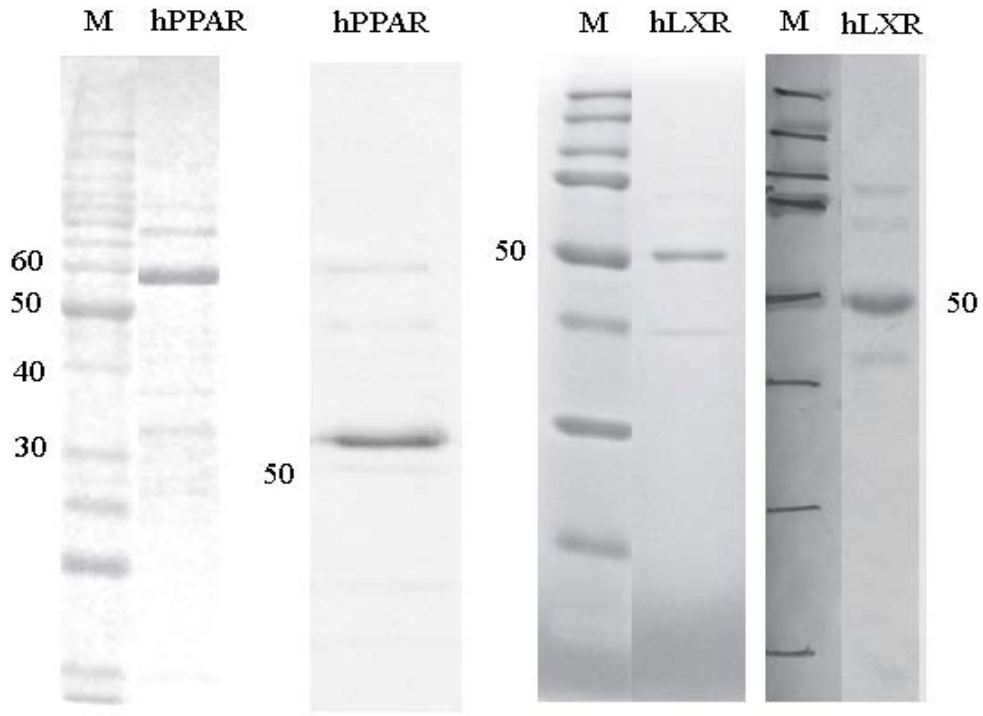

Fig. 16: SDS-PAGE and Coomassie blue staining of purified full-length hPPARα (left) and hLXRα (right) proteins showing the relative purity. The prominent bands correspond to 52 kDa and 50 kDa represent untagged full-length PPARα and LXRα respectively proteins. Anti-PPARα and anti-LXRα antibodies were used to perform Western blot analysis to identify the purified recombinant proteins.

Hex docking of LBDs of LXRα and PPARα: Docking resulted in the generation of possible docking conformations along with model scoring. The most plausible conformations yielded a favorable binding energy value (-590 kcal/mol) and a putative interface between the LBDs of LXRα and PPARα. A Hex based scoring function identified near-native crystallographic orientations. The top 10 scoring poses generated by the docking program were assessed for protein-protein interactions. The resultant interface was determined based on the existing knowledge of the location of interdimer protein binding sites. Most of the interactions predicted by this model occurred between the C-terminus of LXRα and the C-terminus of PPARα. Interestingly, LXRα helix 10 residues, located at the interface of the reported LXRα-RXRβ crystal structure, are positioned differently in LXRα-PPARα model (Fig. 17). This suggests that LXRα might utilize distinct and separate juxtapositions to form interactions with RXR and PPARα. The possibility that all three proteins may bind to form a trimeric complex can be excluded based on the body of evidence gathered from the reported crystal structures and gel filtration assays. These studies demonstrated that whereas RXRα is capable of forming tetramers and heterodimers, PPARα and LXRα exist as dimeric complexes with each other and with RXRα. In addition, LXRα has the ability to form homodimers that implies an unknown functional consequence.

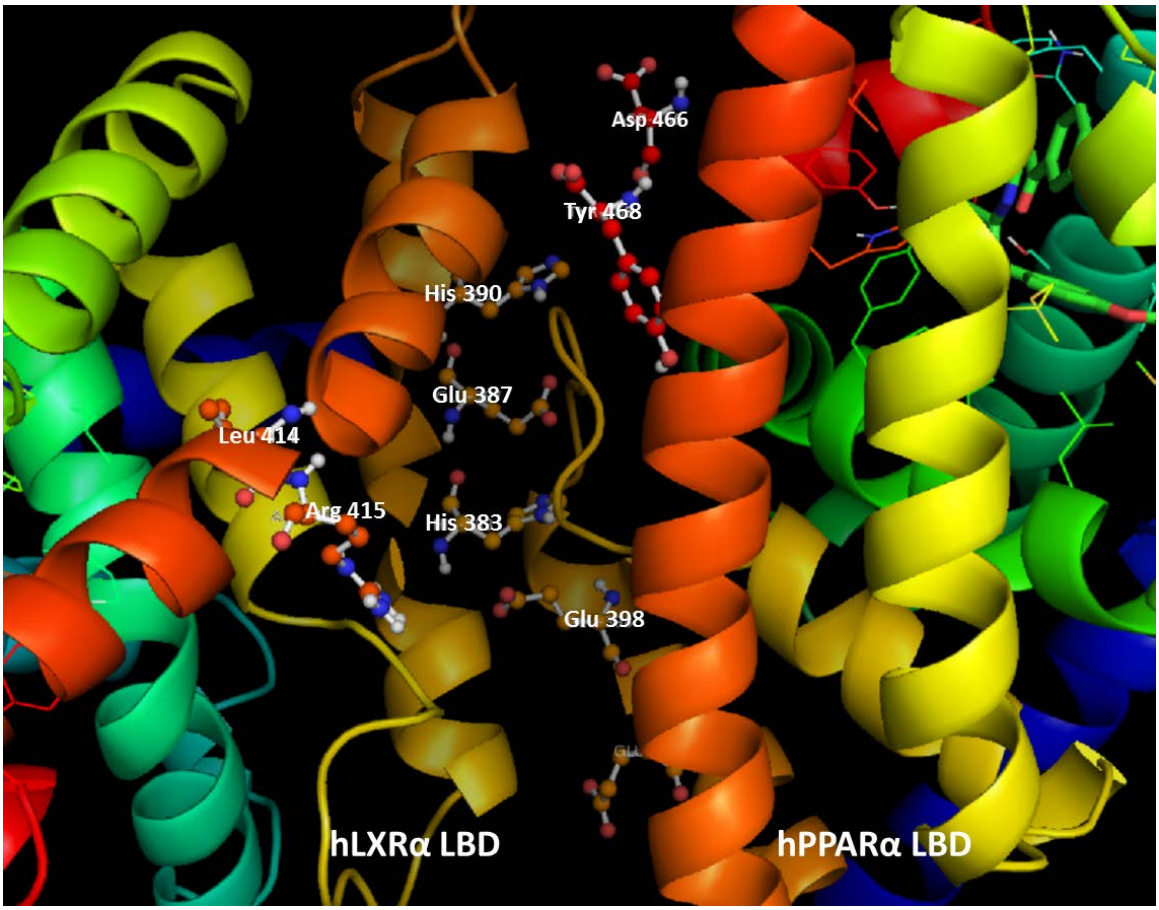
Asp 466
Tyr 468
His 390
Glu 387
Leu 414
Arg 415
His 383
Glu 398
hLXRα LBD
hPPARα LBD

Fig.17. Positions of LXRα and PPARα residues proposed as participating in protein-protein interactions derived from Hex docking of LXRα LBD (extracted from PDB 1UHL) with PPARα LBD (derived from PDB 1K7L). Residues are depicted in white. Helices 9 and 10 of LXRα (shown in light orange and dark orange respectively) have been partly removed to provide a better view of the hypothetical LXRα-PPARα interface.

*Fluorescence monitoring of LXRα-PPARα association***:** We first examined the association of purified full-length proteins, LXRα with PPARα, *in vitro* using recombinant hPPARα fluorescently labeled with Cy3 dye. Fluorescence emission of Cy3-labeled PPARα was measured in the presence or absence of unlabeled LXRα. Fig. 18 shows concentration dependent fluorescence changes induced by LXRα in the presence and absence of exogenous ligands. Quenching of Cy3 dye occurred as a result of a conformational change induced in Cy3-PPARα due to binding with LXRα. The observation that saturation occurred at 8-13nM suggested that the fraction of active Cy3-PPARα protein present in the sample is probably lower than 25 nM. The saturable curve yielded an apparent dissociation constant (K_d) of 7±3 nM using a single site model indicating a high affinity binding between LXRα and PPARα. Addition of saturating concentrations of ligands differentially altered the binding dissociation constants of LXRα-PPARα interaction. The K_d for the LXRα-PPARα dimer affinity were determined to be 25±5 nM (with T-0901317), 11±2 nM (with 25-HC), and 93±43 nM (with C16:0 FA).

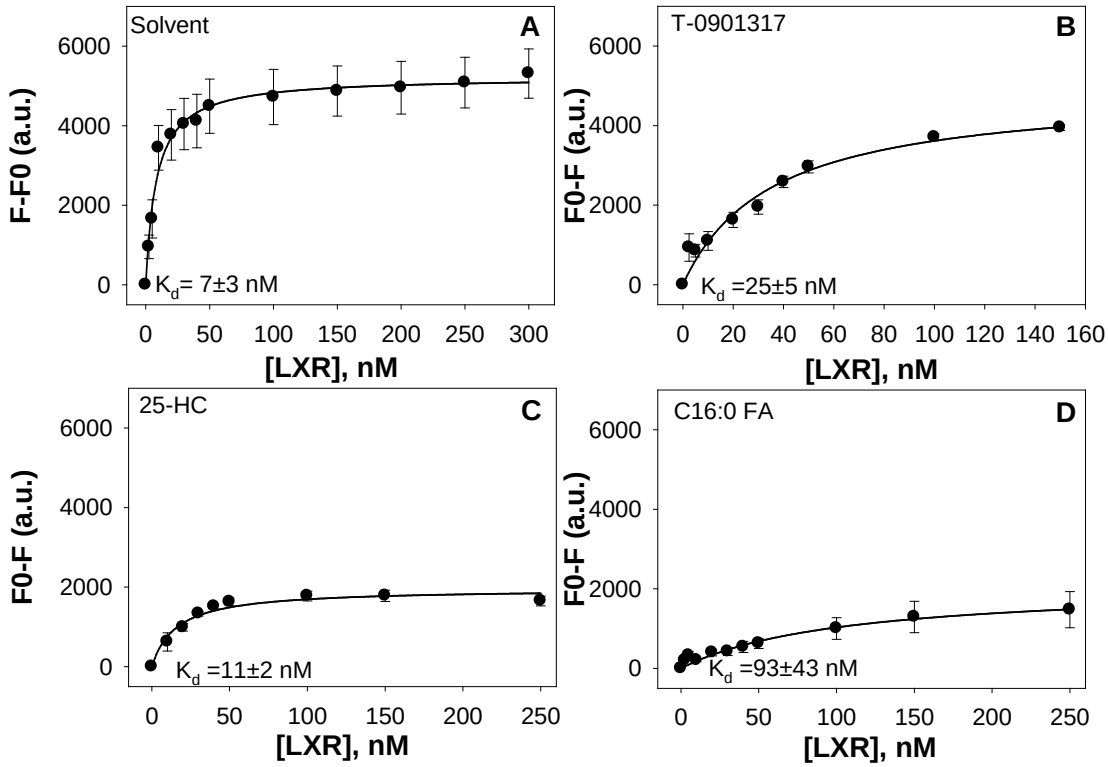
Solvent
A
F-F0 (a.u.)
6000
4000
2000
0
K_d= 7±3 nM
0 50 100 150 200 250 300
[LXR], nM
T-0901317
B
F0-F (a.u.)
K_d =25±5 nM
0 20 40 60 80 100 120 140 160
[LXR], nM
25-HC
C
F0-F (a.u.)
K_d =11±2 nM
0 50 100 150 200 250
[LXR], nM
C16:0 FA
D
F0-F (a.u.)
K_d =93±43 nM
0 50 100 150 200 250
[LXR], nM

Fig. 18: Fluorescent protein-protein binding assays of 25 nM Cy3-labeled hPPARα titrated against increasing concentrations of unlabeled hLXRα in the absence or presence of ligands. The change in fluorescence intensity of 25 nM Cy3-labeled hPPARα was titrated with increasing concentrations (0-250 nM) of hLXRα in the presence of (A) solvent, saturating amount of (B) T-0901317, (C) 25-HC, and (D) C16:0 FA. Values represent means ± the standard error (n = 3-5).

The effect of ligands on the FRET between LXRα heterodimers: Alexa fluor dye labeled proteins were utilized to perform FRET and determine the association of dimers composed of LXRα and PPARαas detected by the emission at 519 nm (Fig. 19A). Since there is minimum overlap of acceptor emission at the donor maximum emission (519 nm), we chose to monitor FRET as a decrease in donor intensity and not an increase in acceptor intensity (580 nm). The apparent K_d for the LXRα-PPARα dimer in the absence of ligand was 8±3 nM (Fig. 19B). By comparison, the K_d value for LXRα-RXRα binding was also determined to be in the low nanomolar concentration range suggesting that both LXRα-PPARα and LXRα-RXRα are high-affinity binding complexes (data not shown). Furthermore, titration experiments allowed us to estimate ligand concentrations required to fully saturate the proteins. Ligands were assessed for their effects on dimerization: synthetic LXR agonist T-0901317, endogenous LXR agonist 25-HC, a PPARα agonist C16:0 FA, and MCFA. All fluorescence based experiments were conducted under saturating ligand concentrations (1 uM for T-0901317, and 10 uM for 25-HC and FA). Our data suggest that the apparent K_d values for dimerization were not similar with all the ligands tested. Compared with the dimers in the absence of ligand, different ligands affected the apparent K_d values by factors ranging from 0.16- to 3-fold. Synthetic agonist T-0901317 increased the heterodimerization K_d by 1.25-fold while the endogenous ligand 25-HC increased the heterodimerization K_d by 1.62-fold. C10:0 FA decreased the heterodimerization K_d by 0.16-fold while C12:0 and C16:0 increased the heterodimerization K_d by 3-fold and 2.25-fold respectively (Fig. 19C-G). The statistical significance of differences using the Student's t-test did not exhibit statistically significant differences between samples treated with solvent and various ligands. A

possible explanation could be that ligands tested might induce subtle structural changes to be detected by intramolecular FRET, which is most sensitive to changes in distance when fluorophores are between 10-100 A^0 apart. Interestingly, T-0901317, compared with all the other ligands, binds LXRα with the highest affinity but this effect is not similar to the change in affinity between LXRα and PPARα.. Taken together, our data demonstrated that classical LXRα ligands increased the K_d values whereas PPARα ligand C16:0 and the newly identified LXRα ligand C10:0 decreased the K_d value. Based on previous findings, it is safe to speculate that distinct conformational changes at the dimer interface induced by ligand binding might modulate the dimerization properties possibly through rearrangement of critical interface residues.

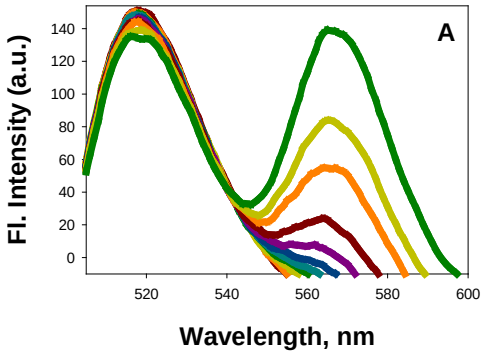
A
Fl. Intensity (a.u.)
Wavelength, nm

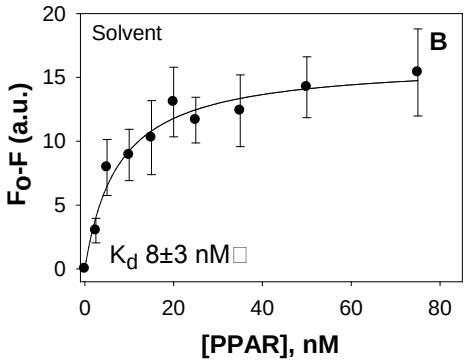
Solvent
B
F_O-F (a.u.)
K_d 8±3 nM
[PPAR], nM

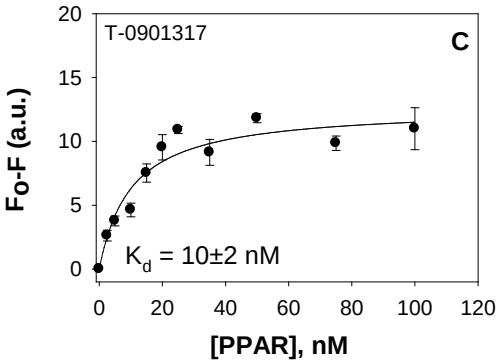
T-0901317
C
F_O-F (a.u.)
K_d = 10±2 nM
[PPAR], nM

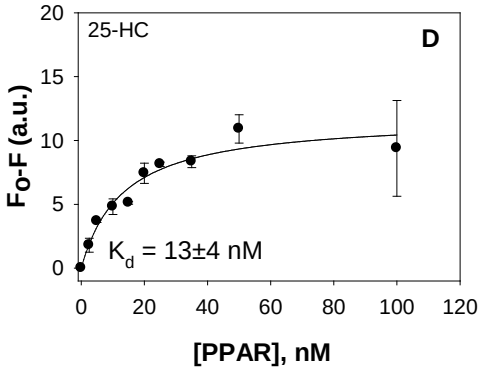
25-HC
D
F_O-F (a.u.)
K_d = 13±4 nM
[PPAR], nM

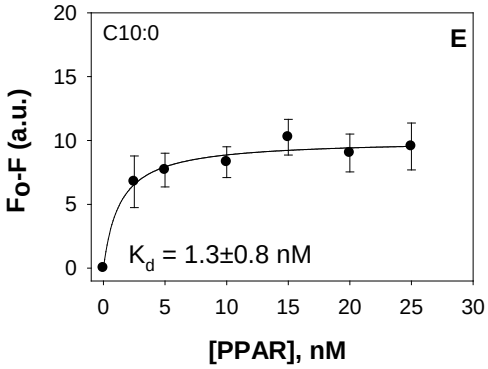
C10:0
E
F_O-F (a.u.)
K_d = 1.3±0.8 nM
[PPAR], nM

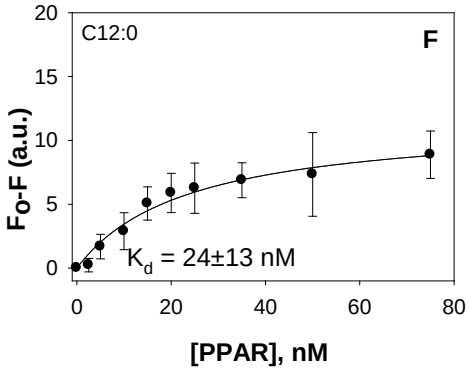
C12:0
F
F_O-F (a.u.)
K_d = 24±13 nM
[PPAR], nM

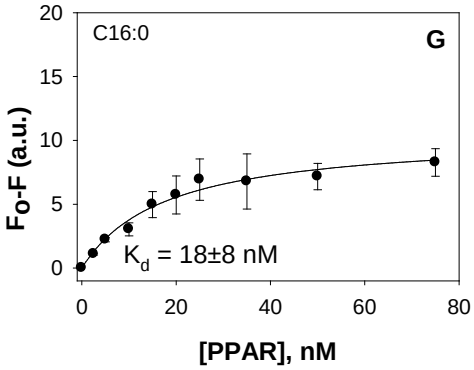
C16:0
G
F_O-F (a.u.)
K_d = 18±8 nM
[PPAR], nM

Fig. 19: Ligands modulate the binding dissociation constants of LXRα-PPARα interaction. FRET from 25 nM donor Alexa fluor 488-labeled LXRα to acceptor Alexa fluor 555-labeled PPARα was detected as quenching of Alexa fluor 488 fluorescence emission (near 519 nm). (A) Emission spectra of Alexa fluor 488-labeled LXRα upon excitation at 488 nm in the absence or presence of increasing concentrations of Alexa fluor 555-labeled PPAR. Plot of the average change in maximal fluorescence intensity at 519 nm (F_0-F) of Alexa fluor 488-LXRα as a function of Alexa fluor 555-PPARα in the presence of (B) solvent, (C) T-0901317, (D) 25-HC, (E) C10:0 FA, (F) C12:0 FA, and (G) C16:0 FA. Values represent the means ± SE, n = 3-5. FRET, Forster resonance energy transfer.

Circular dichroism: To investigate the possibility of the ligands causing conformational changes in the LXRα-PPARα dimer, circular dichroism was used to estimate the secondary structure of proteins under various conditions. As seen in Fig. 20A, the CD spectrum of the individual proteins are different, yet qualitatively similar with PPARα, which exhibits a higher alpha helical content. For the equimolar mixture of the two proteins, the experimentally observed spectrum is different from the spectrum obtained by averaging the spectra of individual proteins (based on the assumption that no interaction exists between the proteins) (Fig. 20B). The changes in the secondary structure composition of the proteins indicate that there is a direct interaction accompanied by conformational changes. To determine the effect of ligands on this interaction, the CD experiment between LXRα and PPARα was repeated in the presence of ligands for LXRα (T-0901317, 25-HC, and fatty acids) and PPARα (C16:0 FA). The presence of T-0901317 or C16:0 resulted in maximal changes at both the 210 and 222 nm minima in the circular dichroic spectra whereas the presence of 25-HC or C12:0 produced small changes in the spectra (Fig. 20 C, D). This observation suggests that ligands differentially affect LXRα-PPARα interactions consistent with previous observations that showed that binding of each ligand resulted in a slightly different LXRα conformational change. The changes in CD may be interpreted in terms of differences between protein structure especially with respect to α–helix content as measured at 210 and 222 nm.

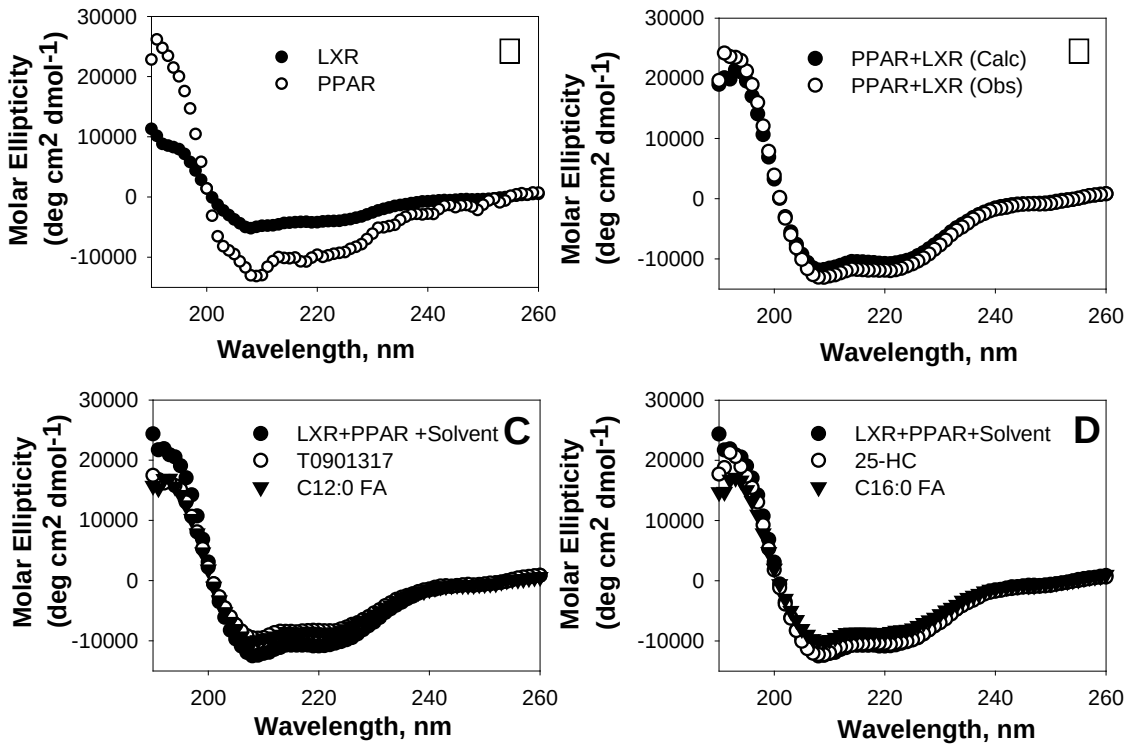
Molar Ellipticity (deg cm2 dmol-1)
Wavelength, nm
LXR
PPAR
PPAR+LXR (Calc)
PPAR+LXR (Obs)
LXR+PPAR +Solvent
T0901317
C12:0 FA
C
LXR+PPAR+Solvent
25-HC
C16:0 FA
D

Fig. 20: Circular dichroic spectra of hLXRα and hPPARα proteins. (A) Circular dichroic spectra of 0.4 uM hLXRα (filled circles) or 0.4 uM hPPARα (open circles). (B) Experimentally observed circular dichroic spectra of a mixture of 0.2 uM hLXRα and 0.2 uM hPPARα (obs, open circles) compared to the calculated average of the individually obtained hLXRα and hPPARα proteins (Calc, closed circles) demonstrating interactions between proteins. Circular dichroic spectra of a mixture of hLXRα and hPPARα proteins in the presence of ligands (C) T-0901317 (open circles) or C12:0 FA (filled triangles), and (D) 25-HC (open circles) or C16:0 FA (filled triangles). Each spectrum is representative of an average of ten scans taken from at least three replicates.

5. Discussion

Dimerization of LXRα, like other nuclear receptors, is a key step in the cascade of events leading to the activation of ligand activated transcription factors. In this study, we have shown that ligand binding influences protein binding kinetics of LXRα. We utilized an *in silico* molecular docking approach combined with fluorescence spectroscopy to characterize LXRα-PPARα interactions. The effects of ligands on LXRα-PPARα dimerization was determined through (1) monitoring the quenching of the fluorophore covalently attached to the protein, and (2) quantifying secondary structural changes induced in the dimer. Our data suggest that most ligands tested, with the exception of C10:0 FA, destabilized LXRα-PPARα interaction. Whether these ligands concomitantly strengthen LXRα-RXRα dimerization or coregulator interactions has yet to be determined. Furthermore, we observed a range in fold changes in the ligand induced K_d values for LXRα-PPARα protein-protein interactions. Together, our data suggest that binding of ligands differentially affect the overall LBD conformation to regulate the protein binding dissociation constants of LXRα. This may have implications in determining the off rate of the LXRα-PPARα dimer in the bound state to its response element and eventually the affinities with which the cofactors bind to the liganded complex. Improved understanding of influences of ligand binding on heterodimer formation may aid development of drugs that could exhibit selectivity in modulating the activities of particular LXRα oligomers.

CHAPTER III

DEFINING REQUIREMENTS FOR HETERODIMERIZATION OF THE HUMAN LIVER X RECEPTOR ALPHA MEDIATED HETERODIMERIC COMPLEXES

1. Abstract

Liver X receptor alpha (LXRα) plays a critical role in the maintenance of lipid and cholesterol homeostasis. Ligand binding and dimerization with retinoid X receptor (RXR) or peroxisome proliferator-activated receptor (PPAR) is required for forming active DNA binding complexes leading to gene regulation. Structure based prediction and solvent accessibility of LXRα LBD shows that residues H383, E387, H390, L414, and R415 which are located in helices 9 and 10 may be critical for mediating protein-protein interactions. In this study, LXRα interface residues were individually mutated to determine their effects on ligand binding, protein-protein association, subcellular localization, and transactivation activity. Ligand binding studies showed that T-0901317 did not bind to mutants L414R and R415A, but binding to 25-HC was retained. Fluorescent protein-protein binding assay demonstrated a decreased affinity of L414R for RXRα, but not for PPARα. Binding of LXRα mutants L414R or R415A with PPARα resulted in little or no conformational changes in the secondary structure of the dimers as determined by circular dichroism spectroscopy. Cell based bimolecular fluorescence complementation assays exhibited a weak fluorescent signal for L414R-RXRα, but strong fluorescent signal for the L414R- PPARα dimers. Furthermore, all LXRα mutants exhibited either lower or similar levels of ligand dependent luciferase activity driven by the SREBP-1c promoter. Taken together, our study demonstrates that charge reversal at the interface surface alters selectivity of LXRα dimerization, ligand binding, and reduces the ligand-dependent transactivation activity in a promoter-dependent manner.

2. Introduction

Nuclear hormone receptors PPARα and LXRα are ligand activated transcription factors that are activated by fatty acids and oxysterols respectively (*1, 66*). These receptors act as sensors of elevated levels of fatty acids and cholesterol derivatives *via* the receptor ligand binding domain (LBD) to regulate the expression of genes involved in controlling cholesterol and lipid metabolism (*74, 100*). PPARα and LXRα can heterodimerize and each also can dimerize with retinoid X receptor (RXR) with high affinities. The corresponding dimers are the functionally active forms of these receptors (*43*). Due to the crucial roles of these receptors in maintaining a constant level of lipids in cells, PPARα and LXRα represent interesting targets for the development of pharmacological compounds in the treatment of metabolic disorders (*101*). Drugs targeting these receptors exhibit anti-atherogenic, anti-inflammatory, and anti-diabetic effects. These effects are also associated with elevated levels of plasma triglycerides due to upregulation of master lipogenic enzyme SREBP-1c (*90, 102*). Thus, there is an interest in investigating regulation of the PPARα-LXRα heterodimer to explore an alternative strategy for the pharmacological manipulation of PPARα and LXRα.

Both nuclear receptors have two well-structured domains, a central DNA binding domain and a C-terminal LBD (*14*). In addition to mediating receptor dimerization, the LBD performs a number of functions such as ligand binding, recruitment of coactivators, transcriptional activation, and repression (*103-105*) Inspection of the crystal structure of LXRα-RXRβ LBDs (PDB entry 1UHL) shows that the LXRα LBD interface is made up of amino acid residues in helices 9 and 10 (*26*). Residues lining these helices provide the locus for the majority of heterodimerization or homodimerization interaction. In particular, amino acid residues H383, E387, and H390 (helix9) and L414 and R415

(helix10) are located on the surface of LXRα and undergo significant changes in the accessible surface area upon receptor dimerization (*26*). Critical determinants of LXRα dimerization have not been characterized yet and variants of LXRα that exhibit selective dimerization or ligand binding properties are unknown.

Previous work suggests that mutations have the ability to confer selectivity in protein binding; RXRα mutants (A416D, R421L, and A416K) exhibit selectivity in binding with thyroid hormone receptors and retinoid acid receptors (*106*). Although similar studies in the LBD of LXRα have not been conducted, mutation at R415 to A was found to lack ligand dependent transactivation activity in the context of the ADH promoter when challenged with T0901317 (*45*). This suggests that residue R415 may stabilize LXRα-RXR complexes, thus it is likely that loss of interactions between R415 and corresponding residues on RXR would abolish or disorganize dimerization. In addition to causing perturbations in the dimer formation, LXRα mutation R415A may have long-range structural and functional consequences. Consistent with this observation, I hypothesized that charge reversal of key residues at LXRα interface may provide selectivity in the choice of heterodimer binding and hence downstream gene regulation. To test our hypothesis and to investigate the effects of mutating interface residues on LXRα function, individual amino acid residues were mutated at putative protein-protein contact points of LXRα and the effects on dimerization, ligand binding, and transactivation activity were measured.

Single point mutations in the LXRα LBD were generated using site-directed mutagenesis and the apparent dissociation constants (K_d) of PPARα -LXRα interactions of mutant proteins relative to wild-type were measured. Circular dichroism (CD) was

applied to study (a) the effect of mutations alone on LXRα secondary structure, and (b) the conformational changes induced in the dimers due to protein-protein binding. Bimolecular complementation assays demonstrated that LXRα mutant, L414R, is selectively impaired in dimerization with RXRα but not with PPARα. A previously identified LXRα mutant, R415A, exhibited intact dimerization but showed selective loss in ligand binding to T0901317. Molecular modeling was performed to visualize the orientation of ligands in the LXRα ligand binding pocket and it showed differences between the positioning of ligands between wild-type and mutant receptors consistent with the previous results. Finally, a transactivation assay showed that LXRα L414R lacked transactivation activity when tested in the context of SREBP-1c promoter. On the other hand, LXRα R415A behaved similar to wild-type LXRα in transactivation activity in the context of SREBP-1c promoter, but exhibited lower activity on ApoA1 promoter.

3. Materials and methods

Chemicals: All ligands were purchased from Sigma-Aldrich (St. Louis, MO). Cy^{TM}3 Ab labelling kit was purchased from GE Healthcare. BiFC cloning vectors pBiFC-VN173 (pFLAG-Venus 1-172), pBiFC-CN173 (pFLAG-Venus 1-172), and pBiFC-CC155 (pHA-ECFP 155-238) were supplied by Dr. Chang-Deng Hu (Purdue University) (*107*).

*Mutagenesis and purification of recombinant mutant hLXRα proteins***:** The purification of recombinant wild-type 6xHis-GST-hLXRα and 6xHis-GST-hPPARα proteins have been described earlier. LXRα mutant proteins were generated through overlap PCR of 6xHis-GST-hLXRα using the following primers:

LXR H383E	Forward 5'- AGAGGCTGCAGGAGACATATGTGGA -3'
	Reverse 5'- TCCACATATGTCTCCTGCAGCCTCT -3'
LXR E387Q	Forward 5'- CACACATATGTGCAAGCCCTGCAT -3'
	Reverse 5'- ATGCAGGGCTTGCACATATGTGTG
LXR H390E	Forward 5'- GAAGCCCTGGAAGCCTACGTC -3'
	Reverse 5'- GACGTAGGCTTCCAGGGCTTC -3'
LXR L414R	Forward 5’-CTGGTGAGCCGCCGGACCCTG-3’
	Reverse 5’-CAGGGTCCGGCGGCTCACCAG-3’
LXR R415A	Forward 5’-CTGGTGAGCCTCGCGACCCTG-3’
	Reverse 5’-CAGGGTCGCGAGGCTCACCAG-3’

The PCR products containing *EcoRI-HF* and *NotI-HF* sites were used to replace wild-type LXRα with the mutant LXRα PCR fragment in the appropriate vectors. The presence of single point mutations was confirmed by DNA sequencing. Plasmids were then transformed into Rosetta 2 competent cells and used to produce recombinant mutant full-length hLXRα proteins through affinity chromatography as described for hPPARα and wild-type hLXRα (*44, 86, 89*). Protein concentration was determined by the Bradford

assay (Bio-Rad, Hercules, CA) and by absorbance spectroscopy using the molar extinction for the protein. Protein purity was determined by sodium dodecyl sulfate-polyacrylamide gel electrophoresis (SDS-PAGE), followed by Coomassie Blue staining.

*Quenching of endogenous fluorescence of Mutant LXR*α *by Ligands:* The direct binding of LXRα mutant recombinant proteins to non-fluorescent ligand T-0901317 was determined by quenching of intrinsic LXRα aromatic amino acid fluorescence. Mutant LXRα (0.1 μM) was titrated with increasing concentrations of T-0901317 in PBS, pH7.4. Emission spectra from 300-400 nm were obtained at 24°C upon excitation at 280 nm with a PC1 photon counting spectrofluorometer (ISS Inc., Champaign, IL). Data were corrected for the bound protein, active protein present, background and inner filter effects, and maximal intensities were used to calculate the apparent dissociation constant (K_d) values as described (*86, 89*).

Circular Dichroism Spectroscopy: Circular dichroism was used to examine changes in the secondary structure upon heterodimerization of hPPARα with each of the mutant hLXRα proteins. Briefly, CD spectra of protein complexes were obtained by use of a Jasco J-815 CD spectrometer. Circular dichroic spectra of a mixture of PPARα and wild-type or mutant LXRα (0.2 μM final concentration each in 30 mM NaCl, 2 mM Tris, pH 8.0, 0.04% glycerol buffer) were measured in the presence and absence of ligands. Spectra was recorded from 260 to 187 nm with a bandwidth of 2.0 nm, sensitivity of 10 millidegrees, scan rate of 50 nm/min and a time constant of 1 s. Ten scans were averaged for percent compositions of α-helices, β-strands, turns and unordered structures with the CONTIN program of the CDpro software package (*44, 86, 88, 89*). The CD spectrum of the mixed proteins was compared to a theoretical spectrum

of combined but noninteracting proteins. The theoretical spectrum was calculated by averaging the spectra of each protein in the mixture analyzed separately at a concentration equal to that in the mixture as described (*44*).

Protein-protein binding experiments- Recombinant PPARα was fluorescently labeled with Cy3 dye using Fluorolink-antibody Cy3 labeling kit (Amersham Biosciences, Pittsburgh, PA) as described (*44*). Emission spectra (560-650 nm) of 25 nM Cy3-labeled PPARα were recorded in PBS, pH 7.4 upon excitation at 550 nm with increasing concentrations of unlabeled LXRα in a Cary Eclipse fluorescence spectrophotometer at 24^0C. The spectra were corrected for background (buffer, solvent, and protein alone), and the maximal intensities were recorded. To determine the effects of ligands on LXRα-PPARα interaction, the experiments were repeated in the presence of each ligand at a concentration determined by their binding affinities. Protein-protein binding curves were analyzed by nonlinear regression analysis using the ligand binding function in Sigma Plot (SPSS Inc., Chicago, IL). The apparent dissociation constant (K_d) values were obtained as previously described (*44*).

Bimolecular Fluorescence Complementation Assay (BiFC) for Visualization of Dimers in Living Cells- Plasmids encoding full-length 6xHis-GST hPPARα, 6xHis-GST hLXRα, and 6xHis-GST hRXRα were digested with *BamH1-HF/Not1-HF* or *EcoR1/Not1* and ligated into pBiFC vectors to generate Venus-hPPARα, ECFP-hLXRα, and Cerulean-hRXRα plasmids. All constructs were verified by DNA sequencing. COS-7 cells were grown to 50-70% confluence in DMEM supplemented with 10% FBS at 37ºC with 5% CO_2 in a humidified chamber. Cells were seeded onto Lab-Tek chambered cover glass and transfected with 0.7 µg of each BiFC plasmid using Lipofectamine 2000. The

growth media and transfection reagent were replaced with serum-free media twenty-four hours after transfection and allowed to grow for additional 20-24 hours before image acquisition using a fluorescence microscope (*107*).

Molecular Docking- The LBD of LXRα was extracted from the crystal structure of LXRα-RXRβ (PDB entry 1UHL) using SPDBV (*26*). The mutant LXRα files utilized as input for docking were prepared using AutoDock Tools and subjected to energy minimization. Docking of T-0901317 to the LXRα LBD was performed using AutoDock Vina 1.1.2 and FlexiDock^{TM} module on SYBYL-X 2.0 as described (*89*). The output generated consisted of docking poses and binding energies that were ranked in the order of the most favorable to the least favorable binding energy.

Mammalian Expression Plasmids: The generation of pSG5-hPPARα and pSG5-hLXRα plasmids has been described (*44*). Mutant hLXRα mammalian expression plasmids were generated by subcloning *MscI-XhoI* hLXRα mutant fragment from 6xHis-GST hLXRα into *MscI-XhoI* site of pSG5-hLXRα. The human sterol regulatory element binding protein 1c (hSREBP-1c) minimal promoter (-520 to -310) (*90*) containing the LXRE was cloned into the pGEM-T easy vector (Promega) and subsequently transferred into *Kpn*I-*Xho*I sites of pGL4.17 (Promega) to produce hSREBP-1c-pGL4.17. The human ApoA1 promoter was amplified with the following primers: tggtaccAGAGGTCTCCCAGGCTAAGG and cgaattcGCAGTAACCTCTGCCTCCTG.

The PCR product was cloned into the pGEM-T easy vector and subsequently transferred into pGL4.17 to produce hApoA1-pGL4.17. All constructs were verified by DNA sequencing.

Cell culture and Transactivation assay: COS-7 cells (ATCC, Manassas, VA) were grown in DMEM supplemented with 10 % fetal bovine serum (Invitrogen, Grand Island, NY) at 37°C with 5% CO_2 in a humidified chamber. Cells were seeded onto 24-well culture plates and transfected with 0.4 µg of each full- length mammalian expression vector (pSG5-hPPARα, pSG5- wild-type or mutant hLXRα or pSG5-hRXRα) or empty plasmid (pSG5), 0.4 µg of the LXRE LUC reporter construct (hSREBP-1c) or hApoA1, and 0.04 µg of the internal transfection control plasmid pRL-CMV (Promega Corp., Madison, WI) with Lipofectamine™ 2000 (Invitrogen, Grand Island, NY). Following transfection incubation, medium was replaced with serum-free medium for 2 h, ligands (10 µM) were added, and the cells were grown for an additional 20 h. Firefly luciferase activity, normalized to *Renilla* luciferase (for transfection efficiency), was determined with the dual luciferase reporter assays system (Promega, Madison, WI) and measured with a SAFIRE^2 microtiter plate reader (Tecan Systems, Inc. San Jose, CA). The sample were normalized against the sample with no ligand (*44*).

Statistical Analysis: Data were analyzed by Sigma Plot™ (Systat Software, San Jose, CA) and a one-way ANOVA was used to evaluate overall significance. The results are presented as mean ± SEM. The confidence limit of $p < 0.05$ was considered statistically significant.

4. Results

Generation of LXRα mutants: To identify putative residues at the LXRα interface that may mediate interactions with PPARα, site specific mutants of LXRα were generated based on solvent accessibility of residues located in helices 9 and 10. These helices form the LXRα interface in the three dimensional structure of LXRα-RXRβ crystal structure [PDB 1UHL] (*26*). As shown in Fig. 21A, amino acid residues H383, E387, H390, L414, and R415 are located on the surface of helices 9 and 10 and undergo changes in solvent accessibility upon dimerization (Table 4). These residues were predicted to stabilize the LXRα interface. With the intent of neutralizing charge at the interface to generate LXRα mutants that may have altered receptor selectivity, H to E, E to Q, and L to R, LXRα mutants were generated. The assignment of helices H9 and H10 together with the point mutations of amino acids implicated in receptor dimerization are shown in Fig. 21B.

A

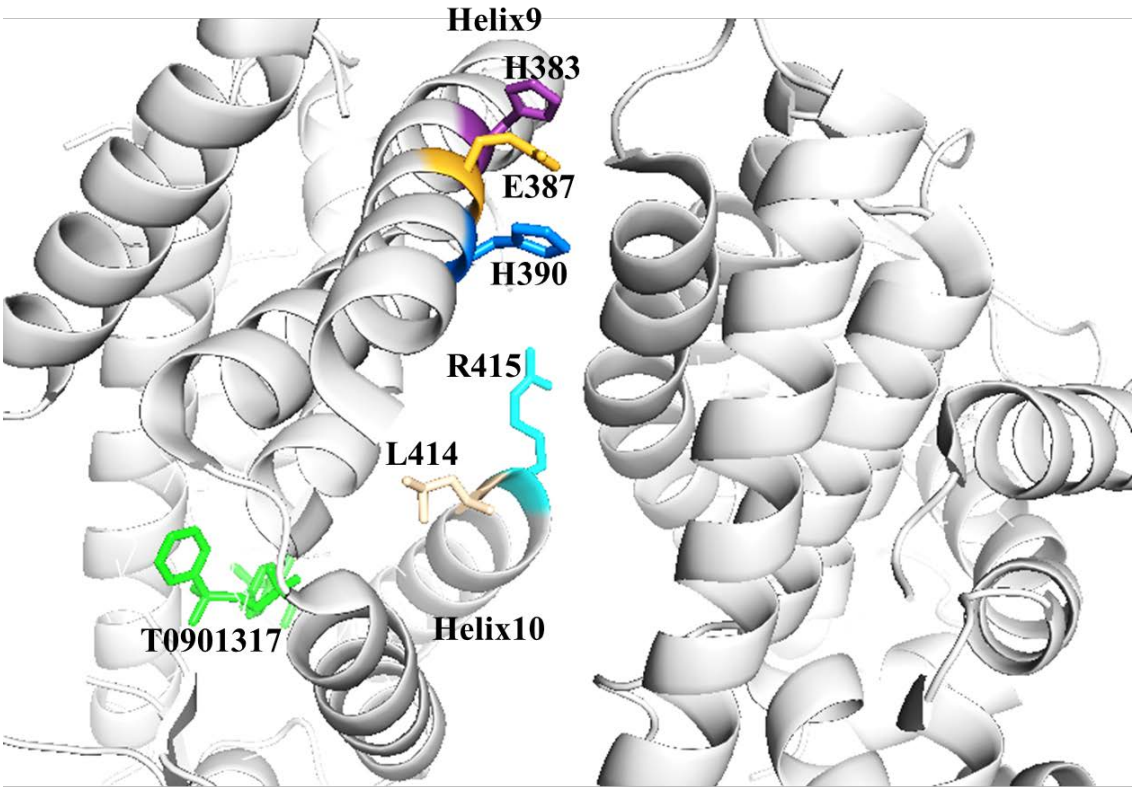

B

Location of LXRα mutation	Helix 9	Helix 10
Mutated LXRα residue	H383E E387Q H390E	L414R R415A

Fig.21. Interface of LXRα-RXRβ heterodimer showing the positioning of solvent accessible residues (**A**) Contacts across the LXRα dimer interface. Location of amino acid residues H383, E387, H390, L414, and R415 in helices 9 and 10 across the LXRα-RXRβ heterodimer as proposed in the crystallographic structure (PDB 1UHL) **(B**) Schematic representation of the LXRα domain structure showing single point mutations.

TABLE 4: Exposure of Amino Acid Residues Predicted at LXRα Interface. Prediction generated using InterProSurf Protein-Protein Interaction Server

Amino Acid Residue	Residue Number	Monomer Area (A^o)	Complex Area (A^o)	Change in Accessible Surface Area
H	383	106.38	66.79	39.59
E	387	79.59	15.15	64.44
H	390	82.98	39.46	43.52
R	415	92.80	17.52	75.28

Full-length mutant LXRα protein purification: Recombinant full-length mutant hLXRα proteins were expressed in Rosetta 2 cells and purified using affinity chromatography as described for wild-type LXRα protein (*44*). SDS-PAGE and Coomassie blue staining indicated predominant bands of 50 kDa corresponding to the expected size of full-length hLXRα, for which the purity was determined to be approximately 75% (Fig. 22). The single point mutations of LXRα did not dramatically alter the secondary structure as was evident using far-UV CD spectrometry (data not shown).

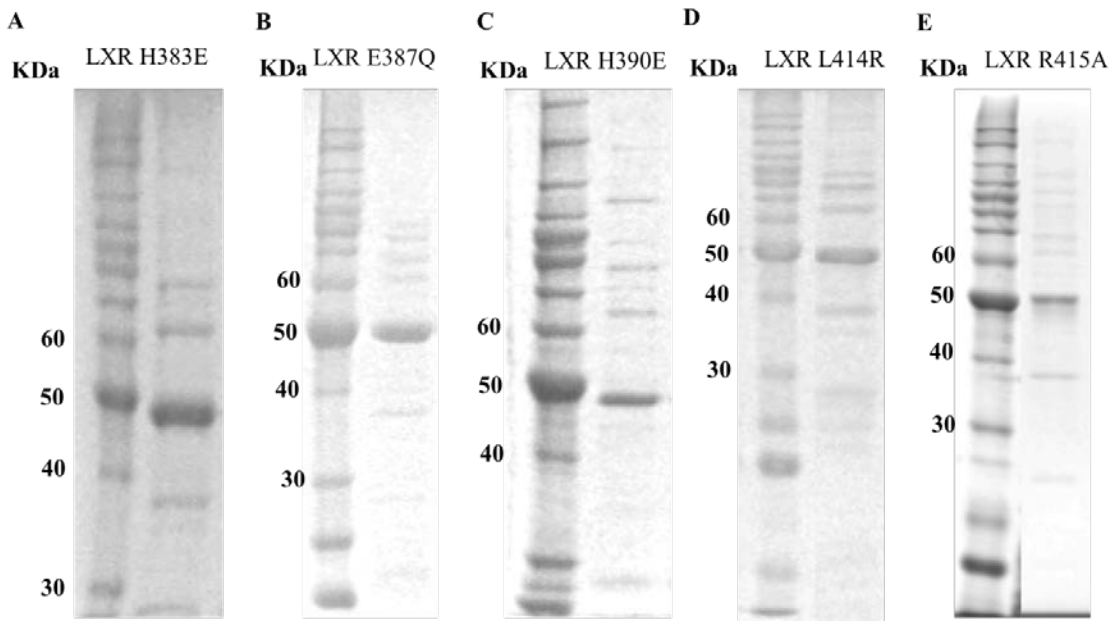

Fig.22. SDS-PAGE and Coomassie blue staining of purified recombinant hLXRα mutant proteins (**A**) H383E, (**B**) E387Q, (**C**) H390E, (**D**) L414R, and (**E**) R415A. The prominent bands at approximately 50kDa are full-length, untagged recombinant mutant LXRα proteins.

Ligand Binding Profile of LXRα mutants: The effect of each LXRα mutation on ligand binding was investigated. Apparent dissociation constant (K_d) values of purified recombinant proteins for T-0901317 were determined using intrinsic quenching of LXRα aromatic amino acids. As seen in Fig. 23A-B, titration of wild-type or H383E LXRα proteins with T-0901317 yielded saturation curves with an apparent K_d = 3±1 nM. Titration of LXRα E387Q and H390E proteins with T0901317 also yielded decrease in protein fluorescence, however, the binding curves exhibited smaller changes than wild-type and H383E LXRα, suggesting lower affinity ligand binding (apparent K_d = 24±7 nM and 26±6 nM respectively) (Fig. 23C-D). T0901317 did not cause significant changes in the intrinsic fluorescence of the L414R and R415A proteins suggesting no binding occurred (Fig. 23E-F). All mutants, except H390E, bound the endogenous ligand 25-HC at nanomolar concentrations similar to that for wild-type LXRα suggesting that mutations did not have detrimental effects on LXRα binding to the relatively weaker endogenous ligand 25-HC (Fig. S5). None of the mutations compromised the folding of the protein as determined by the circular dichroic spectra of the individual proteins (data not shown). The selectivity in ligand binding was further investigated through computational-based molecular modeling of T-0901317 to energy-minimized wild-type, L414R, and R415A LXRα LBDs in the absence of water molecules (Fig. 23G). The deviation from the positioning of ligand in wild-type was greater in the R415A mutant than in the L414R LXRα mutant. Calculation of the corresponding hydrogen bonds and hydrophobic interactions between the ligand and residues lining the LXRα LBP was performed using LIGPLOT analysis. The head group of T-0901317 formed hydrogen bonds with His421 in wild-type, H383E, E387Q, and

H390E, but not with L414R and R415A LXRα (Fig. S6).

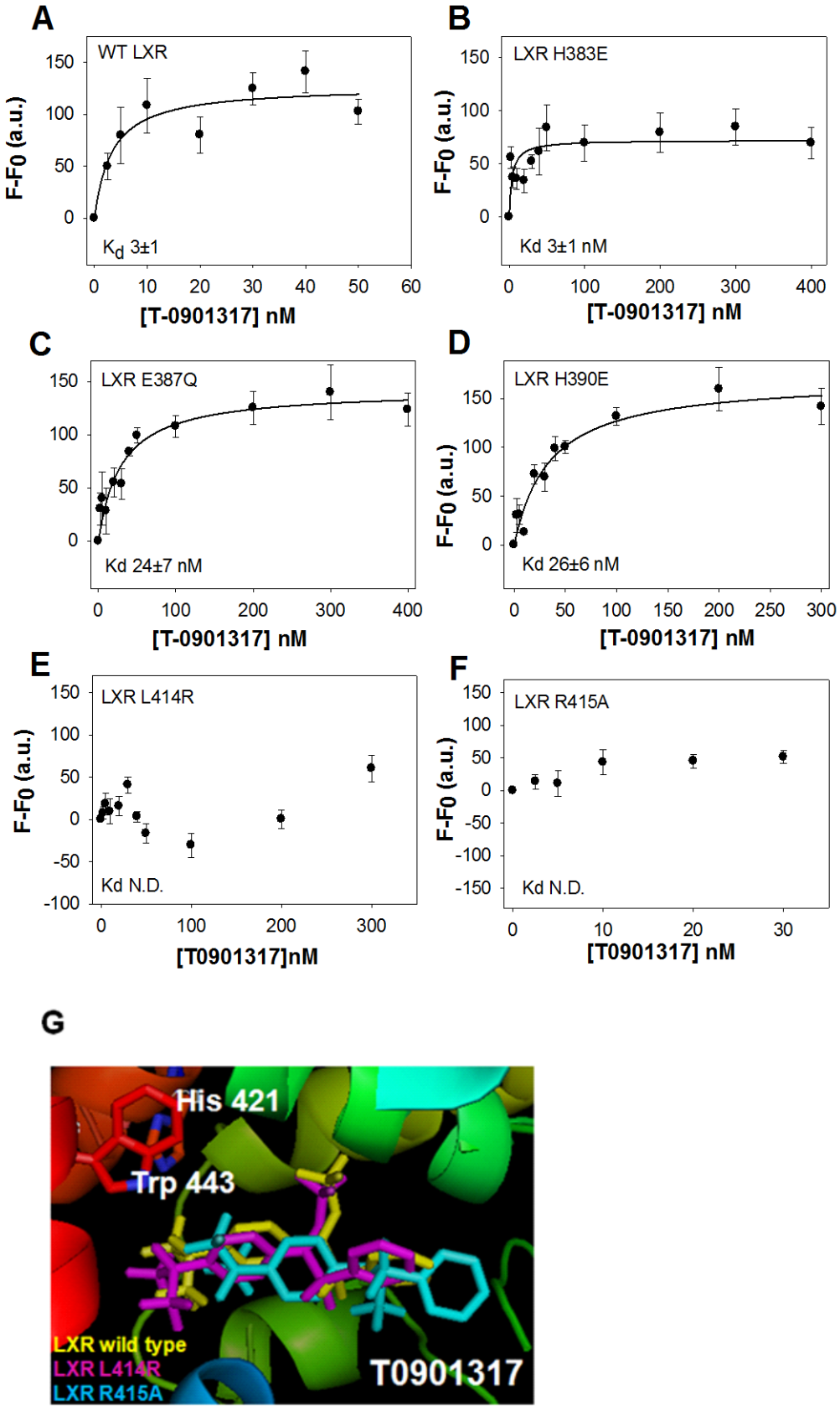
A
WT LXR
F-F0 (a.u.)
Kd 3±1
[T-0901317] nM
B
LXR H383E
F-F0 (a.u.)
Kd 3±1 nM
[T-0901317] nM
C
LXR E387Q
F-F0 (a.u.)
Kd 24±7 nM
[T-0901317] nM
D
LXR H390E
F-F0 (a.u.)
Kd 26±6 nM
[T-0901317] nM
E
LXR L414R
F-F0 (a.u.)
Kd N.D.
[T0901317]nM
F
LXR R415A
F-F0 (a.u.)
Kd N.D.
[T0901317] nM
G
His 421
Trp 443
LXR wild type
LXR L414R
LXR R415A
T0901317

Fig.23. Intrinsic quenching (**A**) wild-type, (**B**) H383E, (**C**) E387Q, (**D**) H390E, (**E**) L414R, and **(F**) R415A LXRα aromatic amino acids by binding to T-0901317. Three independent experiments were performed for each analysis. (**G**) Docking of T-0901317 to the LXRα LBD shows the relative positioning of ligand in the ligand binding pocket of the receptor. LXRα LBD was extracted from the crystal structure of LXRα-RXRβ (PDB entry 1UHL).

Computational–based prediction of free energies of ligand binding in LXRα mutants: *In silico* molecular docking allows distinction of binding molecules from nonbinding molecules and is a method of choice for identification of potential binding sites for ligand-receptor complexes. Docking was employed to evaluate and compare ligand binding free energies of LXRα protein upon introducing mutations at the interface (Table 5). The binding free energies of T-0901317 binding obtained from docking were compared with the experimentally determined binding affinities of T-0901317 binding to LXRα (Figure 23). As seen in Table 5, LXRα mutants exhibited less favorable binding free energies for T-0901317 binding compared to wild-type LXRα. As the apparent K_d values for ligand binding increased in the mutants, the binding free energies also increased suggesting a decrease in affinity of T-0901317 for the mutants. One exception was LXR H383E that bound T-0901317 with a similar affinity as wild-type, but yielded a less favorable binding free energy from the docking simulation. It is important to consider here that the ranking assigned by the docking simulation is not an indication of binding constants, since the proposed models and free binding energies are an approximation made for protein in the absence of water. Hence, caution must be observed when comparing the predicted binding energies to the experimentally determined dissociation constant values.

TABLE 5: The binding free energies of T-0901317 binding to LXRα. The binding free energies (Kcal.mol^{-1}) of the protein-ligand complex were estimated by SYBYL

Protein	**T-0901317**
LXRα wild-type	-2047
LXRα H383E	-1421
LXRα E387Q	-1332
LXRα H390E	-1709
LXRα L414R	-1891
LXRα R415A	-1231

Dimerization of LXRα mutants with PPARα: Fluorescence spectroscopy was used to determine how efficiently each mutated form of LXRα dimerized with PPARα. Purified PPARα protein was fluorescently labeled with Cy3 dye at essentially one dye per protein molecule. Protein-protein binding curves were generated by plotting quenching of Cy3 dye as a function of LXRα concentration as previously described (*44*). The apparent binding dissociation constant values (K_d) of each LXRα mutant- PPARα dimer were determined. In the absence of added ligand, the apparent K_d values determined for PPARα binding to the wild-type LXRα and each of the mutants were found to range between 7 and 20 nM concentrations (Table 6). As seen in Fig. 24A, titration of Cy3-labeled PPARα with increasing concentrations of wild-type LXRα resulted in saturable binding curve at a low protein concentration indicative of high affinity binding. Single amino acid substitutions H383E and E387Q also generated binding curves, with affinities that were comparable to wild-type (Fig. 24B-C). Titration of Cy3-PPARα with H390E, L414R, and R415A exhibited weaker quenching of Cy3 fluorescence and weak binding was detected compared to wild-type LXRα (Fig. 24D-F). Estimation of the apparent dissociation constants of PPARα binding to LXRα mutants showed K_d values to be H383E < E387Q < L414R < Wild-type <R415A < H390E (Table 6). Although K_d values for wild-type or mutant LXRα binding to PPARα were not statistically different, differences were observed in the magnitude of Cy3 quenching by these proteins. H390E, L414R, and R415A were less efficient in quenching Cy3-PPARα compared to other proteins suggesting that the mutants might differentially dimerize with PPARα. Furthermore, L414R showed weaker binding to RXRα (Fig. S7) suggesting that residue L414 may be critical for protein-protein interactions of LXRα.

To determine the potency of ligands to affect protein-protein interactions, the binding affinities of PPARα for each LXRα mutant were determined in the presence of ligands as described (*44).* The K_d values of each complex upon ligand binding are summarized in Table 6. The binding of T0901317 decreased LXRα-PPARα interactions in wild-type, H383E, E387Q, L414R, and R415A mutants. H390E LXRα bound PPARα with three-fold lower affinity compared to wild-type. The addition of LXRα natural ligand, 25HC, decreased binding of PPARα to wild-type, E387Q, and R415A LXRα and enhanced binding to H390E and L414R mutants. The addition of PPARα agonist, palmitic acid decreased the interaction of PPARα with wild-type, E387Q, and R415A LXRα, and enhanced binding of H390E and L414R to PPARα (Table 6). These observations suggest that complexes composed of PPARα and LXRα mutants respond differentially to the addition of ligands.

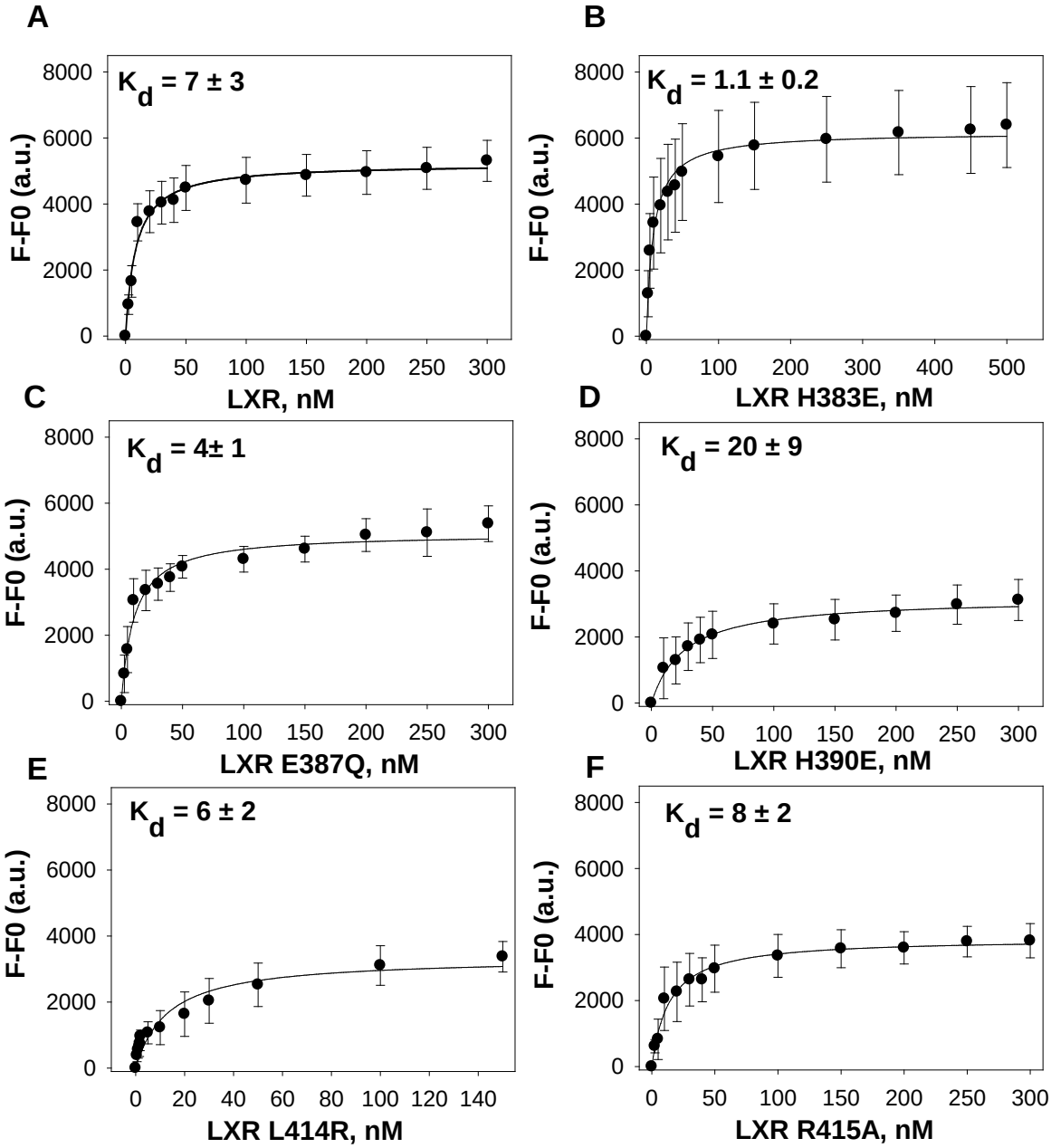
A
K_d = 7 ± 3
F-F0 (a.u.)
LXR, nM
B
K_d = 1.1 ± 0.2
F-F0 (a.u.)
LXR H383E, nM
C
K_d = 4± 1
F-F0 (a.u.)
LXR E387Q, nM
D
K_d = 20 ± 9
F-F0 (a.u.)
LXR H390E, nM
E
K_d = 6 ± 2
F-F0 (a.u.)
LXR L414R, nM
F
K_d = 8 ± 2
F-F0 (a.u.)
LXR R415A, nM

Fig. 24. Effects of mutations on dimerization of LXRα with PPARα. Cy3-labeled PPARα was titrated against increasing concentrations of unlabeled LXRα in the absence of ligand. Representative curves from fluorescence binding experiments are shown for binding of each LXRα mutant to PPARα. At least three independent experiments were performed for each analysis. K_d values represent means ± the standard error.

TABLE 6: Binding affinities of LXRα mutants for PPARα in the absence or presence of ligands (T-0901317 and 25-HC for LXRα and C16:0 FA for PPARα)

Protein	Wild-type K_d (nM)	H383E K_d (nM)	E387Q K_d (nM)	H390E K_d (nM)	L414R K_d (nM)	R415A K_d (nM)
No ligand	7 ± 3	1.1 ± 0.2	4 ± 1	20 ± 9	6 ± 2	8 ± 2
T-0901317	35 ± 6	8± 2	43 ± 7	3 ± 1	28 ± 6	18 ± 13
25-HC	16 ±3	1 ± 0.2	40 ± 9	2 ± 1	2 ± 0.9	56 ± 12
C16:0 FA	104 ±40	5± 0.5	21± 9	3 ± 1	3± 0.6	31 ± 17

Conformational changes in dimers composed of LXRα mutants and PPARα: Nuclear receptors are known to undergo conformational changes in the secondary structure upon binding to ligands or other macromolecules. Previous work demonstrated that PPARα and LXRα undergo a change in conformation upon interaction (*44*). The CD spectra of mutant LXRα proteins alone were qualitatively similar to that of wild-type suggesting that mutations do not impact the overall secondary structure of the mutant proteins (data not shown). To examine protein-protein interactions between PPARα and LXRα mutants, CD spectrum were measured upon mixing of proteins (Obs.) that was compared to the average of the sum of the ellipticities of the unmixed proteins (Calc.). As seen in Fig. 25A-D, spectra of mixtures of each mutant LXRα H383E, E387Q, and H390E with PPARα exhibited a more negative ellipticity at 222 and 208 nm similar to the spectra observed with wild-type LXRα-PPARα mixture. This suggests that binding of wild-type LXRα, and LXR H383E, E387Q, and H390E with PPARα resulted in a slight increase in the overall α-helical content. The observed spectra of LXRα L414R and R415A, in the presence of PPARα, either overlaid the calculated spectra or showed insignificant changes at the wavelengths of 222 and 208 nm (Fig. 25E-F). This suggests that PPARα binds weakly with L414R and R415A or protein binding is not accompanied by conformational changes in the overall secondary structures. Quantitative analyses confirmed these data, with no significant changes observed with L414R and R415A binding to PPARα (Table 7). Since, the mutants retained binding to either T-0901317 or 25-HC, the effect of ligands on the secondary structure of the dimers composed of PPARα and each of the LXRα mutants was investigated. None of the ligands tested caused significant ligand induced structural changes in dimers

composed of PPARα and L414R or R415A (Fig. S8). This suggests that ligands cause structural changes in the individual proteins, but not in the dimer composed of PPARα and LXRα L414R or R415A.

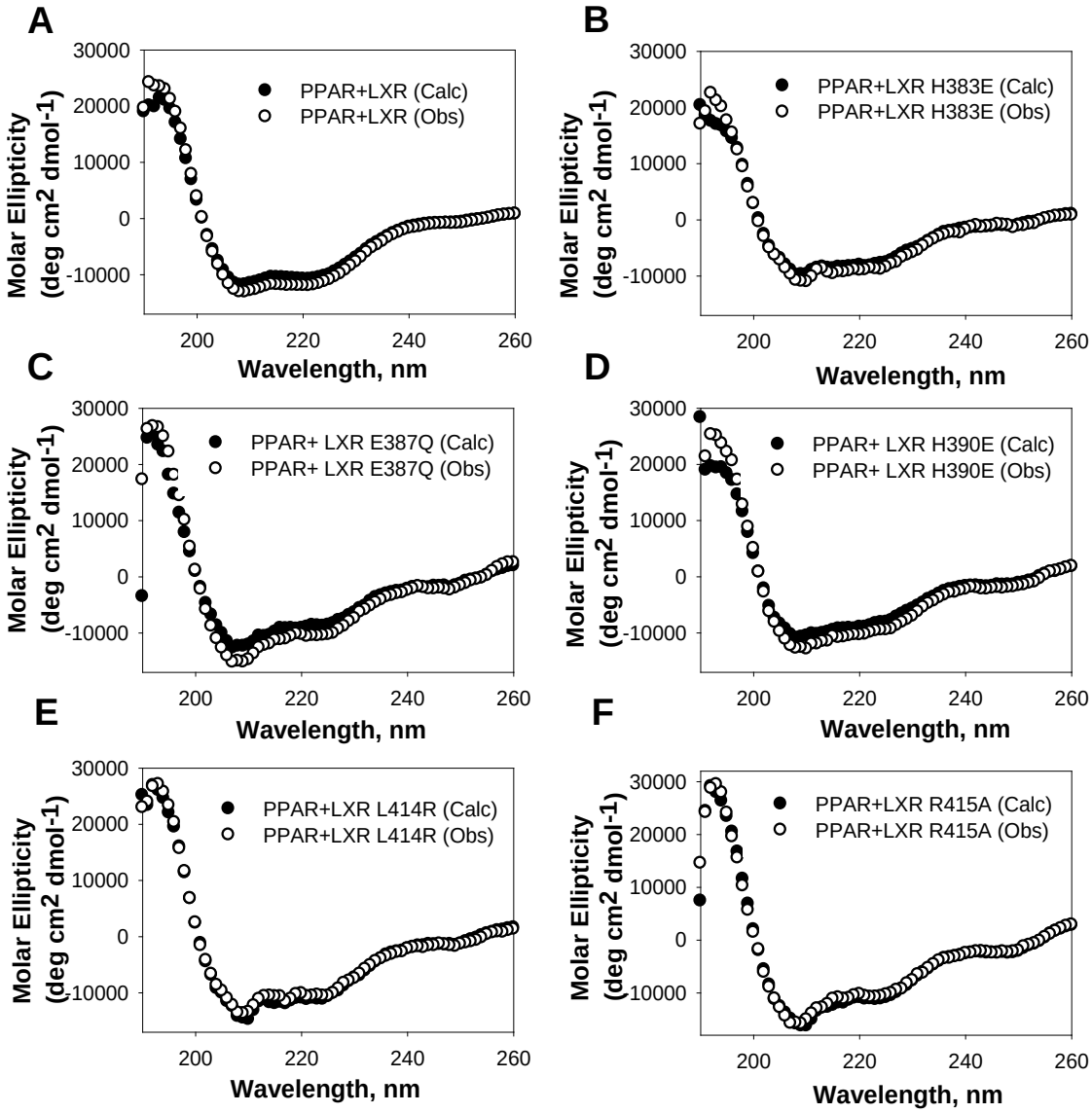
A
Molar Ellipticity (deg cm2 dmol-1)
30000
20000
10000
0
-10000
200
220
240
260
Wavelength, nm
PPAR+LXR (Calc)
PPAR+LXR (Obs)
B
PPAR+LXR H383E (Calc)
PPAR+LXR H383E (Obs)
C
PPAR+ LXR E387Q (Calc)
PPAR+ LXR E387Q (Obs)
D
PPAR+ LXR H390E (Calc)
PPAR+ LXR H390E (Obs)
E
PPAR+LXR L414R (Calc)
PPAR+LXR L414R (Obs)
F
PPAR+LXR R415A (Calc)
PPAR+LXR R415A (Obs)

Fig. 25. Far UV CD of the mixture of PPARα and LXRα proteins. Experimentally observed (Obs, open circles) circular dichroic spectrum of a mixture of 0.2 μM PPARα and 0.2 μM (A) wild-type, (B) H383E, (C) E387Q, (D) H390E, (E) L414R, and ((F) R415A LXRα compared to the calculated average (Calc, closed circles) of the individually obtained PPARα and LXRα spectra representing non-interacting proteins. The amino acid molarity for each spectrum was 0.0002 M, and each spectrum represents the average of at least three replicates, scanned 5 times per replicate.

TABLE 7: Secondary structures of hLXRα and hPPARα proteins in the absence of ligands[a]

Proteins	α-helix regular H(r)%	α-helix distort H(d)%	β-sheet regular S(r)%	β-sheet distort S(d)%	Turns T%	Unordered U%
LXRα	29.7 ± 1.0	23.3 ± 0.8	10.0 ± 1.0	11.0 ± 1.0	14.3 ± 2.0	11.0 ± 2.0
PPARα	28.0 ± 0.0	19.0 ± 1.0	9.3 ± 1.0	8.0 ± 1.0	14.3 ± 0.6	20.3 ± 2.0
PPARα/LXRα (Obs)	32.3 ± 1.2[b]	25.7 ± 0.6[b]	8.3 ± 0.6	8.0 ± 1.0	12.3 ± 0.3	13.0 ± 2.0
PPARα/LXRα (Calc)	27.0 ± 0	22.0 ± 1.0	8.0 ± 0.0	10.0 ± 0.0	15.0 ± 1.0	17.5 ± 1.5
PPARα/LXRα H383E (Obs)	24.0 ± 2.0	16.0 ± 1.0	10.5 ± 0.5[b]	8.0 ± 0.0	17.5 ± 1.5	24.5 ± 0.5[b]
PPARα/LXRα H383E (Calc)	21.5 ± 1.5	17.5 ± 1.5	14.0 ± 0.5	10.5 ± 3.5	17.0 ± 2.0	19.5 ± 0.6
PPARα/LXRα E387Q (Obs)	28.0 ± 0.0[b]	22.3 ± 0.6	8.6 ± 0.3	8.0 ± 1.0[b]	13.7 ± 0.3	19.9 ± 1.5[b]
PPARα/LXRα E387Q (Calc)	23.5 ± 0.5	23.5 ± 0.5	9.5 ± 1.5	14.0 ± 0.0	15.0 ± 1.0	13.5 ± 0.5
PPARα/LXRα H390E (Obs)	31.5 ± 0.5[b]	17.0 ± 1.0	10.0 ± 0.0	9.0 ± 1.0	12.0 ± 2.0	20.5 ± 0.5[b]
PPARα/LXRα H390E (Calc)	25.5 ± 0.9	15.8 ± 0.8	9.5 ± 1.1	8.7 ± 0.7	14.5 ± 0.6	25.2 ± 0.5
PPARα/LXRα L414R (Obs)	26.7 ± 0.8	19.3 ± 0.8	7.6 ± 0.3[b]	6.6 ± 0.3	16.0 ± 0.5	23.3 ± 0.8[b]
PPARα/LXRα L414R (Calc)	27.5 ± 0.5	18.0 ± 0.0	5.5 ± 0.5	6.0 ± 0.0	16.5 ± 0.5	26.0 ± 0.0
PPARα/LXRα R415A (Obs)	29.2 ± 0.8	23.4 ± 0.8	10.8 ± 0.5[b]	8.0 ± 0.6	12.8 ± 0.9	16.4 ± 1.3
PPARα/LXRα R415A(Calc.)	30.5 ± 0.5	23.5 ± 1.5	7.0 ± 1.0	8.5 ± 3.5	13.0 ± 2.0	16.5 ± 4.5

[a]Definitions: Obs, obtained experimentally; calc, calculated average. Significant difference between observed and calc for each protein mixture (n = 4-6). [b]$p < 0.05$.

Analysis of dimers in living cells using Bimolecular Fluorescence Complementation (BiFC): The ability of LXRα mutants to form heterodimers with RXRα and PPARα in living cells using fluorescence complementation was determined. BiFC plasmids encoding ECFP-LXRα, Cerulean-RXRα, and Venus-PPARα were generated for transfection in mammalian cells. The cells were transiently co-transfected with BiFC plasmids and dimerization was evaluated by fluorescence microscopy. As seen in Fig. 26, ECFP LXRα-Cerulean RXRα and ECFP LXRα-Venus PPARα complexes yielded CFP and YFP fluorescent signals respectively in a substantial fraction of cells suggesting that the BiFC system has the sensitivity to detect LXRα-RXRα and LXRα-PPARα interactions.

A similar approach was used to investigate the effect of LXRα interface mutations on dimerization. As seen in Fig. 26, complexes of LXRα mutants H383E, E387Q, H390E, and R415A with PPARα or RXRα showed nuclear localization and were indistinguishable from wild-type complexes. Co-transfection of mutant L414R with RXRα and PPARα resulted in a robust YFP fluorescence but non-existent levels of CFP fluorescence suggesting that LXR L414R specifically inhibited LXRα interaction with RXRα but not with PPARα. Immunoblot analysis revealed lower expression of RXRα protein levels in samples co-transfected with L414R mutant compared to wild-type and other mutated LXRα mutants (Fig. S9). This suggests that partner receptor that is unable to dimerize with LXRα or binds poorly to PPARα is unstable and undergoes proteolytic degradation.

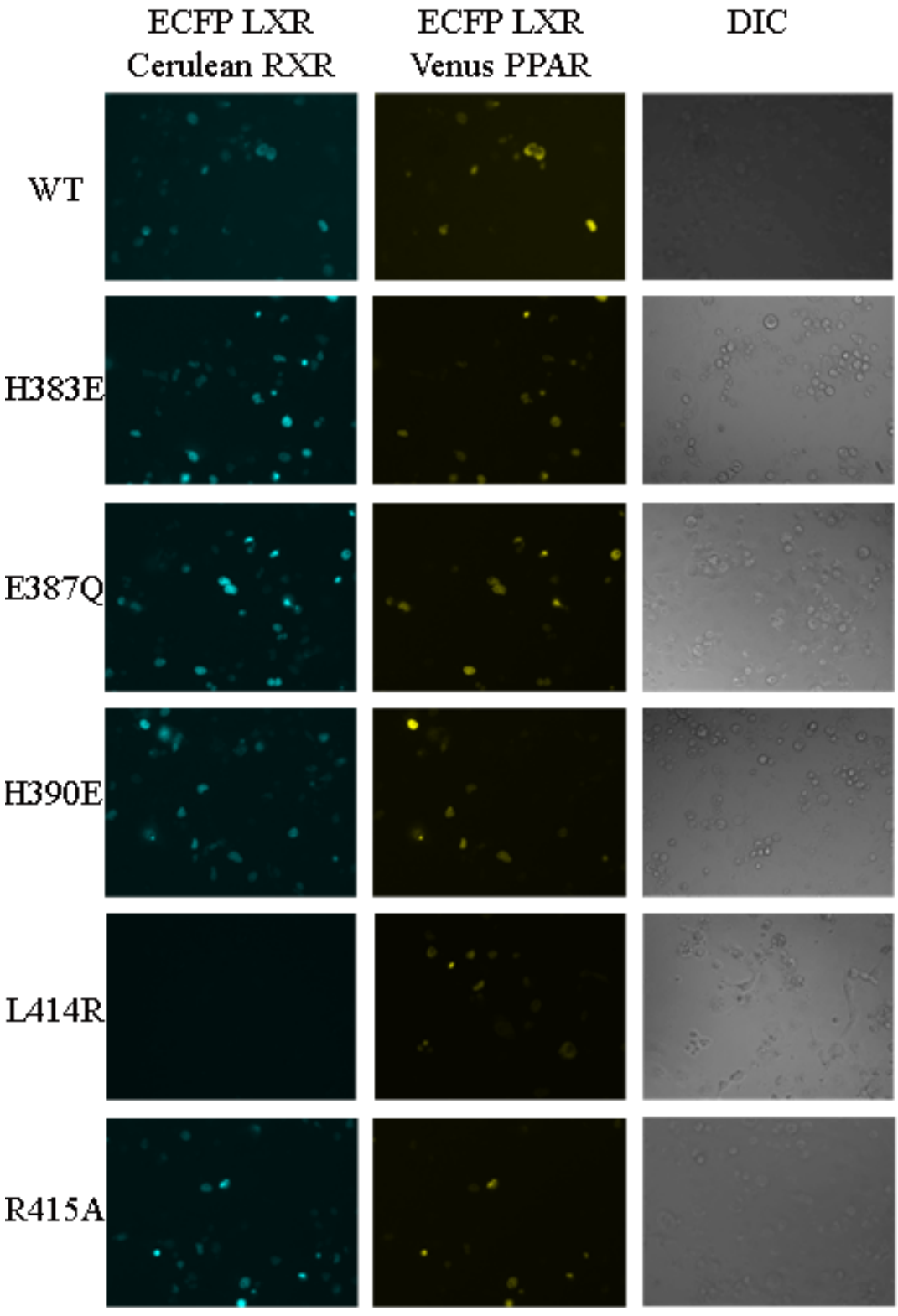
ECFP LXR
Cerulean RXR
ECFP LXR
Venus PPAR
DIC
WT
H383E
E387Q
H390E
L414R
R415A

Fig.26. Visualization of protein complexes composed of PPARα and (A) wild-type, (B) H383E, (C) E387Q, (D) H390E, (E) L414R, and (F) R415A LXRα in living cells using Bimolecular Fluorescence Complementation (BiFC) analysis. Fluorescence images of COS-7 cells expressing ECFP-LXR, Venus-PPAR, and Cerulean-RXR proteins were acquired 24 hours after transfection with indicated plasmids.

Residues at the LXRα interface are required for ligand-dependent transactivation activity: The SREBP-1c promoter contains two LXREs and is activated by LXR overexpression presumable through dimerization with endogenous RXR (*108*). No information exists on the identity of genes regulated by LXRα-PPARα heterodimers. However, unpublished data from our laboratory have identified human ApoA1 promoter to contain putative nucleotide sequences that preferentially binds LXRα-PPARα heterodimer. The effects of mutations on the ability of LXRα to dimerize efficiently and hence transactivate a known promoter (SREBP-1c) and a novel promoter (ApoA1) were evaluated using a luciferase reporter assay. Figure 27 illustrates the effects of overexpression of wild-type or mutant LXRα in COS7 cells in the absence or presence of 25HC on SREBP-1c promoter activity. Since COS7 cells express low levels of endogenous LXRα and PPARα proteins, interference of endogenous protein with the analysis of expressed proteins was unlikely. As shown in Fig. 27, wild-type LXRα activation of SREBP-1c promoter was slightly enhanced with the addition of 25-HC. Overexpression of mutants H383E, E387Q, and H390E exhibited an increase in basal promoter activity, whereas R415A exhibited similar basal activity, and L414R exhibited lower basal activity compared to wild-type LXRα. The basal activities of LXR H383E, E387Q, and H390E were higher than the levels displayed by wild-type LXRα in the presence of 25-HC. This suggests that these mutations resulted in a functional change that was independent of ligand binding for interacting with the SREBP-1c promoter.

LXRα activation of the SREBP-1c promoter in transfected COS7 cells was suppressed by cotransfection of PPARα (data not shown) consistent with the findings of Yoshikawa *et al* (*108*). Mutants H383E, E387Q, and H390E exhibited a ligand-induced

repression of the promoter activity, whereas, L414R and R415A showed no change in promoter activity with the addition of ligand. The effects on ligand-dependent activation of the promoter were not due to effects on ligand binding as all the mutants bind 25-HC as determined through intrinsic quenching assay (Fig. S6). Collectively, these data demonstrate a reduced ability of LXRα mutants to transactivate SREBP-1c promoter in a ligand dependent manner.

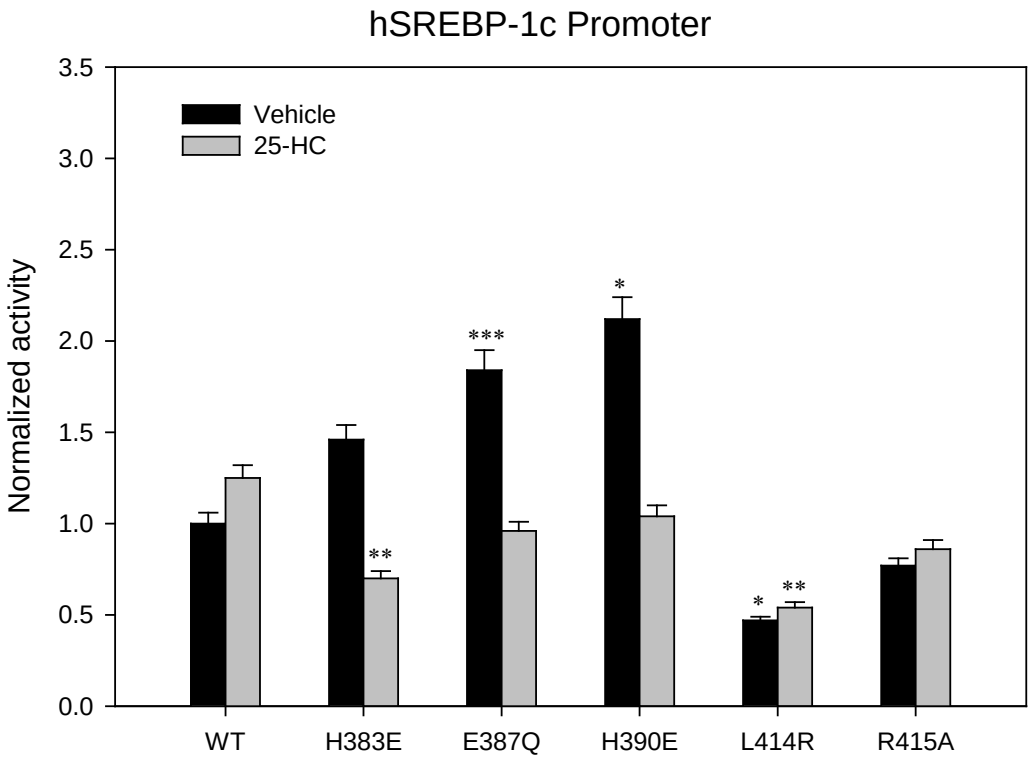
hSREBP-1c Promoter
Vehicle
25-HC
Normalized activity
3.5
3.0
2.5
2.0
1.5
1.0
0.5
0.0
*
***
*
**
*
**
WT
H383E
E387Q
H390E
L414R
R415A

Fig.27. Effect of LXRα interface mutations on luciferase reporter activation of human SREBP-1c promoter. COS-7 cells were co-transfected with pSG5 empty vector or each indicated LXRα plasmid and transactivation of the SREBP-1c LXRE-luciferase reporter construct in the presence of vehicle (solid bars) and 25-HC (Gray bars) was measured. Luciferase reporter activity was measured 18 hrs after the addition of vehicle or ligand and normalized using *Renilla* as an internal control. Asterisks denote significant differences due to single point mutations compared to wild-type LXRα for vehicle or 25-HC treated cells: *$p < 0.05$, **$p < 0.01$, ***$p < 0.001$.

Figure 28 shows the effect of LXRα mutations on the ability of LXRα to transactivate ApoA-1 promoter. Overexpression of each of the mutants H383E, E387Q, and L414R alone exhibited similar basal activity as wild-type LXRα. LXRα H390E exhibited enhanced basal activity, whereas R415A exhibited decreased basal activity compared to wild-type LXRα overexpression. This suggests that R415, but not L414, H383E, E3387, and H390, is critical for basal transactivation activity of ApoA1 promoter. All LXRα mutants tested exhibited decreased ligand-induced activation suggesting that the presence of each of these residues is required for ligand-dependent transactivation function of ApoA1 promoter. Cotransfection of LXRα and PPARα resulted in suppression of ApoA1 promoter activity similar to the effects observed on SREBP-1c promoter (data not shown).

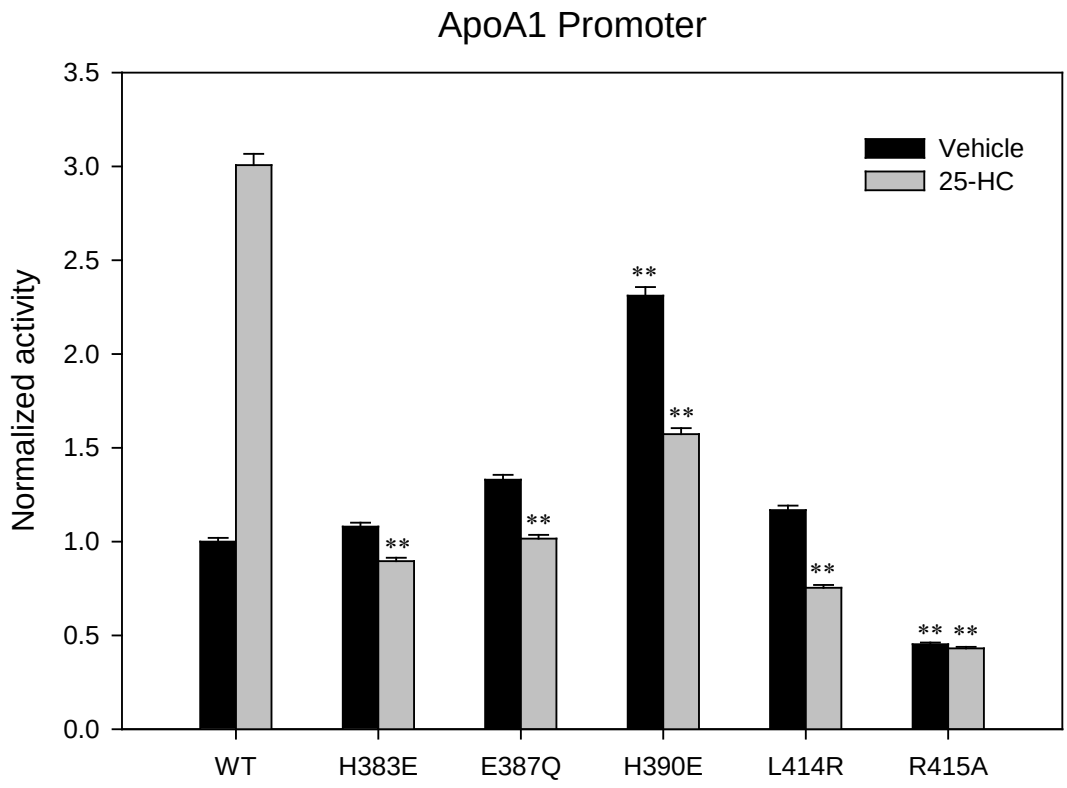
ApoA1 Promoter
Normalized activity
3.5
3.0
2.5
2.0
1.5
1.0
0.5
0.0
Vehicle
25-HC
**
**
**
**
**
**
**
WT
H383E
E387Q
H390E
L414R
R415A

Fig.28. Effect of LXRα interface mutations on luciferase reporter activation of human ApoA1 promoter. COS-7 cells were co-transfected with pSG5 empty vector or each indicated LXRα plasmid and transactivation of the ApoA1 luciferase reporter construct in the presence of vehicle (solid bars) and 25-HC (Gray bars) was measured. Luciferase reporter activity was measured 18 hrs after the addition of vehicle or ligand and normalized using *Renilla* as an internal control. Asterisks denote significant differences due to the single point mutations compared to wild-type LXRα for vehicle or 25-HC treated cells: *$p < 0.05$, **$p < 0.01$, ***$p < 0.001$.

5. Discussion:

The LBD of LXRα, similar to other nuclear receptors, is a multifunctional domain that mediates ligand binding, heterodimerization, cofactor recruitment, and ligand-dependent transactivation function. The three dimensional crystal structure of LXRα-RXRα LBD complex provides useful information regarding the identity of LXRα amino acid residues essential for dimerization. As proposed in the LXRα-RXRβ crystal structure, residues H383, E387, H390, and R415 in LXRα showed significant changes compared with other RXR dimers (*26*). Sequence alignment coupled with solvent accessibility further showed that residue L414 may also stabilize the dimer interface to mediate LXRα heterodimerization. Dimerization was evaluated through two approaches: (1) *in vitro* protein-protein binding assays, and by (2) bimolecular fluorescence complementation system in living cells. Our results demonstrate that the carboxyl-terminal amino acid of hLXRα (L414) is required for the formation of LXRα-RXRα complexes. Cell based BiFC analysis demonstrated that mutation of L414 to arginine resulted in disruption of LXRα-RXRα interactions, but not LXRα-PPARα interactions consistent with the *in vitro* findings. Complete conservation of LXRα L 414 in the corresponding sequences of other NRs suggests that this residue stabilizes protein-protein interactions with RXR in other heterodimeric pairs as well. Interestingly, a previous work identified a hPPARα point mutation (L433R corresponding to L414 in LXRα) that also abolished dimerization with RXR (*109*). Our findings combined with these previous results strongly suggest that the dimerization interface contains a leucine residue in LXRα, PPARα, and possibly other NRs that is indispensable for protein-

protein interactions with RXR.

Since LXRα H390E and L414R were less efficient in binding PPARα compared to wild-type LXRα, the possibility that these changes might reflect altered receptor conformations due to mutations themselves was considered. CD spectrum of each of the purified mutant LXRα proteins was found to be qualitatively similar to the spectra observed with wild-type LXRα protein suggesting that mutations alone did not result in gross conformational changes in the secondary structure of the proteins (data not shown). However, the calculated and the observed spectra of mixture of PPARα with either L414R or R415A were indistinguishable suggesting no observable conformational changes occurred in the proteins due to protein-protein binding. Subtle differences were observed between the calculated and the observed CD spectra for H383E, E387Q, and H390E LXRα in the presence of PPARα suggesting that binding of these proteins is accompanied by conformational changes in the dimer structure. It can be concluded that PPARα binding to LXRα H383E, E387Q, H390E, but not L414R and R415A, resulted in conformational changes in the secondary structure of the dimers.

Introduction of mutations L414R and R415A abolished binding of LXRα to synthetic agonist T-0901317, but not to 25-HC. A previous study with R415A mutant demonstrated that mutation at this position abolishes ligand dependent transactivation of ADH promoter in response to T-0901317 addition (*45*). The present results support previous conclusions that R415A is unable to respond to LXR ligand in a cell based reporter assay. Although the purification properties and the protein yield for the mutants were similar to those observed for wild-type LXRα protein, the altered ligand binding properties of L414R and R415A suggest that changes at the interface might cause subtle

rearrangement in the helices lining the LXRα ligand binding pocket.

To interpret the mutagenesis data with respect to ligand binding, molecular docking of ligands to the LXRα LBD extracted from the LXRα-RXRβ crystal structure (1UHL) was performed. The docked models revealed differences in the positioning of T-0901317 in the ligand binding pocket of the energy-minimized mutant receptors. In agreement with the experimental results presented here, docking of T-0901317 to the LBDs of LXR L414R and R415A was associated with unfavorable binding energies suggesting that these residues are critical for high affinity ligand interactions. LigPlot analysis showed that the head group of T-0901317 is positioned further away from His421 in the ligand pocket of LXRα mutant R415A (Fig. S6). Residue His421 in the LBP has been reported to be critical for agonist binding to LXRα (*26*) and differential positioning of T-0901317 in R415A relative to wild-type LXRα could explain the inability of this mutant to bind T-0901317.

The effect of mutations on the ability of LXRα to transactivate two promoters: SREBP-1c and ApoA1was also examined. The data demonstrated that residues H383, E387, and H390 are not necessary for basal activity of unliganded LXR, but are required for ligand-dependent transactivation function. Replacement of L414 with arginine significantly reduced SREBP-1c promoter reporter activity in a ligand dependent as well as ligand independent fashion without affecting the nuclear localization of LXRα. This supports the idea that conserved L414 in LXRα may be essential for ligand-independent and ligand-dependent transactivation functions. We postulate that substitution of a non-polar, hydrophobic amino acid, leucine, for the basic amino acid residue arginine may disrupt an ionic interaction or change the hydrophobic nature of the LXRα interface. As

most of the residues involved in the interactions between proteins and alpha-helices are hydrophobic in nature (*110),* introducing charge may prove detrimental for the formation of LXRα-RXRα, but not for LXRα-PPARα interactions. Moreover, the presence of two arginine residues adjacent to each other in L414R mutation may further contribute to destabilization of the dimer.

We next investigated whether the effect of L414R mutation on transactivation is promoter specific. The basal transactivation activity of L414R was indeed similar to that of wild-type LXRα on the ApoA1 promoter. However, the ligand dependent transactivation activity on the promoter was abolished. These findings suggest that the LXRα mutants have differential effects dependent upon promoter context. Thus, a mutant that is non responsive to the addition of ligands and unable to regulate a specific gene may be activated by different agonists and could regulate different subset of genes. The findings here have important implications for the development of novel therapies, in particular for the design of LXR modulators in the treatment of metabolic disorders. For example, it would be desirable to design a molecule that mimics the effects of L414R mutation such that it exhibits modest SREBP-1c activity (to prevent hypertriglyceridemia) whilst up-regulating transcription of beneficial genes such as ApoA1 (to enhance reverse cholesterol transport).

In conclusion, this study provides insights into the functional roles of LXRα helices 9 and 10 and the long-range effects mutations may have in modulating various functions of LXRα. Evidence was provided that maintenance of hydrophobic interaction mediated by L414 at LXRα interface is required for dimerization with RXR and for optimal ligand-dependent transactivation function of LXRα. The data suggests that LXRα

mutants (identified here and other mutants implicated in metabolic disorders) may behave differently depending upon the nature of: (a) mutation, (b) ligand tested, and (c) the promoter under consideration. Moreover, the fact that the conserved leucine is also required for dimerization and transactivation of PPARα (and possibly other NRs) suggests the existence of a common mechanism for ligand-dependent transactivation among lipid sensing nuclear receptors.

SUMMARY AND CONCLUSIONS

Cholesterol plays several structural and metabolic roles that are vital for human biology. However, excess cholesterol can lead to pathological conditions such as atherosclerosis, which is a consequence of the accumulation of cholesterol into the cells of the arterial wall. As cholesterol is both crucial and lethal, organisms have developed regulatory networks to ensure maintenance of lipid homeostasis. LXR functions as a cholesterol sensor that regulates cholesterol transport and metabolism. The popularity of LXRs as attractive pharmacological targets stems from the fact that, in addition to playing a key role in maintaining cholesterol homeostasis, these receptors contain a hydrophobic pocket that binds a variety of small hydrophobic molecules (*111, 112*). Various synthetic LXR ligands that display anti-atherogenic properties in mice have been developed. Despite the favorable responses induced by LXR agonists in animal models, these compounds have not progressed to human trials due to side effects such as hypertriglyceridemia. Hence, there has been an immense interest in identifying novel ligands for LXRs, synthetic as well as natural, that may be tweaked to design better drugs with fewer adverse effects in the treatment of metabolic disorders.

The identification of ligands may be performed based on function, such as transactivation of a reporter gene in a transient transfection assay or via direct binding to the receptor. Herein, we have utilized both strategies to investigate the effects of chain length and degree of unsaturation on fatty acid binding to LXRα. We have reported interactions between full-length LXRα protein and fatty acids in quantitative terms

(dissociation constant values) and demonstrated that transactivation activity of LXRα is modulated in response to 25-HC (canonical endogenous ligand) and medium chain fatty acids (novel ligand). Although transactivation assays are a method of choice for identifying novel ligands and/or potential drugs, these assays may lead to false positives by identifying receptor activators, of which only a subclass may actually be bona fide ligands. The compounds could, for example, alter a signal transduction pathway that in turn affects the phosphorylation state of the receptor, and it is that phosphostate, and not direct ligand binding, that affects function. It is also possible in reporter gene assays that a compound may activate an endogenous receptor, which in turn affects the expression and/or activity of the ectopically expressed receptor being tested (*113*). Alternatively, a compound could be a precursor to the true ligand, as may be the case for the free fatty acids that were originally identified as ligands for PPARα by transfection assays (*114*). To circumvent these problems, we utilized a variety of biophysical assays to provide evidence of direct binding of fatty acids to LXRα. Our data strongly suggests that medium chain fatty acids and/or their acyl CoA derivatives bind LXRα with high affinities (low nanomolar concentrations) and that such binding may or may not involve drastic changes in the secondary structure of the protein. Interestingly, there is a structural similarity between oxysterols and 25-dihydroxy-vitamin D3 suggesting that this metabolite could also potentially act as an LXRα agonist. The relative binding affinities and the functional significance of vitamin D binding to LXRα will be worth investigating in future.

The finding that dietary fatty acids can bind to LXRα and exhibit enhanced activity on SREBP-1c promoter suggests that these lipids are not just energy sources but

regulators of LXRα target genes. But the obvious question that arose was whether medium chain fatty acids have the potential to reach high enough concentrations in cells to activate LXRs. Although MCFA constitute a very minor fraction of the free fatty acids in plasma, these FA can be greatly elevated in certain disease states (*115*). Under these conditions, MCFA are likely to be present intracellularly at concentrations that are in good agreement with their dissociation constant (K_d) values. Thus, MCFA binding to LXRα is biologically relevant.

The activity of LXR is not only modulated through ligand binding, but also through posttranslational modifications such as glycosylation, ubiquitination, acetylation, sumoylation, and phosphorylation (*51-54*). One of the major concerns with the use of bacterially purified proteins in enzymatic assays is that the preparation might not be identical to the naturally occurring wild-type protein. The lack of efficient posttranslational modifications in bacterial cells might result in the purification of protein that might be largely insoluble or is improperly folded (*116*). Although we did not encounter such issues in the purification of recombinant LXRα, the possibility remains that lack of posttranslational modifications may have profound effects on responses to nutritional cues, receptor stability, or interactions with other nuclear proteins such as coactivators/corepressors etc. However, findings of our mammalian cell based transactivation assays were found to be in close agreement with the *in vitro* data obtained with bacterially purified proteins. This suggests that the *in vitro* results were not an artifact of the reaction conditions.

MCFA as treatment for metabolic disorders- Lifestyle-related diseases, such as obesity, hyperlipidemia, atherosclerosis, type 2 diabetes and hypertension, are

widespread and increasingly prevalent in industrialized countries. Subjects with metabolic syndrome have a threefold higher risk of developing coronary heart attack or stroke, and a twofold higher cardiovascular mortality than those without the syndrome. MCFA, present in coconut oil, palm kernel oil, butter, milk, yogurt and cheese, have been used for the dietary treatment of malabsorption syndrome because of their metabolic properties (*117*). Additionally, several reports suggest that MCFAs/MCTs offer the therapeutic advantage of preserving insulin sensitivity in animal models and patients with type 2 diabetes and cardiac diseases (*118*). Whether MCFAs/MCTs regulate these processes through modulation of LXRα will be of great interest in future studies. Since MCFA have also been shown to bind and modulate PPARγ, the therapeutic potential of MCFAs/MCTs in treating metabolic syndrome may be a combinatorial effect mediated through both receptors. Despite promiscuity displayed by nuclear receptors with respect to ligand binding, our data strongly suggests that MCFA are natural physiologically relevant LXRα modulators.

A recent study revealed three critical mutations in the LXRα LBD comprising of amino acids E324, P327, and R328. This mutation is responsible for the inability of LXRα LBD to interact with its endogenous ligands leading to deregulation of target genes (*119*). As the classical endogenous LXRα ligands mostly comprise of four linked hydrocarbon rings, it is possible that the distorted LBD in the triple mutant receptor is unable to accommodate the bulky steroid structure of oxysterols. On the other hand, MCFA that lack the bulky ring structures are more likely to fit in the LXRα triple mutant LBD. Future studies might explore MCFA as an alternative therapeutic option that may be used for treating such patients.

Ligand regulated dimerization of LXRα and PPARα- One of the debated questions is whether dimerization between LXRα and PPARα is induced by ligand binding. Several previous studies have utilized truncated forms of proteins to measure the binding affinities of LXRα mediated complexes (*43*). In contrast, this study focused on the interactions of full-length proteins (LXRα and PPARα) to demonstrate that binding dissociation constants of full-length proteins are different from those of LBDs. Unliganded LXRα protein bound PPARα at low nanomolar concentrations (K_d value of 8±2nM) indicative of high affinity binding. Furthermore, presence of ligands modulated the K_d, values for dimerization possibly through amino acid side-chain rearrangements. Although we have previously reported that the high affinity interaction between PPARα and LXRα proteins is abolished by the addition of polyunsaturated fatty acids and enhanced by the addition of relatively shorter saturated fatty acids (*44*), the effect of LXRα ligands on these interactions had not been investigated. This study allowed us to determine quantitatively the effects of LXRα ligands on LXRα-PPARα heterodimer. All ligands tested induced distinct conformational changes that either promoted or destabilized the formation of heterodimers. Interestingly, the control of dimerization by LXRα ligands did not always correlate with the binding affinities of these compounds for the receptor highlighting the complexity of regulation of dimerization of LXRα-PPARα by ligand binding. Although I did not test the effect of pre-formed LXRα-PPARα dimers on ligand binding, the expectation is that dimerization is likely to influence ligand binding due to allosteric effects propagated from the receptor interface to the ligand binding pocket.

It is worthwhile to mention here that our assays suggest a combination of both ligand-mediated association of monomers into dimers as well as ligand-mediated changes in the conformation of dimers. Whether treatment with ligand modulates the level of LXRα homodimers has not been addressed in the study. Enhancement of homodimerization has been reported for a few GPCRs in which agonist treatment leads to a decrease in the level of dimers, with a corresponding increase in the level of monomers (*120*). Unpublished data from our laboratory suggests that LXRα has a higher affinity for partner receptors compared to LXRα monomers. Although the effect of ligand on homodimers was not investigated, we anticipate that receptor homodimerization is likely to be modulated through ligand binding.

Given that LXRα homodimeric and heterodimeric complexes may exhibit unique functional characteristics, the presence of ligands could selectively target homodimeric species in favor of heterodimeric complexes or vice versa. Regardless of the effect of ligands on homodimers or heterodimers or both, this study provides evidence that ligand binding leads to both qualitative and quantitative changes in heterodimerization that might have significant therapeutic implications.

LXRα L414 may be critical for LXRα-RXRα but not LXRα-PPARα interactions: The role of the LXRα-LBD interface in the functioning of the full-size receptor was verified through functional analysis of carefully selected mutations of residues exposed on the contact surface. I demonstrated that mutations can be computationally predicted and could be applied to design LXRα variants that show selective binding. Using the known crystal structure of LXRα LBD, I generated five LXRα single point mutants for experimental testing. LXRα interactions with both RXRα and PPARα were considered.

Ligand binding and mutations at the LXRα interface modulated protein-protein interactions of LXRα with partner receptors. I identified mutations at the LXRα interface that exhibited altered apparent dissociation constant values with respect to binding PPARα and synthetic LXRα ligand T-0901317. Replacements were predicted to either disrupt or enhance dimerization without major impact on the secondary structure of LXRα and without altering other important functions. In fact, we detected minor changes in ligand-binding properties for LXRα variants with respect to binding 25-HC. All substitutions tested had dramatic consequences on the transactivation activities. Interestingly, all LXRα variants showed higher basal transactivation activity than the wild-type receptor. How interface mutants exhibited enhanced basal transactivation remains unclear. L414R nearly completely disrupted activity when tested with SREBP-1c promoter but retained wild-type like activity with ApoA1 promoter. On the other hand, R415A exhibited strongly reduced transactivation activity with ApoA1 promoter. Our results are consistent with published data on LXRα R415A that has previously been reported to affect transactivation (ADH promoter) and/or ligand binding (T-0901317) (*45*). Our data now points out that the detrimental effects of R415A on transactivation are not due to disruption in LXRα dimerization, but probably due to defective DNA binding or cofactor recruitment. Altogether, the current findings demonstrate that LXRα LBD dimerization surface is critical for the transcriptional activity of the LXRα. Furthermore, dimer contacts at the LXRα interface may provide a link between ligand binding and dimerization and the relationship between ligand binding and dimerization in LXRα is probably more complex than previously thought.

To date, a few mutations in the LXR-LBD have either been linked to human diseases or demonstrated to disrupt ligand binding or transactivation properties. Previously available structures of monomeric LXR-LBD allowed for a straightforward rationalization of the impact of mutations that directly affect hormone binding or protein-protein interactions. Mutations in residues that line AF-2 explain further the basis for ligand dependent transactivation activity. The current LXRα-RXRβ structure suggests an elegant map of allosteric connections between major LXRα functional sites with important implications for signal transmission across the LBD. We provide structure-function insights into how mutations of key residues that cluster at the dimer interface alter key functions of the LXRα. Even though caution must be exercised when extrapolating the current results to other NRs, strong conservation of residues at corresponding positions in other nutrient sensing receptors argues in favor of similar roles in other NRs as well. Despite the inherent challenges in developing protein–protein modulators, our findings suggest that small molecules that may modulate LXRα dimerization could be potentially useful in the treatment of cardiovascular diseases.

Phenocopy- The identification of LXRs as regulators of cholesterol makes them important drug targets to stimulate cholesterol efflux from lipid-laden macrophages (*18*). Presently, several pharmaceutical companies are working to develop agonists that exhibit beneficial effects without the detrimental stimulation of triglyceride synthesis inherent to existing LXRα agonists. This study identified L414R variant as having selective dimerization properties. The observation that L414R selectively binds PPARα, and not RXRα, and responds to the endogenous ligand 25-HC, and not T0901317, has potential implications in drug discovery and development. Moreover, this mutant has

lower transactivation activity when challenged with ligand on SREBP-1c promoter but retains normal wild-type like activity on ApoA1 promoter. Since ApoA1 is the protein component of high density lipoproteins and mediates efflux of cholesterol from the macrophages, L414R presents a possible solution for dissociating the favorable effects of LXRα stimulation from their unwanted effects. The phenocopy phenomenon has been used for drug discovery processes through inhibiting a drug target with different functional modulation technologies and thereby mimicking a phenotype of interest (*121*). The term phenocopy was introduced by Goldschmidt to describe environmentally induced developmental defects which resemble mutant phenotypes (*122*). Inhibition can be achieved using RNA interference (RNAi), to knockdown a target, or by small molecule inhibitors to block or inhibit the activity of the target. Final proof that phenocopy of L414R may offer a solution to the triglyceride-raising problems of the LXR stimulation must await the identification of molecules that will mimic L414R effects in the receptor. However, evidence presented herein makes a compelling case for attempting to identify such molecules to develop strategies in combating metabolic disorders.

BIBLIOGRAPHY

1. Francis, G. A., Fayard, E., Picard, F., and Auwerx, J. (2003) Nuclear Receptors and the Control of Metabolism. Annu Rev. Physiol. 65:261-311.

2. Chawla, A., Repa, J. J., Evans, R. M., and Mangelsdorf, D. J. (2001) Nuclear Receptors and Lipid Physiology: Opening the X-files. Science. 294: 1866-1870.

3. Shulman, A. I., and Mangelsdorf, D. J. (2005) Retinoid X Receptor Heterodimers in the Metabolic Syndrome. Journal of Medicine. 353:604-615.

4. Hsu, I. R., Kim, S. P., Kabir, M., and Bergman, R. N. (2007) Metabolic syndrome, hyperinsulinemia, and cancer. Am J Clin Nutr. 86(3):s867-71.

5. Tozawa, M., Iseki, C., Tokashiki, K., Chinen, S., Kohugura, K., Kinjo, K., Takishita, S., Iseki, K. (2007) Metabolic syndrome and risk of developing chronic kidney disease in Japanese adults. Hypertens Res. 30:937-943.

6. Falkner, B., and Cossrow, N. D. (2014) Prevalence of metabolic syndrome and obesity-associated hypertension in the racial ethnic minorities of the United States. Curr Hypertens Rep. 16(7):449

7. Hegele, R. A., Cao, H., Frankowski, C., Mathews, S. T., Leff, T. (2002) PPARG F388L, a transactivation-deficient mutant, in familial partial lipodystrophy. Diabetes. 51:3586-3590.

8. Gurnell, M., Savage, D. B., Chatterjee, V. K., and O'Rahilly, S. (2003) The metabolic syndrome: peroxisome proliferator-activated receptor gamma and its therapeutic modulation. J Clin Endocrinol Metab. 88(6):2412-21.

9. Savage, D. B., Tan, G. D., Acerini, C. L., Jebb, S. A., Agostini, M., Gurnell, M., Williams, R. L., Umpleby, A. M., Thomas, E. L., Bell, J. D., Dixon, A. K., Dunne, F., Boiani, R., Cinti, S., Vidal-Puig, A., Karpe, F., Chatterjee, V. K., and O'Rahilly, S. (2003) Human metabolic syndrome resulting from dominant-negative mutations in the nuclear receptor peroxisome-proliferator-activated receptor-gamma. Diabetes. 52(4):910-7.

10. Greschik, H., Wurtz, J.-M., Hublitz, P.,Kohler, F., Moras, D., and Schule, R. (1999) Characterization of the DNA-binding and dimerization properties of the nuclear orphan receptor germ cell nuclear factor. Mol. Cell. Biol. 19:690-703.

11. Pawlak, M., Lefebvre, P., and Staels, B. (2012) General molecular biology and architecture of nuclear receptors. Curr Top Med Chem. 12(6):486-504.

12. Kuipers, I., Li, J., Vreeswijk-Baudoin, I., Koster, J., van der Harst, P., Sillje, H. H., Kuipers, F., van Veldhuisen, D. J., van Gilst, W. H., de Boer, R. A. (2010) Activation of liver X receptors with T0901317 attenuates cardiac hypertrophy in vivo. Eur J Heart Fail. 12(10):1042-50.

13. Tontonoz, P., and Mangelsdorf, D. J. (2003) Liver X receptor signaling pathways in cardiovascular disease. Mol Endocrinol. 17(6):985-93.

14. Willy, P. J., Umesono, K., Ong, E. S., Evans, R. M., Heyman, R. A. and Mangelsdorf, D. J. (1995) LXR, a nuclear receptor that defines a distinct retinoid response pathway. Genes Dev. 9(9):1033-45.

15. Janowski, B. A., Grogan, M. J., Jones, S. A., Wisely, G. B., Kliewer, S. A., Corey, E. J., and Mangelsdorf, D. J. (1999) Structural requirements of ligands for the oxysterols liver X receptors LXRα and LXRβ. Proc Natl Acad Sci USA. 96(1):266-271.

16. Steffensen, K. R., and Gustafsson, J. A. (2004) Putative metabolic effects of the liver X receptor (LXR). Diabetes. 53 Suppl 1:S36-42.

17. Ulven, S. M., Dalen, K. T., Gustafsson, J. A., and Nebb, H. I. (2005) LXR is crucial in lipid metabolism. Prostaglandins Leukot Essent Fatty Acids. 73(1):59-63.

18. Hong, C., and Tontonoz, P. (2014) Liver X receptors in lipid metabolism: opportunities for drug discovery. Nature Reviews Drug Discovery. 13: 433-444.

19. Peet, D. J., Janowski, B. A., and Mangelsdorf, D. J. (1998) The LXRs: a new class of oxysterols receptors. Curr Opin Genet Dev. 8 (5):571-5.

20. Aagaard, M. M., Siersbaek, R., and Mandrup, S. (2011) Molecular basis for gene-specific transactivation by nuclear receptors. Biochimica et Biophysica Acta (BBA) - Molecular Basis of Disease. 1812(8): 824-835.

21. Ricci, C. G., Silveira, R. L., Rivalta, I., Batista, V. S., and Skaf, M. S. (2016) Allosteric pathways in the PPARγ-RXRα nuclear receptor complex. Sci Rep. 6:19940.

22. Vivat-Hannah, V., Bourguet, W., Gottardis, M., and Gronemeyer, H. (2003) Separation of Retinoid X Receptor Homo- and Heterodimerization Functions. Mol Cell Biol. 23(21): 7678-7688.

23. Locker, J. Transcription Factors 1st Edition (2000). Academic Press. 9780080924366.

24. Lark, A. K., Wilder, J. H., Grayson, A. W., Johnson, Q. R., Lindsay, R. J., Nellas, R. B., Fernandez, E. J., and Shen, T. (2016) The Promiscuity of Allosteric Regulation of Nuclear Receptors by Retinoid X Receptor. J Phys Chem B. 120 (33); 8338-8345.

25. Giguere, V. (1999) Orphan Nuclear Receptors: From Gene to Function. Endocrine Reviews. 20(5):689-725.

26. Svensson, S., Ostberg, T., Jacobsson, M., Norstrom, C., Stefansson, K., Hallen, D., Johansson, I. C., Zachrisson, K., Ogg, D., and Jendeberg, L. (2003) Crystal structure of the heterodimeric complex of LXRalpha and RXRbeta ligand-binding domains in a fully agonistic conformation. EMBO J. 22(18):4625-33.

27. Hoerer, S., Schmid, A., Heckel, A., Budzinski, R. M., and Nar, H. (2003) Crystal structure of the Human Liver X Receptor Beta Ligand- Binding Domain in Complex with a Synthetic Agonist. J. Mol. Biol. 334: 853-861.

28. Fradera, X., Vu, D., Nimz, O., Skene, R., Hosfield, D., Wynands, R., Cooke, A. J., Haunso, A., King, A., Bennett, D. J., McGuire, R., and Uitdehaag, J. C. (2010) X-ray structures of the LXR alpha LBD in its homodimeric form and implications for heterodimer signaling. J. Mol. Biol. 399:120-132.

29. Matsui, Y., Yamaguchi, T., Yamazaki, T., Yoshida, M., Arai, M., Terasaka, N., Honzumi, S., Wakabayashi, K., Hayashi, S., Nakai, D., Hanzawa, H., and Tamaki, K. (2015) Discovery and structure-guided optimization of tert-butyl 6-(phenoxymethyl)-3-(trifluoromethyl) benzoates as liver X receptor agonists. Bioorg. Med. Chem. Lett. 25: 3914-3920.

30. Yang, C., Li, Q., and Li, Y. (2014) Targeting Nuclear Receptors with Marine Natural Products. Mar Drugs. 12(2): 601-635.

31. Darimont, B. D., Wagner, R. L., Apriletti, J. W., Stallcup, M. R., Kushner, P. J., Baxter, J. D., Fletterick, R. J., and Yamamoto, K. R. (1998) Structure and specificity of nuclear receptor-coactivator interactions. Genes Dev. 12(21):3343-3356.

32. Lou, X, Toresson, G., Benod, C., Suh, J. H., Philips, K. J., Webb, P., and Gustafsson, J. A. (2014) Structure of the retinoid X receptor alpha-liver X receptor beta (RXRα-LXRβ) heterodimer on DNA. Nat. Struct. Mol. Biol. 21(3):277-81.

33. Yang, C., McDonald, J. G., Patel, A., Zhang, Y., Umetani, M., Xu, F., Westover, E. J., Covey, D. F., Mangelsdorf, D. J., Cohen, J. C., and Hobbs, H. H. (2006) Sterol Intermediates from Cholesterol Biosynthetic Pathway as Liver X Receptor Ligands. 281(27816-27826).

34. Ecker, J., Liebisch, G., Patsch, W., and Schmitz, G. (2009) The conjugated linoleic acid isomer trans-9, trans-11 is a dietary occurring agonist of liver X receptor alpha. Biochem Biophys Res Commun. 388(4):660-6.

35. Yoshikawa, T., Shimano, H., Yahagi, N., Ide, T., Amemiya-Kudo, M., Matsuzaka, T., Nakakuki, M., Tomita, S., Okazaki, H., Tamura, Y., Lizuka, Y., Ohashi, K., Takahashi, A., Sone, H., Osuga, J-I., Gotoda, T., Ishibashi, S., and Yamada, N. (2001) Polyunsaturated Fatty Acids Suppress Sterol Regulatory Element-binding Protein 1c Promoter Activity by Inhibition of Liver X Receptor (LXR) Binding to LXR Response Elements. The Journal of Biological Chemistry. 277: 1705-1711.

36. Ou, J., Tu, H., Shan, B., Luk, A., DeBose-Boyd, R. A., Bashmakov, Y., Goldstein, J. L., and Brown, M. S. (2001) Unsaturated fatty acids inhibit transcription of the sterol regulatory element-binding protein -1c (SREBP-1c) gene by antagonizing ligand-dependent activation of the LXR. PNAS. 98(11): 6027-6032.

37. Huang, C. (2014) Natural modulators of liver X receptors. Journal of Integrative Medicine. 12(2): 76-85.

38. Komati, R., Spadoni, D., Zheng, S., Sridhar, J., Riley, K. E., and Wang, G. (2017) Ligands of Therapeutic Utility for the Liver X receptors. Molecules. 22, 88; doi: 10.3390.

39. Schultz, J. R., Tu, H., Luk, A., Repa, J. J., Medina, J. C., Li, L., Schwendner, S., Wang, S., Thoolen, M., Mangelsdorf, D. J., Lustig, K. D., and Shan, B. (2000) Role of LXRs in control of lipogenesis. Genes Dev. 14(22):2831-8.

40. Houck, K. A., Borchert, K. M., Hepler, C. D., Thomas, J. S., Bramlett, K. S., Michael, L. F., and Burris, T. P. (2004) T0901317 is a dual LXR/FXR agonist. Mol Genet Metab 83(1-2):184-7.

41. Aravindhan, K., Webb, C. L., Jaye, M., Ghosh, A., Willette, R. N., DiNardo, N. J., and Jucker, B. M. (2006) Assessing the effects of LXR agonists on cellular cholesterol handling: a stable isotope tracer study. The Journal of Lipid Research. 47:1250-1260.

42. Lund, E. G., Menke, J. G., and Sparrow, C. P. (2003) Liver X receptor Agonists as Potential Therapeutic Agents for Dyslipidemia and Atherosclerosis. Arteriosclerosis, Thrombosis, and Vascular Biology. 23:1169-1177.

43. Yue, L., Ye, F., Gui, C., Luo, H., Cai, J., Shen, J., Chen, K. Shen, X., and Jiang, H. (2005) Ligand-binding regulation of LXR/RXR and LXR/PPAR heterodimerizations: SPR technology-based kinetic analysis correlated with molecular dynamics simulation. Protein Sci. 14(3):812-822.

44. Balanarasimha, M., Davis, A. M., Soman, F. L., Rider, S. D., and Hostetler, H. A. (2014) Ligand-Regulated Heterodimerization of Peroxisome Proliferator-Activated Receptor α with Liver X Receptor α. Biochemistry. 53(16):2632-2643.

45. Shulman, A. I., Larson, C., Mangelsdorf, D. J., and Ranganathan, R. (2004) Structural Determinants of Allosteric Ligand Activation in RXR Heterodimers. Cell. 116, 417-429.

46. Zhang, X. K., Salbert, G., Lee, M. O., and Pfahl, M. (1994) Mutations That Alter Ligand-Induced Switches and Dimerization Activities in the Retinoid X Receptor. Molecular and Cellular Biology. 14(6): 4311-4323.

47. Aggelldou, E., Lordanidou, P., Demetriades, C., Piltsi, O., and Hadzopoulou-Cladaras, M. (2006) Functional characterization of hepatocyte nuclear factor-4 α dimerization interface mutants. FEBS Journal. 273: 1948-1958.

48. Wojcicka, G., Jamroz-Wisniewska, A., Horoszewicz, K., and Beltowski, J. (2007) Liver X receptors (LXRs). Part 1: Structure, function, regulation of activity, and role in lipid metabolism. Postepy Hig Med Dosw. (Online) 61:736-759.

49. Ruan, X. Z., Moorhead, J. F., Fernando, R., Wheeler, D. C., Powis, S. H., Varghese, Z. (2003) PPAR agonists protect mesangial cells from interleukin 1 beta-induced intracellular lipid accumulation by activating the ABCA1 cholesterol efflux pathway. J Am Soc Nephrol. 14(3):593-600.

50. Baranowski, M. (2008) Biological Role of Liver X Receptors. Journal of Physiology and Pharmacology. 59, suppl 7, 31-55.

51. Wang, Y., Viscarra, J., Kim, S. J., Sui, H. (2016). Transcriptional Regulation of Hepatic Lipogenesis. Nat Rev Mol Cell Biol. 16(11):678-689.

52. Cagen, L. M., Deng, X., Wilcox, H. G., Park, E. A., Raghow, R., and Elam, M. B. (2005) Insulin activates the rat sterol-regulatory-element-binding protein 1c (SREBP-

1c) promoter through the combinatorial actions of SREBP, LXR, Sp-1 and NF-Y cis-acting elements. Biochem J. 385(Pt 1): 207-216.

53. Chen, M., Bradley, M. N., Beaven, S. W., Tontonoz, P. (2006) Phosphorylation of the liver X receptors. FEBS Letters. 580(20):4835-4841.

54. Delvecchio, C. J. and Capone, J. P. (2008) Protein Kinase C alpha modulates liver X receptor alpha. J Endocrinol 197(1): 121-30.

55. Laffitte, B. A., Repa, J. J., Joseph, S. B., Wilpitz, D. C., Kast, H. R., Mangelsdorf, D. J., and Tontonoz, P. (2001) LXRs control lipid-inducible expression of the apolipoprotein E gene in macrophages and adipocytes. PNAS. 98: 507-512.

56. Luo, Y. and Tall, A. R. (2000) Sterol upregulation of human CETP expression in vitro and in transgenic mice by an LXR element. J. Clin. Invest. 105: 513-520.

57. Venkateswaran, A., Repa, J. J., Lobaccaro, J. M., Bronson, A., Mangelsdorf, D. J., and Edwards, P. A. (2000) Human white/murine ABC8 mRNA levels are highly induced in lipid-loaded macrophages: A transcriptional role for specific oxysterols. J. Biol. Chem. 275:14700-14707.

58. Yoshikawa, T., Shimano, H., Amemiya-Kudo, M., Yahagi, N., Hasty, A. H., Matsuzaka, T., Okazaki, H., Tamura, Y., Lizuka, Y., and Ohashi, K, et al. (2001) Identification of liver X receptor-retinoid X receptor as an activator of the sterol regulatory element-binding protein 1c gene promoter. Mol Cell Biol. 21:2991-3000.

59. Joseph, S. B., Laffitte, B. A., Patel, P. H., Watson, M. A., Matsukuma, K. E., Walczak, R., Collins, J. L., Osborne, T. F., and Tontonoz, P. (2002) Direct and indirect mechanisms for regulation of fatty acid synthase gene expression by liver X receptors. The Journal of Biological Chemistry. 277:11019-11025.

60. Zhao, C., and Dahlman-Wright, K. (2010) Liver X receptor in cholesterol metabolism. Journal of Endocrinology. 204:233-240.

61. Santamarina-Fojo, S., Remaley, A. T., Neufeld, E. B., and Brewer Jr, H. B. (2001) Regulation and intracellular trafficking of the ABCA1 transporter. The Journal of Lipid Research. 42: 1339-1345.

62. Eren, E., Yilmaz, N., and Aydin, O. (2012) High Density Lipoprotein and its Dysfunction. Open Biochem J. 6:78-93.

63. Vu-Dac, N., Schoonjans, K., Laine, B., Fruchart, J-C., Auwerx, J., and Staels, B. (1994) Negative Regulation of the Human Apolipoprotein A-1 Promoter by Fibrates can be Attenuated by the Interaction of the Peroxisome Proliferator-activated Receptor with its Response Element. The Journal of Biological Chemistry. 269(49): 31012-31018.

64. Hafiane, A., and Genest, J. (2013) HDL, Atherosclerosis, and Emerging Therapies. Cholesterol. 2013: 891403.

65. Zadelaar, S., Kleemann, R., Verschuren, L., De Vries-Van der Weij, J., van der Hoorn, J., Princen, H. M., and Kooistra, T. (2007) Mouse Models for Atherosclerosis and Pharmaceutical Modifiers. Arteriosclerosis, Thromobosis, and Vascular Biology. 27:1706-1721.

66. Janowski, B.A., P. J.Willy, T. R. Devi, J. R. Falck, and D. J.Mangelsdorf. (1996) An oxysterol signalling pathway mediated by the nuclear receptor LXR alpha. Nature. **383**:728-731.

67. Katzenellenbogen, J.A. and B.S. Katzenellenbogen. (1996) Nuclear hormone receptors: ligand-activated regulators of transcription and diverse cell responses. Chemistry & Biology.**3**:529-536.

68. Schulman, I. G., C. Li, J. W. R. Schwabe, and R. M. Evans. (1997) The phantom ligand effect: allosteric control of transcription by the retinoid X receptor. Genes & Development.**11**: 299-308.

69. Georgiadi, A and S. Kersten. (2012) Mechanisms of Gene Regulation by Fatty Acids. Adv. Nutr. 3:127-134.

70. Lu, T. T., J. J. Repa, and D. J. Mangelsdorf. (2001) Orphan nuclear receptors as eLiXiRs and FiXeRs of sterol metabolism. The Journal of Biological Chemistry. 276:37735-37738.

71. Rochette-Egly, C. and P. Germain. (2009) Dynamic and combinatorial control of gene expression by nuclear retinoic acid receptors (RARs). Nuclear Receptor Signaling., 7, e005.

72. Repa, J. J. and D. J. Mangelsdorf. (2000) The role of orphan nuclear receptors in the regulation of cholesterol homeostasis. Annu. Rev. Cell. Dev. Biol. 16: 459-481.

73. Zhang, Y., D. J. Mangelsdorf, and I. G.Schulman. (2012) Liver LXRα expression is crucial for whole body cholesterol homeostasis and reverse cholesterol transport in mice. *J Clin Invest*. **122**:1688-1699.

74. Peet, D. J., S. D. Turley, W. Ma, B. A. Janowski, J. M. Lobaccaro, R. E. Hammer, and D. J. Mangelsdorf. (1998) Cholesterol and bile acid metabolism are impaired in mice lacking the nuclear oxysterol receptor LXR alpha. Cell. 93: 693-704.

75. Alberti, S., G. Schuster, P. Parini, D. Feltkamp, U. Diczfalusy, M. Rudling, B. Angelin, I. Bjorkhem, S Pettersson., and J. A. Gustafsson. (2001) Hepatic cholesterol metabolism and resistance to dietary cholesterol in LXRbeta deficient mice. J Clin Invest. 107: 565-573.

76. Lima-Cabello, E., M. V. Garcia-Mediavilla, M. E. Miquilena-Colina, J. Vargas-Castrillon, T. Lozano-Rodriquez, M. Fernandez-Bermejo, J. L. Olcoz, J. Gonzalez-Gallego, C. Garcia-Monzon, S. Sanchez-Campos. (2011) Enhanced expression of pro-inflammatory mediators and liver X-receptor-regulated lipogenic genes in non-alcoholic fatty liver disease and hepatitis C. Clin Sci.120: 239-250.

77. Kohjima, M., N. Higuchi, M. Kato, K. Kotoh, T. Yoshimoto, T. Fujino, M. Yada, R. Yada, N. Harada, M. Enjoji, R. Takayanagi, and M. Nakamuta (2008) SREBP-1c, regulated by the insulin and AMPK signaling pathways, plays a role in nonalcoholic fatty liver disease. Int J Mol Med. 21:507-511.

78. Higuchi, N., M. Kato, Y. Shundo, T. Hirotaka, T. Masatake, Y. Naoki, K. Motoyuki, K. Kazuhiro, N. Makoto, T. Ryoichi, and E. Munechika (2008) Liver X receptor in cooperation with SREBP-1c is a major lipid synthesis regulator in nonalcoholic fatty liver disease. Hepatol Res. **38**.1122-1129.

79. Joseph, S. B., E. Mckilligin, L. Pei, M. A. Watson, A. R. Collins, B. A. Laffitte, M. Chen, G. Noh, J. Goodman, G. N. Hagger, J. Tran, T. K. Tippin, X. Wang, A. J. Lusis, W. A. Hsueh, R. E. Law, J. L.Collins, T. M. Willson, and P. Tontonoz (2002) Synthetic LXR ligand inhibits the development of atherosclerosis in mice. Proc Natl Acad Sci U.S.A. 99: 7604-9.

80. Schulman, I. G. (2010) Nuclear Receptors as Drug Targets for Metabolic Disease. Adv Drug Deliv Rev. 62:1307-1315.

81. Cannon, M. V., H. H. Sillje, J. W. Sijbesma, M. A. Khan, K. R. Steffensen, W. H. van Gilst, and R. A. de Boer (2016) LXRα improves myocardial glucose tolerance and

reduces cardiac hypertrophy in a mouse model of obesity-induced type 2 diabetes. Diabetologia. 59: 634-643.

82. Pawar, A., D. Botolin, D. J. Mangelsdorf, and D. B. Jump (2003) The role of Liver X Receptor- α in the Fatty Acid Regulation of Hepatic Gene Expression. The Journal of Biological Chemistry, 278:40736-40743.

83. Sampath, H. and J. M. Ntambi (2005) Polyunsaturated Fatty Acid Regulation of Genes of Lipid Metabolism. Annu. Rev. Nutr. 25: 317-340.

84. Vallim, T. and A. M. Salter (2010) Regulation of hepatic gene expression by saturated fatty acids. Prostaglandins Leukot Essent Fatty Acids. 82: 211-218.

85. Hostetler, H.A., A. D. Petrescu, A. B. Kier, and F. Schroeder (2005) Peroxisome proliferator-activated receptor alpha interacts with high affinity and is conformationally responsive to endogenous ligands. Journal of Biological Chemistry. 280:18667-18682.

86. Oswal, D. P., M. Balanarasimha, J. K. Loyer, S. Bedi, F. L. Soman, S. D. Rider, Jr., and H. A. Hostetler (2013) Divergence between human and murine peroxisome proliferator-activated receptor alpha ligand specificities. J Lipid Res. 54: 2354-65.

87. Hostetler, H.A., H. Huang, A.B. Kier, and F. Schroeder (2008) Glucose directly links to lipid metabolism through high affinity interaction with peroxisome proliferator-activated receptor alpha. J Biol Chem. 283: 2246-54.

88. Sreerama, N. and R.W. Woody (2000) Estimation of protein secondary structure from circular dichroism spectra: comparison of CONTIN, SELCON, and CDSSTR methods with an expanded reference set. Anal Biochem. 287: 252-60.

89. Oswal, D. P., G. M. Alter, S. D. Rider, Jr., and H.A. Hostetler. (2014) A single amino acid changes humanizes long-chain fatty acid binding and activation of mouse peroxisome proliferator-activated receptor α. J Mol Graph Model. 51: 27-36.

90. Fernandez-Alvarez, A., M. Soledad Alvarez, R. Gonzalez, C. Cucarella, J. Muntane, and M. Casado. (2011) Human SREBP1c Expression in Liver Is Directly Regulated by Peroxisome Proliferator-activated Receptor α (PPARα). J Biol Chem. 286: 21466-21477.

91. Van Holde, K. E., Johnson, W. C., and Ho, P.S. (1998) Principles of Physical Biochemistry. Prentice Hall, NJ (ISBN 0-13-720459-0).

92. Mitro, N., P. A. Mak, L.Vargas, C. Godio, E. Hampton, V. Molteni, A. Kreusch, and E. Saez. (2007) The nuclear receptor LXR is a glucose sensor, Nature.445: 219-223.

93. Howard, B. V. and D. Kritchevsky (1970) Free fatty acids in cultured cells. Lipids. 5: 49-55.

94. Sridharan, R., J. Zuber, S. M. Connelly, E. Mathew, and M.E. Dumont (2014) Fluorescent Approaches for Understanding Interactions of Ligands with G Protein Coupled Receptors, Biochim Biophys Acta.1838:15-33.

95. Hannah, V. C., J. Ou, A. Luong, J. L. Goldstein, and M.S. Brown (2001) Unsaturated fatty acids down-regulate SREBP isoforms 1 a and 1 c by two mechanisms in HEK-293 cells. J. Biol. Chem. 276: 4365-72.

96. Hostetler, H. A., A. B. Kier, and F. Schroeder (2006) Very-long-chain and branches-chain fatty acyl-CoAs are high affinity ligands for the peroxisome proliferator-activated receptor alpha (PPARalpha). Biochemistry. 45:7669-81.

97. Huang, P., Chandra, V., and Rastinejad, F. (2010) Structural Overview of the Nuclear Receptor Superfamily: Insights into Physiology and Therapeutics. Annu Rev Physiol. 72: 247-272.

98. Ritchie, D. W., and Kemp, G. J. (2000) Protein docking using spherical polar Fourier correlations. Proteins. 39: 178-194.

99. Hostetler, H. A., McIntosh, A. L., Atshaves, B. P., Storey, S. M., Payne, H. R., Kier, A. B., and Schroeder, F. (2009) The Journal of Lipid Research. 50: 1663-1675.

100. Varga, T., Czimmerer, Z., and Nagy, L. (2011) PPARs are a unique set of fatty acid regulated transcription factors controlling both lipid metabolism and inflammation. Biochim Biophys Acta. 8, 1007-1022.

101. Barish, G. D. (2006) Peroxisome Proliferator-Activated Receptors and Liver X Receptors in Atherosclerosis and Immunity. J. Nutr. 136, 690-694.

102. Repa, J. J., Liang, G., Ou, J., Bashmakov, Y., Lobaccaro, J. A., Shimomura, L., Shan, B., Brown, M. S., Goldstein, J. L., and Mangelsdorf, D. J. (2000) Regulation of mouse sterol regulatory element-binding protein-1c gene (SREBP-1c) by oxysterol receptors, LXRα and LXRβ. Genes and Development. 14, 2819-2830.

103. Chambon, P. (1996) A decade of molecular biology of retinoic acid receptors. FASEB J. 10, 940-954.

104. Gronemeyer, H., and Laudet, V. (1995) Transcription factors 3: nuclear receptors. Protein Profile. 2, 1173-1308.

105. Perlmann, T., and Evans, R. M. (1997). Nuclear receptors in Sicily: all in the famiglia. Cell. 90, 391-397.

106. Lee, S. K., Lee, B., and Lee, J. W. (2000) Mutations in Retinoid X Receptor That Impair Heterodimerization with Specific Nuclear Hormone Receptor. The journal of Biological Chemistry. 275, 33522-33526.

107. Hu, C. D., Chinenov, Y., and Kerppola, T. K. (2002) Visualization of Interactions among bZip and Rel Family Proteins in Living Cells Using Bimolecular Fluorescence Complementation. Molecular Cell. 9(4): 789-798.

108. Yoshikawa, T., Ide, T. Shimano, H., Yahagi, N., Amemiya-Kudo, M., Matsuzaka, T., Yatoh, S., Kitamine, T., Okazaki, H., Tamura, Y., Sekiya, M., Takahashi, A., Hasty, A. H., Sato, R., Sone, H., Osuga, J., Ishibashi, S. and Yamada, N. (2003) Cross-Talk between Peroxisome Proliferator-Activated Receptor (PPAR) α and Liver X Receptor (LXR) in Nutritional Regulation of Fatty Acid Metabolism. 1. PPARs Suppress Sterol Regulatory Element Binding Protein-1c Promoter through Inhibition of LXR Signaling. Molecular Endocrinology. 17, 1240-1254.

109. Juge-Aubry, C. E., Gorla-Bajszczak, A., Pernin, A., Lemberger, T., Wahli, W., Burger, A. G., and Meier, C. A. (1995) Peroxisome Proliferator-activated receptor mediates cross-talk with thyroid hormone receptor by competition for retinoid X receptor- Possible role of a leucine zipper-like heptad repeat. The Journal of Biological Chemistry. 270(3):18117-18122.

110. Moreira, I. S., Fernandes, P. A., and Ramos, M. J. (2007) Hot spots- A review of the protein-protein interface determinant amino-acid residues. Proteins. 68, 803-812.

111. Schulman, I. G. and Heyman, R. A. (2004) The flip side: Identifying small molecule regulators of nuclear receptors. Chem Biol 11:639-646.

112. Chen, T. (2008) Nuclear receptor drug discovery. Curr Opin Chem Biol. 12, 418-426.

113. Bookout, A. L., Jeong, Y., Downes, M., Yu, R. T., Evans, R. M., and Mangelsdorf, D. J. (2006) Anatomical profiling of nuclear receptor expression reveals a hierarchical transcriptional network. Cell. 126, 789-799.

114. Chakravarthy, M. V., Lodhi, I. J., Yin, L., Malapaka, R. R., Xu, H. E., Turk, J., Semenkovich, C. F. (2009) Identification of a physiologically relevant endogenous ligand for PPARalpha in liver. Cell. 138, 476-488.

115. Kenyon, M. A. and Hamilton, J. A. (1994) ^{13}C NMR studies of the binding of medium-chain fatty acids to human serum albumin. The Journal of Lipid Research. 35, 458-467.

116. Ferrer-Miralles, N., Villaverda, A. (2013) Bacterial cell factories for recombinant protein production; expanding the catalogue. Microb Cell Fact. 12:113. Doi: 10.1186/1475-2859-12-113.

117. Nagao. K. and Yanagita, T. (2010) Medium-chain fatty acids: Functional lipids for the prevention and treatment of the metabolic syndrome. Pharmacological Research. 61, 208-212.

118. St-Onge, M. P. and Jones, P. J. (2002) Physiological effects of medium-chain triglycerides: potential agents in the prevention of obesity. J Nutr. 132, 329-32.

119. Dave, V. P., Kaul, D., Sharma, Y., and Bhattacharya, R. (2009) Functional genomics of blood cellular LXR- gene in human coronary heart disease. Journal of Molecular and Cellular Cardiology. 46, 536-544.

120. Smith, N. J. and Milligan, G. (2010) Allostery at G Protein-Coupled receptor Homo- and Heterodimers: Uncharted Pharmacological Landscapes. Pharmacol Rev. 62, 701-725.

121. Baum, P., Schmid, R., Ittrich, C., Rust, W., Fundel-Clemens, K., Siewert, S., Baur, M., Mara, L., Gruenbaum, L., Heckel, A., Eils, R., Kontermann, R. E., Roth, G. J., Gantner, F., Schnapp, A., Park, J. E., Weith, A., Quast, K. and Mennerich, D. (2010) Phenocopy- A Strategy to Qualify Chemical Compounds during Hit-to-Lead and/or lead Optimization. PLoS One, 5(12):e14272.

122. Goldschmidt, R. B. (1935a). Gen Und Asseneigenschaft. I, Zeitschrift fver Induktive Abstammungs –und Vererbungslehre. 69, 38-69.

APPENDIX

Supp. Table 1. Affinity of hLXRα for non-fluorescent ligands determined by quenching of hLXRα aromatic amino acid fluorescence (K_d) and ligand efficiencies determined by displacement of hLXRα-bound BODIPY C16-CoA (K_i).

Ligand	Chain length: double bonds (position)	K_d (nM)	K_i (nM)
Palmitoleic acid	C16:1 (n-7)	102±58	N.D.
Palmitoleoyl-CoA	C16:1 (n-7)	34±12	N.D.
Stearic acid	C18:0	16±5	N.D.
Stearoyl-CoA	C18:0	>197	N.D.
Oleic acid	C18:1 (n-9)	45±15	N.D.
Oleoyl-CoA	C18:1 (n-9)	>68	N.D.
Linoleic acid	C18:2(n-6)	16±4	N.D.
Linoleoyl-CoA	C18:2(n-6)	>61	N.D.
Arachidonic acid	C20:4 (n-6)	27±8	N.D.
Arachidonoyl-CoA	C20:4 (n-6)	16±7	N.D.
Docosahexanoic acid	C22:6	>80	N.D.
Docosahexaenoyl-CoA	C22:6	19±4	N.D.
22 (R) Hydoxycholesterol		N.D.	1.2±0.3
25-Hydroxycholesterol		17±4	N.D.

Values represent the mean ± S.E. ($n \geq 3$). ND, not determined.

Supp. Table 2. *Secondary structures of hLXRα protein in the presence of fatty acids and fatty acyl-CoAs*

Ligand	α-helix regular H(r)%	α-helix distort H(d)%	β-sheet regular S(r)%	β-sheet distort S(d)%	Turns T%	Unordered U%
Ethanol	13.9 ± 0.4	11.9 ± 0.2	13.3 ± 0.3	8.8 ± 0	19.6 ± 0.8	32.4 ± 1.5
C16:1	14.0 ± 1.0	11.3 ± 0.9	17.0 ± 3	10.1 ± 0.9	20.9 ± 0.5*	26.5 ± 2.4
C16:1-CoA	14.3 ± 0.6	11.6 ± 0.6	13.7 ± 1.4	9.3 ± 0.3	20.6 ± 0.6	30.2 ± 1.1
C18:0	16.4 ± 3.2	11.7 ± 0.8	10.1 ± 5.1	9.2 ± 0.4	16.9 ± 3.4	35.4 ± 4.8
C18:0-CoA	10.3 ± 1.3	9.7 ± 0.7	19.0 ± 2.4	10.4 ± 0.5	20.1 ± 1.1	30.4 ± 2.0
C18:1	14.0 ± 1	11.3 ± 0.9	17.0 ± 3	10.1 ± 0.9	20.9 ± 0.5	26.6 ± 2.4
C18:1-CoA	14.0 ± 0.2	10.9 ± 0.8	12.0 ± 6	9.0 ± 0.1	18.9 ± 0.2	35.2 ± 0.6
C18:2	14.1 ± 1.1	11.6 ± 1.2	15.0 ± 2	9.4 ± 1.1	20.9 ± 1.1	28.9 ± 1.3
C18:2-CoA	7.4 ± 0.3	8.5 ± 0.1	28.2 ± 9.8	10.8 ± 0.1	25.4 ± 0.4	19.4 ± 9.7
C20:4	13.2 ± 0.2	10.3 ± 0.1	16.1 ± 2.9	10.1 ± 0.1	21.3 ± 0.5	28.7 ± 0.2
C20:4-CoA	13.9 ± 0.6	12.1 ± 0.3	14.21 ± 0.9	8.9 ± 0.2	20.9 ± 0.3	30.0 ± 0.5
C20:5	13.1±0.1	11.6±0.2	14.8±0.8*	9.1±0.1	20.8±0.1	30.5±0.7
C22:5	15.7±1.9	12.2±0.4	10.1±4	8.3±0.6	19.8±1.5	33.8±4
C22:6	15.6±1.1	12.2±1	14±3	9.5±0.8	21±0.4	27.5±1.8
KH_2PO_4	12.3±0.1	9.8±0.3	16.5±1.8	9.7±0.3	19.2±0.3	32.4±0.7
C20:5-CoA	14.2±0.7	12±0.5	14±0.1	8.8±0.4	21.1±0.5	29.9±0.1
C22:5-CoA	13.4 ± 1.1	11.6 ± 0.5	14.9 ± 1.7	9.2 ± 0.3	20.6 ± 0.6	30.2 ± 1.1
C22:6-CoA	14.3 ± 0.4	12.4 ± 0.2	13.2 ± 0.8	8.5 ± 0.1	20.6 ± 0.5	30.9 ± 0.9

Significant difference between hLXRα with solvent compared to the absence or presence of fatty acids or fatty acyl-CoA dissolved in either ethanol or in KH_2PO_4 were determined by t-test * = $P<0.05$, ** = $P<0.01$, *** = $P<0.001$.

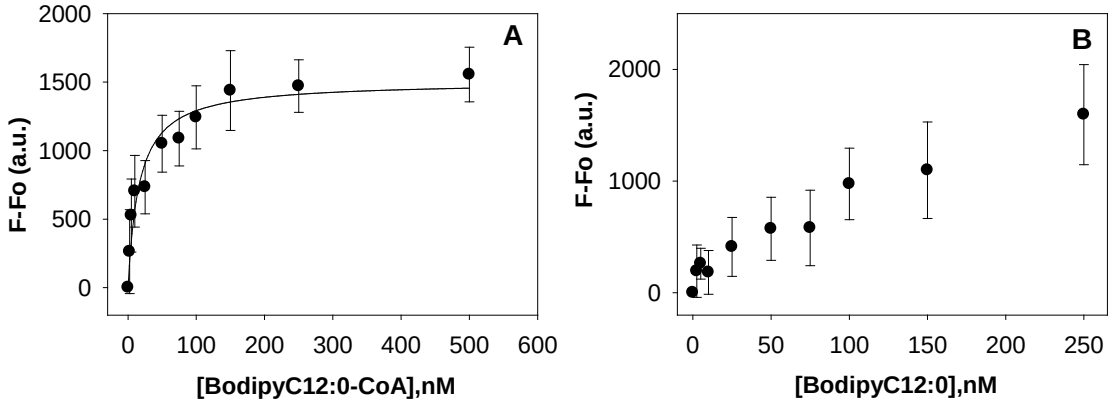

Fig S1: Forster resonance energy transfer (FRET). Unlabeled LXRα (donor) (excitation wavelength 280 nm) was titrated against increasing concentrations of BODIPY C12:0 or BODIPY C12:0-CoA (acceptor) (emission wavelength 300-540 nm). Changes in the fluorescence intensity at 341 nm wavelength were plotted as a function of ligand concentration to determine apparent dissociation constant (K_d) values.

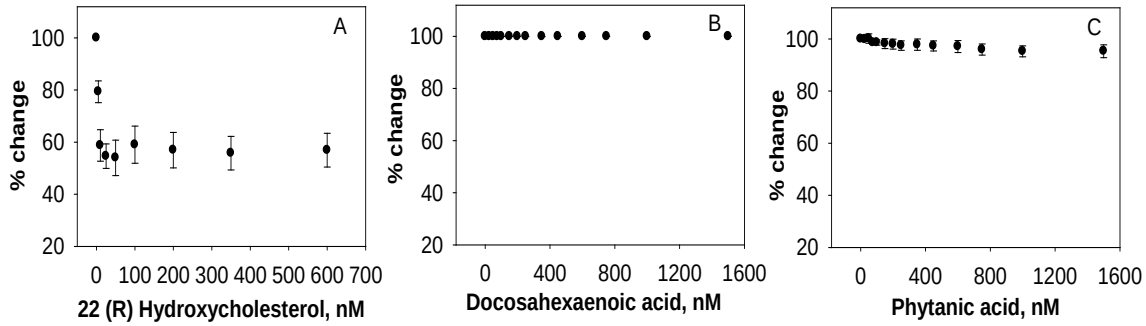

Fig. S2: Displacement assay of BODIPY C16:0-CoA bound LXRα. BODIPY C16:0-CoA bound to LXRα was displaced with LXRα endogenous ligand 22 (R) Hydroxycholesterol, but not with long chain fatty acids docosahexaenoic acid and phytanic acid.

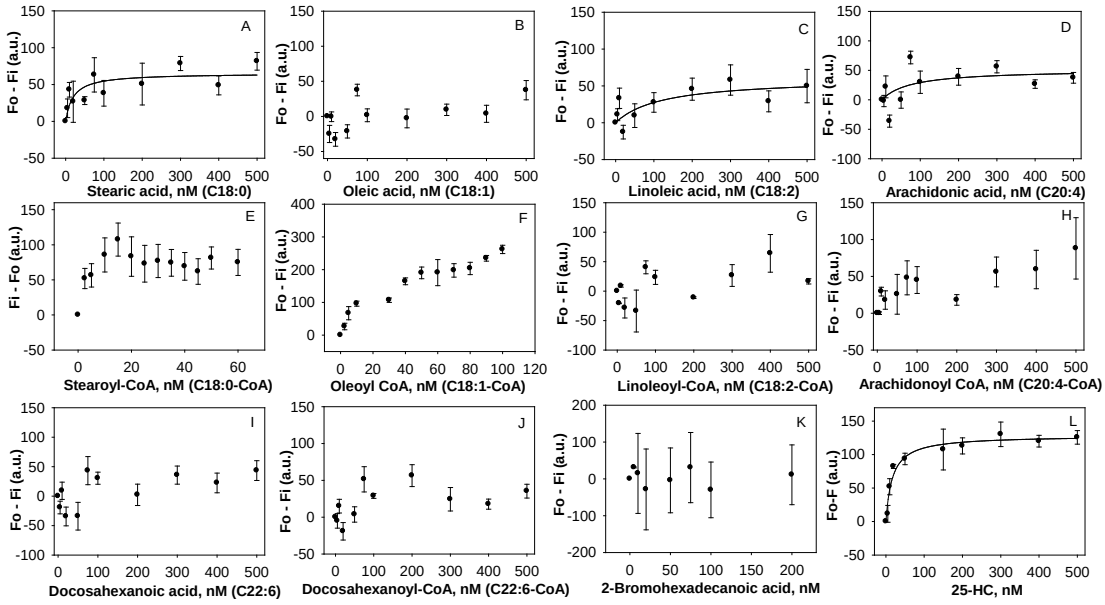

Fig. S3: Direct binding assay based on quenching of LXRα aromatic amino acid fluorescence emission when titrated with the following ligands (A) Stearic acid, (B) Oleic acid, (C) Linoleic acid, (D) Arachidonic acid, (E) Stearoyl-CoA, (F) Oleoyl-CoA), (G) Linoleoyl-CoA, (H) Arachidonoyl-CoA, (I) Docosahexanoic acid, (J) Docosahexanoyl-CoA, (K) 2-Bromohexadecanoic acid, and (L) 25-Hydroxycholesterol

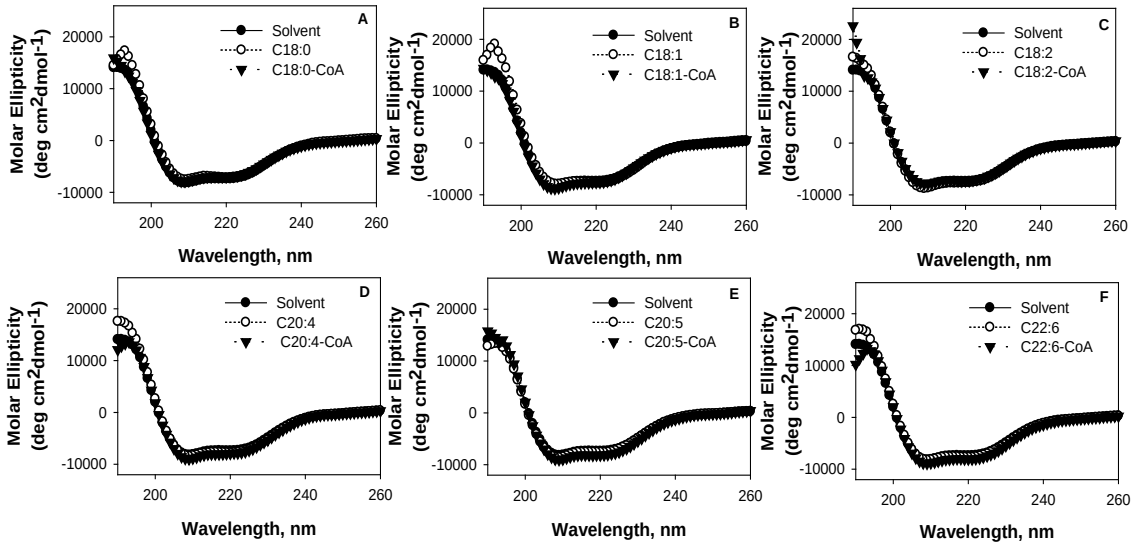

Fig. S4: Far UV circular dichroic spectra of LXRα in the absence (filled circles) and presence of added ligand: (**A**) C18:0 FA (open circles) or C18:0-CoA (filled triangles); (**B**) C18:1 FA (open circles) or C18:1-CoA (filled triangles); (**C**) C18:2 FA (open circles) or C18:2-CoA (filled triangles); (**D**) C20:4 FA (open circles) or C20:4-CoA (filled triangles); (**E**) C20:5 FA (open circles) or C20:5-CoA (filled triangles), and (**F**) C22:6 FA(open circles) or C22:6-CoA (filled triangles). Each spectrum represents an average of 10 scans for a given representative spectrum from at least three replicates.

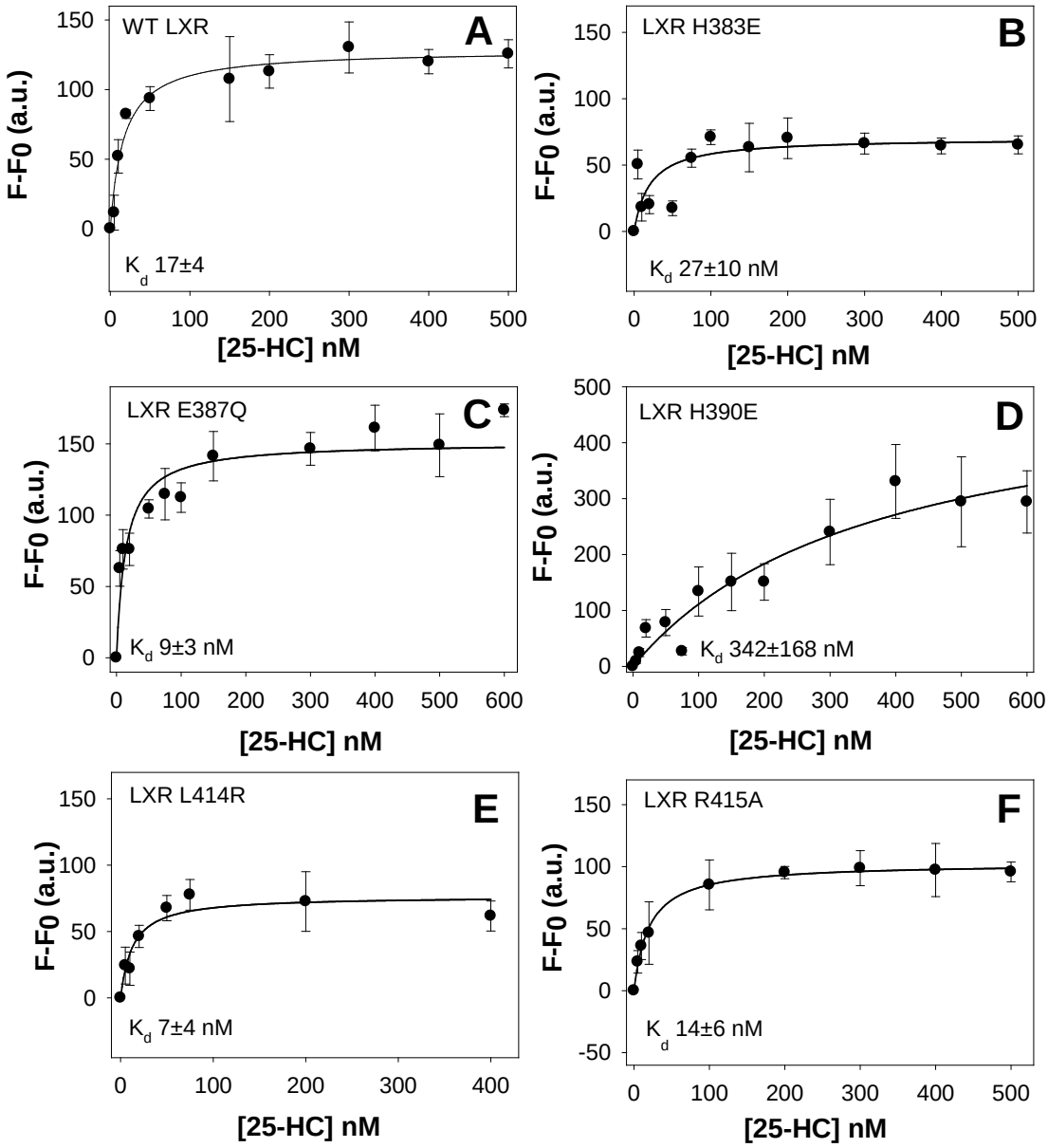

Fig. S5. Effects of LXRα interface mutations on ligand binding of (A) wild-type, (B) H383E, (C) E387Q, (D) H390E, (E) L414R, and (F) R415A LXRα to 25-HC. All mutants, except H390E, showed reduced binding affinity compared to the wild-type. Three independent experiments were performed for each analysis.

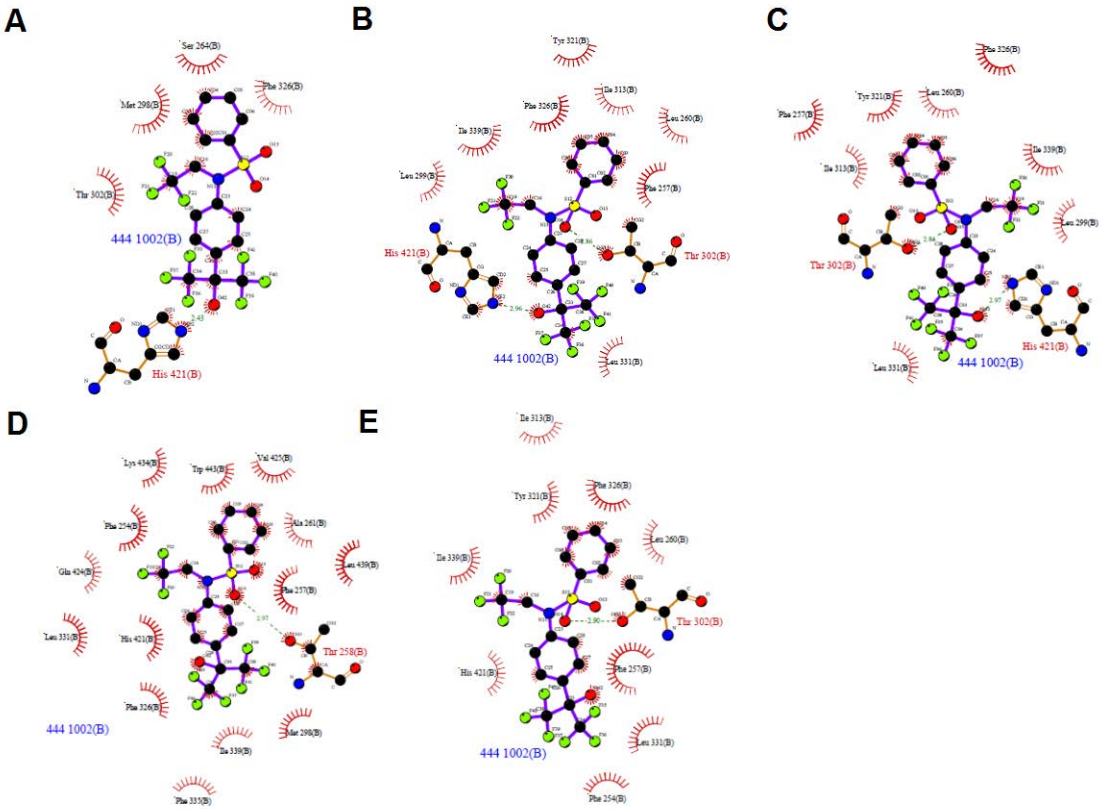

Fig. S6: Ligplot representations of hydrogen bonds and hydrophobic interactions between T-0901317 and (A) wild-type, (B) H383E, (C) E387Q, (D) H390E, (E) L414R, and (F) R415A LXRα. Dashed lines represent hydrogen bonds and spiked residues form hydrophobic contacts with the ligand. Figures were generated in Ligplot+ and LigEd.

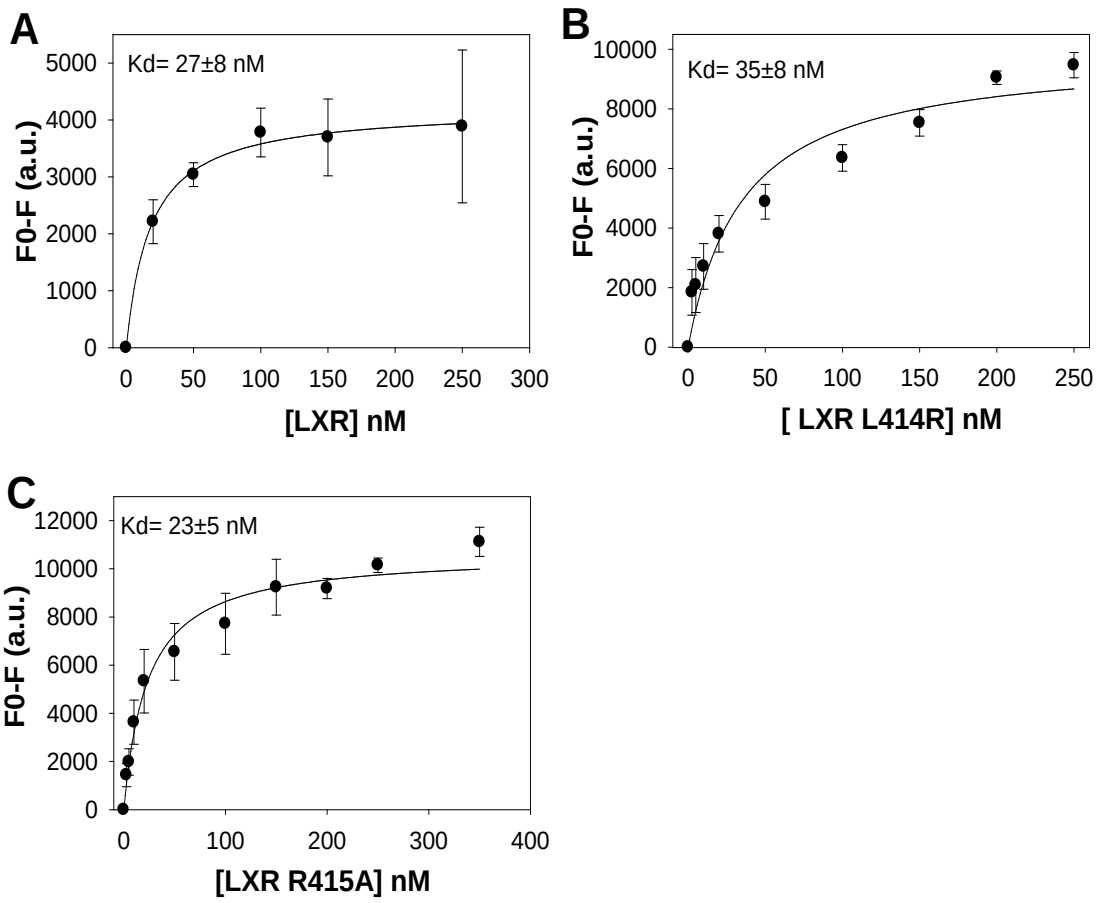

Fig. S7. Fluorescent protein-protein binding assay of Cy3-labeled RXRα titrated against increasing concentrations of unlabeled LXRα. The change in fluorescence intensity of 25nM Cy3-labeld RXRα was titrated with increasing concentrations (0-250 nM) of (**A**) Wild-type LXRα, (**B**) L414R LXRα, (**C**) R415A LXRα.

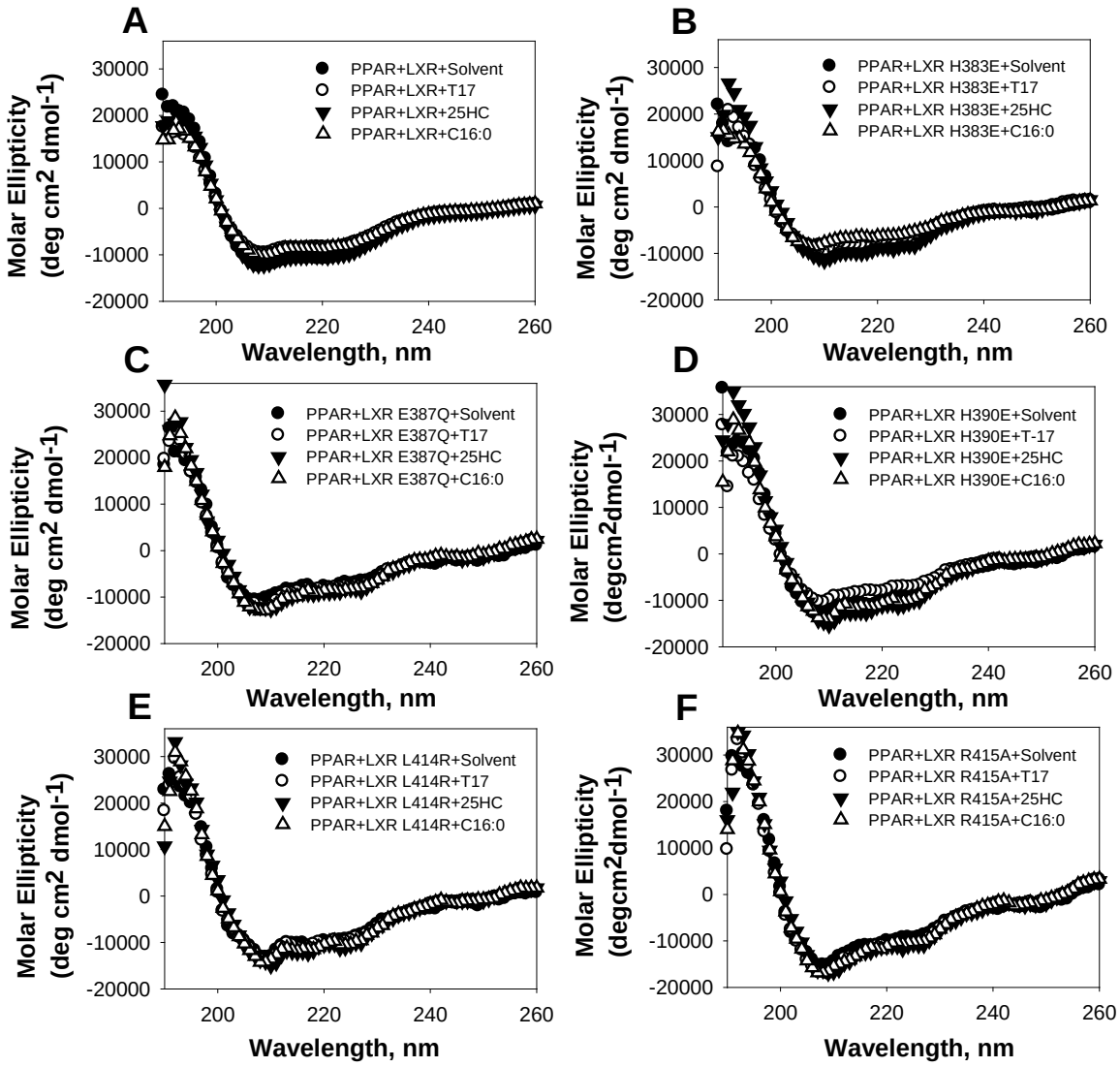

Fig. S8. Far UV CD of the PPARα and (A) wild-type; (B) H383E; C) E387Q; (D) H390E; (E) L414R; or (F) R415A LXRα proteins in the absence (filled circles) and presence of added ligands: T-0901317 (open circles) or 25-HC (filled triangle) or C16:0 FA (open triangle). The amino acid molarity for each spectrum was 0.0002 M, and each spectrum represents the average of at least three replicates, scanned 5 times per replicate.

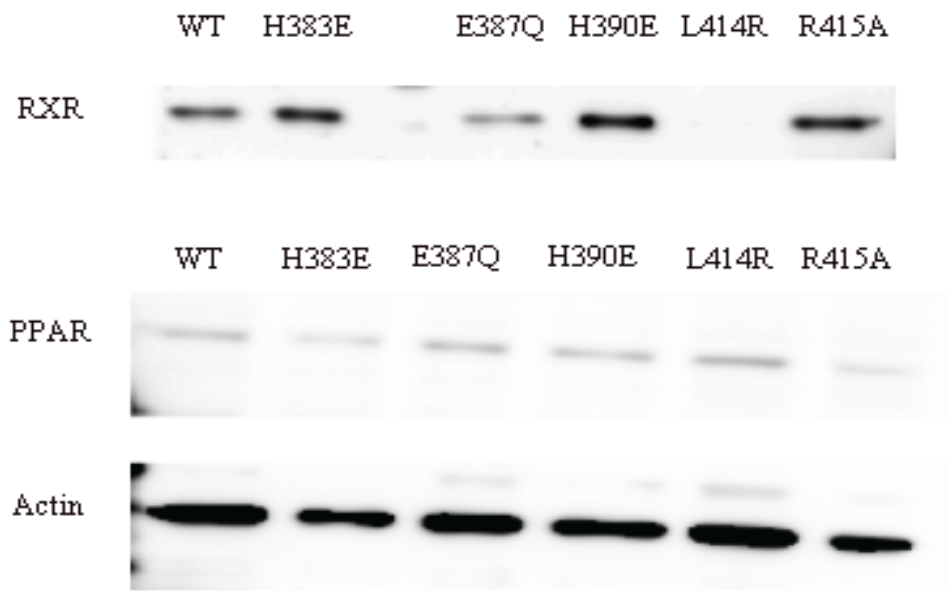

Fig. S9. Detection of the expression levels of BiFC proteins by western blot analysis. COS-7 cells were transfected with the indicated expression plasmids (700 ng). Cell lysates were analyzed by 12% SDS-PAGE and transferred to a nitrocellulose membrane. The expression of BiFC-PPARα and BiFC-RXRα proteins were detected by using a rabbit anti-PPARα serum (provided by Dr. Hardwick) and rabbit anti-RXRα antibody (SC-553, Santa Cruz).

LIST OF ABBREVIATIONS

ABCA1	ATP- cassette transporter A1
ACC	Acetyl-CoA carboxylase
AF-1	Ligand-independent transactivation function
AF-2	Ligand-dependent transactivation function
apo-A1	apolipoprotein A-1
apoE	apolipoprotein E
BiFC	Bimolecular Fluorescence Complementation
Bodipy	Boron-dipyrromethene
CD	Circular Dichroism
CETP	Cholesteryl ester transfer protein
CYP7A	Cholesterol 7 alpha-hydroxylase
DBD	DNA binding domain
DMEM	Dulbecco's modified Eagle's media
DMSO	Dimethyl sulfoxide
DR 4	Direct repeat 4
ECFP	Enhanced cyan fluorescent protein
EDTA	Ethylenediaminetetraacetic acid
FA	Fatty acid
FAS	Fatty acid synthase
FBS	Fetal-bovine serum

FRET	Forster resonance energy transfer
FXR	Farnesoid X receptor
GW3965	3-[3-[N-(2-Chloro-3-trifluoromethylbenzyl)-(2, 2-diphenylethyl) amino] propyloxy] phenylacetic acid hydrochloride
HAT	Histone acetyltransferase activity
HDAC	Histone deacetylase activity
HDL	High density lipoprotein
hPPARα	Human peroxisome proliferator activated receptor α
22-R HC	22R- Hydroxycholesterol
25-HC	25-Hydroxycholesterol
IL-1	Interleukin-1
IL-6	Interlukin-6
LBD	Ligand binding domain
LBP	Ligand binding pocket
LCFA	Long chain fatty acids
LCFA-acyl CoA	Long chain fatty acyl CoA
LDL	Low density lipoprotein
LDL-C	Low-density lipoprotein cholesterol
LXRα	Liver X Receptor α
LXRβ	Liver X Receptor β
LXRE	LXR response element
MCFA	Medium chain fatty acids
MCFA-acyl CoA	Medium chain fatty acyl CoA

NAFLD	Non-alcoholic fatty liver disease
NCoR	Nuclear receptor corepressor
NR	Nuclear receptor
PC	Photon counting spectrofluorometry
PDB	Protein Data Bank
PPRE	PPAR response element
PUFA	Polyunsaturated fatty acids
PXR	Pregnane X receptor
RAR	Retinoic acid receptor
RCSB	The Research Collaboratory for Structural Bioinformatics
RXR	Retinoid X receptor
SCD-1	Stearoyl-CoA desaturase
SDS PAGE	Sodium dodecyl sulfate polyacrylamide gel electrophoresis
SMILE	Small heterodimer partner interacting leucine zipper protein
SMRT	Silencing mediator of retinoid acid and thyroid hormone receptor
SPDBV	Swiss PDB Viewer
SRC-1	Steroid receptor coactivator
SREBP	Steroid regulatory element-binding protein
T-0901317	N-(2,2,2-trifluoroethyl)-N-[4-[2,2,2-trifluoro-1-hydroxy-1-(trifluoromethyl)ethyl]phenyl]-benzenesulfonamide
UGT	UDP-glucuronosyltransferase
VDR	Vitamin D receptor